

ADVANCED OCCUPANT DETECTION SYSTEM: DETECTION OF HUMAN VITAL SIGNS BY SEAT-EMBEDDED FERROELECTRIC FILM SENSORS AND BY VIBRATION ANALYSIS

Pierre Orlewski
CRP Gabriel Lippmann
Laurent Federspiel
IEE SA
Luxemburg
Mark Cuddihy
Manoharprasad Rao
Ford Motor Company,
Stephen Fuks
IEE Sensing Inc.
USA
Paper Number 11-0205

ABSTRACT

The concepts of human seat occupancy detection and driver's drowsiness monitoring require a sophisticated, sensing technology capable of capturing human vital signs in a reliable manner. The concept discussed in this paper may help enable the development of future systems capable of detecting an occupant in a seat.

The present study explores the feasibility of detecting humans based on a polymer sensor fitted into the seat cushion and capable of capturing human vital signs. A bulk, polypropylene ferroelectric film has been charged and polarized in a strong external electric field prior to the sensor assembly. The resulting 323 sq cm sensors displayed a high piezoelectric d_{33} coefficient of approximately 200 pC/N, considerably higher than vibration sensors made of PVDF or PVDF-TR piezoelectric films. This type of electroresponsive polymer has been used for medical respiration, heartbeat and epileptic seizure monitors.

We employed dedicated, microprocessor-based electronics including charge and variable gain amplifiers and 4th-order anti-aliasing filter for data collection. Three different types of algorithms have been fitted or developed and tested: i) a commercial medical monitor with estimation of respiratory and heart beat rates, ii) a signal extraction, filtering and matching wavelet-based algorithm for vital sign detection and (iii) a frequency domain, 2nd-order classifier for humans/objects, using knowledge-based discrimination.

Experimental data involved a minimum of 20 human subjects ranging from a 5-month old infant in a child restraint to a 95th percentile male, both in fully

static (sleeping like) and non-static scenarios. Recordings using test loads and a pack of water bottles were also collected as the counterpart to the passengers.

Human-specific presence detection and discrimination from objects by detection of vital signs was achieved within a relatively short detection time in this conceptual study. Infants and small children were placed in dedicated child restraint seats (CRS) and not moved during the data collection, thus simulating sleeping children. All subjects were detected typically within a 20 seconds sampling interval. In a few cases and with additional time, their respective signals could be extracted from collected data as confirmed by a medical monitor used in parallel.

INTRODUCTION

The concept of human seat occupancy detection requires a sophisticated, sensing technology. Any proposed solution should be capable of quickly and reliably capturing and analyzing data to identify characteristics of the human body (such as vibration frequency eigen-values) and human vital signs (such as respiration rate and/or heart beat). The constraint of seat-specific detection rather than entire vehicle interior monitoring implies the use of seat-embedded sensors. This brings additional functional restrictions of sensor size and materials as directly impacting the seating comfort, seat designs and seat manufacturing process. For all those reasons, the use of thin, electromechanical polymer was the approach investigated in this study.

SENSOR TECHNOLOGY

Over the past decade a lot of research has been carried out on multilayer electret films extruded from various polymer materials like polyethylene (PE), polystyrene (PS), polyurethane (PU), and polyethylene terephthalate (PET). Those successfully brought to the large scale commercial applications included polytetrafluoro-ethylene (PTFE), polyvinylidene fluoride (PVDF) and its copolymer (PVDF-TR) and more recently a porous, monolayer polypropylene (PP) film [1,2,3]. Even employed in relatively slim thickness of 90 μ m, the latter displays excellent sensitivity in the 130 - 200 pC/N range and at vibration frequencies spanning from 1 to 150 KHz. Those principal characteristics, together with the simplicity of the sensor setup, as well as its cost effectiveness, made this intrinsically sensing material attractive for slim acoustic and photoacoustic transducers [4], paramedical, patient in bed monitoring [5], vital sign monitoring including both, respiration rate and heart activity [6] and recently for the wireless ballistographic chair [7]. Detectors built with such a ferroelectric material are transient state sensors reacting only on transient compression or release and are insensitive to the constant force or load applied to its surface.

INITIAL PROOF OF CONCEPT

In the early part of our study we employed an A4-size electromechanical sensor including a 90 μ m polypropylene EMFi film (Emfit Ltd.) and two bottom and top PET layers, both covered with ca. 6 μ m screen-printed silver paste. All three layers have been assembled using double-sided bonding spacer (3M) exclusively applied to the contour of vibration sensitive PP layers. It allowed a stable electrical contact between the sensing layer and the conductive electrode paste and finally a direct charge change measurement instead of a capacitive measurement, which is generally noisier. An additional silver and dielectric double-layer was printed on top of one PET film to protect the sensor from external electromagnetic disturbances (shielding). The sensor was simply deployed on horizontal portion of the vehicle rear bench. It was interfaced to the DAS1000 data logger via original electronics used for a para-medical bed exit and seizure monitor supplied from Emfit Ltd (Finland). Initial testing included a sample of 3 adult male passengers covering the range from 50th- 95th percentile and a variety of objects up to the weight of approximately 15kg, supposed to be transported on the rear bench seat. Our attention was initially focused on two major questions: (1) Would it be possible to extract human vital signals captured by the sensor exclusively fitted to the seating portion of the vehicle bench seat (no backrest sensor present), while the vehicle is operating at low

vibration noise conditions (parked with engine on or cruising on smooth paved roads)? (2) Would it be possible to use this information for a robust discrimination of human passengers from transported cargo? Collected vibration time-domain data has been denoised by using classical Coiflet's wavelets [8] with universal thresholding method as proposed by Donoho and Johnstone [9].

Each human test subject was monitored for 60 seconds of steady seating at a sampling frequency of 1 kHz. A reduced sample of 32 seconds was used for analysis in order to avoid the bias from initial and continuing compression of seat materials. As shown on Figure 1 below, we were able to extract a quite regular and reliable vital sign signal especially from steady vehicle with engine on. Signal periodicity coincides well with the typical human respiration rate and a higher frequency component, probably in relation to the heart beat, is clearly perceptible on the top of every peak.

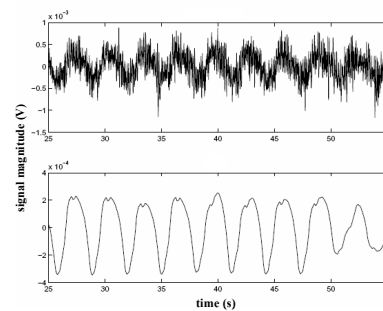


Figure 1. Vital signals from 50thile male passenger in steady vehicle with engine on: raw signal (upper) and extracted human respiration after wavelet denoising (bottom).

A similar approach, except with 2 (backrest and seat cushion) ferroelectric EMFi sensors fitted to an office chair, and a wavelet analysis has been adopted in the past by Postolache et al. [6] for a remarkably good separation of respiration signal embedded in the heart rate ballistocardiogram (BCG).

Test conditions and sampling

For the setup of a discrimination algorithm, a larger data set has been collected consisting of a 5 x 32 data series recorded in a non-moving vehicle with the engine ON and OFF. The test series included 4 objects (5, 10, 15kg load stamps and a 9L 6x1.5L water pack), 3 adult males and 1 empty seat, every sequence being repeated twice. The second set of data was collected while the vehicle was cruising. It totaled 5x16 data series (incl. 2 repetitions) from 4 objects, 3 humans and 1 empty seat. The third set of data (2x48) has been collected in similar

conditions as previously described but with intentionally aged sensors. Finally, 40 data series were collected while the vehicle was traveling at 70 km/h on very smooth paved road and at 50 km/h on a paved but non-smooth road. From the total number of 371 useable vibration profiles (out of the first 376 recordings, 5 were damaged), 144 profiles were used in algorithm setup and discrimination training while the remaining 227 were used in further testing.

Discrimination Algorithm

A three-step discrimination algorithm was established. In the first step a data sequence of an arbitrarily selected 50th percentile male test subject was collected in a steady vehicle with engine on. After extracting a 32.7sec window and performing wavelet decomposition, the noise was removed from the signal using universal hard thresholding. A representative *physiological pattern* was manually picked up from the cleaned signal. In the second, still off-line stage, all 144 test sequences were employed in a setup of the *training database* (Fig.2). The following wavelet-based signal denoising and reconstruction, autocorrelation, correlation with physiological pattern and FFT analysis, resulted in 5 primary signal characteristics (max DSP frequency, max DSP value, max FFT frequency, max FFT value and max correlation with physiological pattern). These physical signal parameters were then converted to a set of classification features among which, the barycentres (centers of mass) of the Human and non-Human (cargo or empty seat) clusters were the most prominent classifiers.

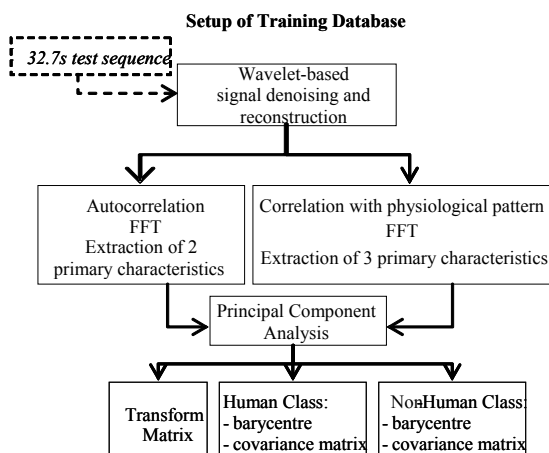


Figure 2. Off line setup of Training Database.

In the on-line phase, every incoming, “unknown” vibration sequence from the 227 testing data sets was submitted to exactly the same wavelet denoising procedure as previously employed with the training sequences.

Decision-making Process

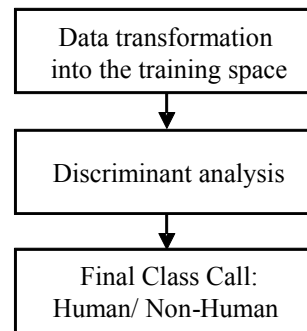


Figure 3. On-line decision-making process.

After data transformation into the training space, the final (Human or non-Human) discrimination call (Fig. 3) was issued from Discriminant Analysis (DA). The prevalent discriminators in the DA were the respective distances to the human and non-human class barycentres and the likeness to the canonical *physiological pattern*. The overall human / cargo (or empty seat) discrimination performance during this part of the study reached 93.5% of correct decisions. As expected, most of the errors (false positives) came from driving scenarios, while non- detection (false negatives) errors resulted exclusively from testing with parked vehicle (Tab.1). This result was obtained without any *a priori* knowledge about the state of vehicle (stationary or moving). In real life, this information may be retrieved from the vehicle CAN bus which would improve the performance. In the present study, use of this information improved the final discrimination, with up to 98.8% of the decisions correctly classified.

Table 1. Confusion matrix of the final discrimination: FN–false negatives, FP–false positives.

	Steady vehicle with engine ON	Cruising vehicle
FN	5	0
FP	0	17
Total	224	112

In this conceptual study, extraction of the vital signs from the electromechanical film sensor fitted into the vehicle seat cushion was achieved, even in presence of relatively large vibration noise background generated by a moving vehicle. It was realized that with currently available sensor technology, one needs to address also other human body characteristics for the robust discrimination over the large number of passengers and objects potentially carried in the rear seats and to cover real-world driving scenarios (e.g., road quality, vehicle velocity and acceleration, types of chassis)

DETECTION TRIALS OF TODDLERS AND INFANTS

One of the sensors employed in the previous study was fitted into the rear bench seat with thick foam trim. We used both the original electronic interface for paramedic vital sign monitoring (from Emfit Ltd., Finland) and its modified version with reduced amplification gain. The principal point of interest was the feasibility of vital sign capture and detection of infants installed in a CRS. All tests were made with a rearward-facing class 1 child restraint seat and with a forward facing seat (Fig. 4). Two infants (4 and 5 months old) and two toddlers (22 and 24 months old) were involved in detection trials in a parked vehicle with the engine off. These tests were conducted during the winter period, with the children warmly dressed. The thick clothes constituted an additional damping factor of the vital signals supposed to propagate through the base of the CRS. As at this stage we were exclusively interested in vital signs, all of children were encouraged to stay motionless, simulating a sleeping child scenario.



Figure 4. Detection trials with child restraint seats (from left to right 4 month old infant in rearward-facing seat and 22 month old toddler in a forward-facing seat)

All tests were repeated at least 5 times with both types of electronic interface. With the original Emfit interface setting, typically 20 seconds were required to detect vital signs within preset signal robustness and quality requirements. Even with the inevitable high frequency movements of the children, the software was able to yield realistic, average heart beat rates of approximately 115 beats / min and 90 beats / min respectively for the infants and for toddlers. Trials with modified electronics and modified amplification gains and filtering parameters accelerated the detection of vital signs down to approximately 15 sec (toddlers) and 10 sec (infants) but computed heart rates were unrealistically low.

This assessment demonstrated the conceptual feasibility of detection of infants with a very

sensitive vibration sensor installed in the car seat, with both ballistocardiograph and respiration signals of acceptable quality. The “child detected” decision exclusively relied on vital signals and did not account for other captured signals, generated by small body movements of the children.

Additionally, in order to detect a child with this conceptual approach, a sensor-CRS contact surface is necessary and complete absorption of vibrations within a physiological frequency range from 0.1 to 2.0 Hz by the CRS cannot occur.

TOWARDS A VERSATILE INTELLIGENT PEOPLE DETECTOR IN THE VEHICLE SEATS

Although conceptual feasibility was shown in laboratory testing, the robustness of in-vehicle occupant detection by vital signals will be limited in the real-world driving due to the vibration noise. Therefore, human vital signs cannot be the exclusive detection target and must be accompanied by another “human factor”, well distinguishable from the surrounding vibration background of a moving vehicle. Such a physical entity, moderately influenced by chassis vibrations, is apparent mass resonance frequency of the human body, which significantly differs from empty seat and seat cargo resonance frequencies (Fig. 5 and Fig. 6).

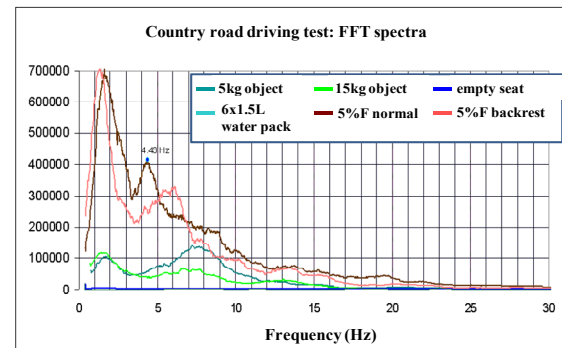


Figure 5. Frequency spectrum of 5th percentile female and of seat cargoes up to 15 kg during 50 km/h cruising on smooth road.

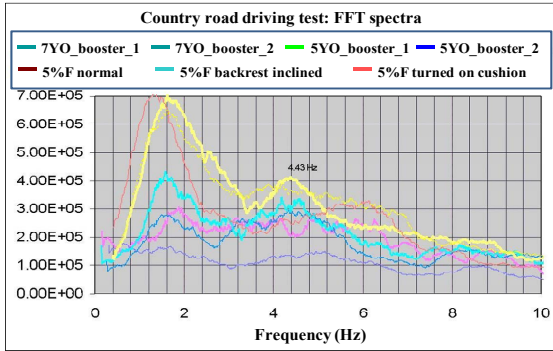


Figure 6. Frequency spectrum of 5th percentile female (various seating postures) and of 5&7 YO children seated on booster seats during 50 km/h cruising on smooth road.

In the test cases using human occupants, a 5th percentile female adopting different seating postures and 5 and 7 year old children in booster seats, the human mass resonance peaks at approximately 4.43Hz and is perceptible and in agreement with data found in the literature [10,11]. In contrast, the resonance frequency of unanimated seat cargo peaks at higher frequencies, starting from 7-8Hz on and thus allows for the human /non-human seat occupancy discrimination.

Dual mode discrimination strategy and new algorithm setup

After basic detection assessments were conducted both in parked and in moving vehicles, the focus was shifted to the dual mode detection scenario. The magnitude of the vehicle chassis vibrations was selected as the trigger between vital signals and apparent mass vibration characteristics in the dedicated algorithm (Fig. 7). For study, the vehicle vibration noise level was assumed to be known, which in practice is achievable in the vehicle either by retrieving this information from the CAN bus or by installing a dedicated, vertical accelerometer.

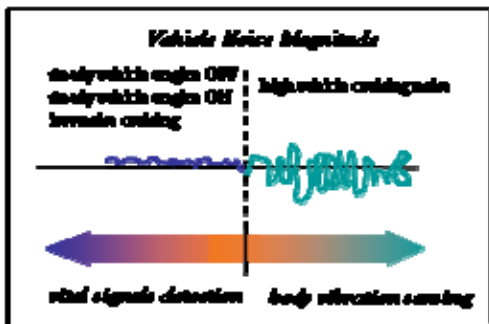


Figure 7. Dual mode discrimination strategy triggered by vehicle's noise magnitude.

The sensors (Fig.8) were modified and their sensitive surface was reduced to ca. 323 cm² in order to fit 3 places of a sedan rear bench seat.

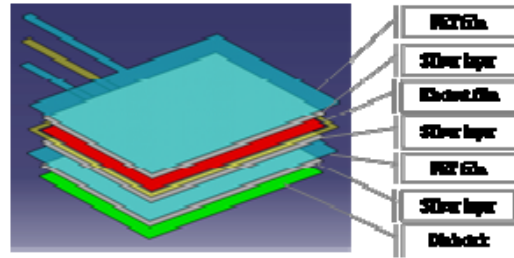


Figure 8. Electromechanical sensor setup with 90µm porous polypropylene ferroelectric film (length: 214 mm, width: 152 mm, thickness: 370 µm).

All three sensors fitted into the rear bench were quasi-simultaneously controlled by an electronics module specially developed for this purpose. It included (Fig.9) a 12 bit Field Programmable Gate Array microprocessor (µC), a 3-channel multiplexer (MUX), a 12 bit ADC converter, charge- and variable gain amplifiers and a 4th-order antialiasing filter. All data was stored on the laptop PC hosting the graphical user interface. The discrimination software operated alternatively in the real-time and in the off-line mode.

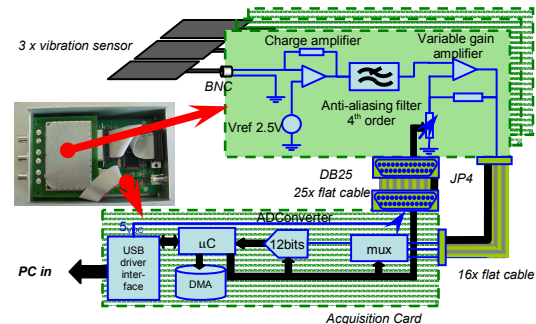


Figure 9. Block diagram of acquisition electronic interface.

A new, dedicated algorithm was developed, different from the computation-intensive algorithm with wavelet filtering used in the initial proof of concept. It involved several discrete discrimination features computed both from the time domain and frequency domain spectra, depending on the vehicle noise magnitude (a major feature trigger) and specifically addressing vital signs and/or vibration properties of the human beings. Current front outboard seat belt reminder systems emit their warning within 30-60 seconds. For this reason, we limited a spectral window to only 8 seconds in order to be able to collect and average the discrimination status over at least 3 samples.

During the algorithm setup (training) and validation, data was collected with both a parked vehicle (engine on and off) and with a vehicle moving with three different velocities (50, 70 and 90 kph) on three types of roads (smooth paved, rough paved and gravel roads). The human test subjects (collected with 2 to 5 repetitions) were: 95th and 50th percentile adult males, 5th percentile female, 3 and 6 year old children sitting on booster seats. A few tests also involved additional objects like a thick blanket or wooden comfort mat. The cargo transported on the seat included 5, 10 and 15 kg metal load stamps, 6x2L water containers and a 5 kg backpack. The data from the empty seat was also collected.

In total, the performance validation sample consisted of not less than 153 tests repeated up to 8 times, which resulted in more than 163 hours of elapsed testing time. Final performance evaluation was run with 8 second samples without any higher level decision, smoothing or filtering. Thus, the system was required to classify the occupant within 8 seconds for performance evaluation.

Results and discussion

The parked vehicle discrimination evaluation was performed with motionless passengers and separately with passengers behaving normally (moving) on the seat. The test population included various adults as well as 6 year old children on boosters. The test cargo was manually agitated by the test operator during the moving testing scenario, which had a significant impact on the sensor response (Tab.2).

Table 2.
Discrimination performance in parked vehicle with engine on and with steady and moving seat occupants. Decision exclusively based on algorithm features addressing human vital signs.

SEAT OCCUPANT	Steady	Moving
adults	100%	100%
Children on boosters	75%	92%
cargo	92%	20%

In many cases of manually agitated seat cargo the signal was saturated to the point that precise occupancy discrimination was no longer feasible, except for the classification of an occupied seat. According to this logic, the detection of empty seat and occupied seat has reached 100% performance. In both, steady and moving passenger scenarios in the vehicle with engine on, the system seemed to reach its detection limit for 3 year old children seated on booster seats. With the engine off, this limit seemed to be much lower but was still very

dependent on the design and materials of the CRS hosting the child.

More exhaustive, driving tests conducted with a Ford Taurus covered 3 different vehicle velocities and 3 different road types.

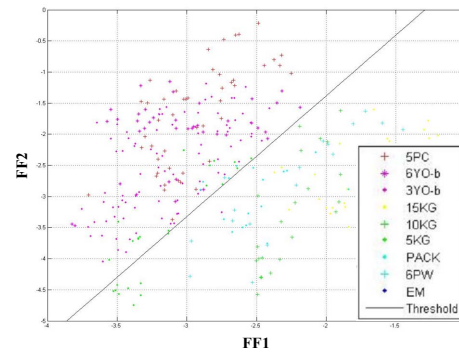


Figure 10. Example of discrimination among the most critical occupants from the last test campaign. Three different road styles and vehicle velocities of 50, 70 and 90 kph.

As vehicle vibrations become more prominent, seat occupancy discrimination occurred principally through the algorithm features addressing human body vibration properties and less via vital signs. Figure 10 depicts separation achieved by two principal “dynamic” features FF1 and FF2. There were very few issues with classification of the 5th percentile female, but signals generated by 3YO children in boosters were usually below the preset sensitivity threshold, and are therefore not shown in the Table 3 below.

Table 3.
Estimated discrimination performance in driving test with static passengers.

SEAT OCCUPANCY	Smooth paved road		Rough paved road		Gravel road		
	Car seat	boosters	Car seat	boosters	Car seat	boosters	
Human	5 th percentile female	100%	-	100%	-	100%	-
	6YO child A	-	91%	-	100%	-	97%
	6YO child B	-	78%	-	100%	-	85%
Cargo	Backpack	100%	-	63%	-	88%	-
	9L water pack	100%	-	41%	-	100%	-
	10kg stamp load	67%	-	71%	-	100%	-
	Empty seat	100%	-	100%	-	100%	-

The performance was moderately affected by the quality of the road, with the rough paved road being the most difficult for cargo discrimination. Also, additional objects in the seat (thick blanket, wooden comfort mats) and occupant motion (still, moving) seemed to have little influence on the spectra of adult passengers (Fig. 11).

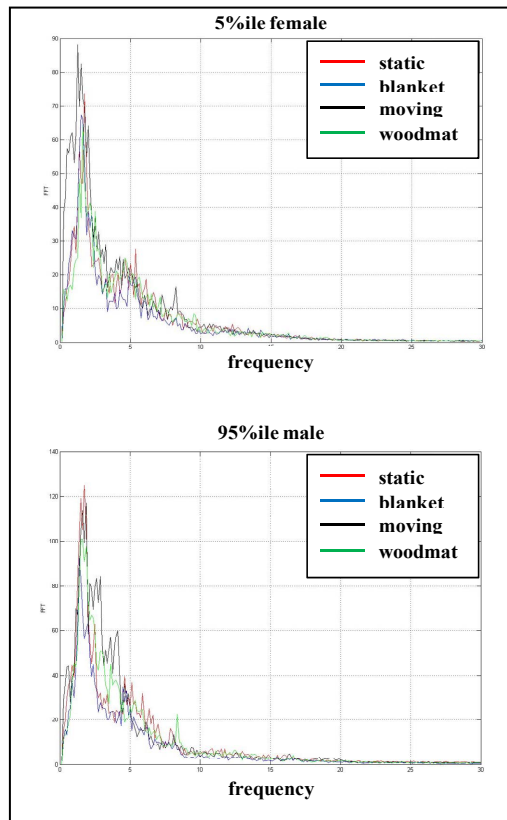


Figure 11. Seat resonance spectra of 5th percentile female (top) and 95th percentile male (bottom) sitting on other objects (blanket, wooden mat).

OUTLOOK

This study suggests some limitations of the concepts evaluated due to the core functional material employed. Additional research is necessary to evaluate these shortcomings in more detail.

The ultrasensitivity of the highly porous, charged polymer led to detection performance reduction as far as vehicle rear seating positions are concerned. Seating position which are not physically separated or at least, not mechanically decoupled will have the potential to generate vibration crosstalk in case of simultaneous bench occupation by passenger(s) and by cargo. The latter can then be misclassified as a human being.

The stability of the sensitivity over a broad temperature range for the material evaluated in this study has not been demonstrated. Preliminary analysis of deliberately degraded (aged) sensors suggests that a minimum sensitivity of 50-80 pC/N would have to be preserved over the seat and sensors lifetime to guarantee successful detection of human vital signs. The current ferroelectric material will probably not meet these requirements as it is based on polypropylene film injected with

nitrogen and corona charged air pockets, which seem to progressively lose their charge and polarization in temperature ranges above 75°C. Therefore it will be necessary to investigate alternative materials further in view of an application in automotive environment.

CONCLUSIONS

This paper describes the use of a conceptual electromechanical, ferroelectric polymer for advanced occupant detection and occupancy discrimination in a variety of vehicle scenarios.

It also demonstrates the possibility of the capture of human vital signals (especially respiration) by the detector fitted into the seat cushion. A means to address the limitations caused by chassis vibrations is presented.

Based on this study, further research into the utilization of ultrasensitive vibration sensor as an occupant detection technology is warranted. If researchers can address the material-related limitations, this technology may become a viable approach to monitoring human body physiological characteristic in a motor vehicle environment.

ACKNOWLEDGMENTS

The authors would like to thank Dr Radu Ranta from Centre de Recherche en Automatique in Nancy, France for his comprehensive introduction of wavelet theory and practice and his contribution into the preliminary proof of concept. We also thank Heikki Räisänen from Emfit Ltd., Finland for his active support over the complete program duration.

REFERENCES

- [1] Savolainen AK. and Kirjavainen K. "Electromechanical film : Part 1. Design and Characteristics", (1989), J. Macromol. Sci –Chem., A26(2-3) 583-591.
- [2] Kirjavainen K. "Electromechanical film and procedure for manufacturing same", U.S. Patent No. 4654 546, 1987.
- [3] Paajanen M., Lekkala, J. and Kirjavainen K. "ElectroMechanical Film (EMFi) – a new multipurpose electret material", (2000), Sensors and Actuators 84:95-102.
- [4] Manninen A., Sand J., Saarela J., Sorvajärvi T., Toivonen J. and Harnberg R., "Electromechanical film as a photoacoustic transducer", (2009), Optics Express, 19:16994-16999.
- [5] Emfit Ltd., Vaajakoski, Finland, www.emfit.com/en/care/
- [6] Postolache O., Silva Girão P., Postolache G. and Pereira M. "Vital Signs Monitoring System

- Based on EMFi Sensor and Wavelet Analysis”, (2007), Instrumentation and Measurement Technology Conference – IMTC2007, Warsaw, Poland, 1:4.
- [7] Junnila S., Akhbaradeh A. and Värri A. “An Electromechanical Film Sensor Based Wireless Ballistographic Chair: Implementation and performance”, (2009), J Signal Process Syst 57:305-320.
- [8] Coifman, R. and Wickerhauser, M., “Adapted waveform de-noising for medical signals and images”, (1994), Engineering in Medicine and Biology Magazine, vol. 14, 5:78–586,
- [9] Donoho, D. and Johnstone, I., “Ideal spatial adaptation via wavelet shrinkage”, (1994), Biometrika 81:455
- [10] Fairley T.E. and Griffin M.J. “The apparent mass of the seated human body in the fore-and-aft and lateral directions”,(1990), Journal of Sound and Vibration, 139, 2: 299-306
- [11] Smith S.D. “Modelling differences in the vibration response characteristics of the human body”,(2000), Journal of Biomechanics, 33, 11:151

ANALYSIS OF CHILD DUMMY RESPONSES AND CRS PERFORMANCE IN FRONTAL NCAP TESTS

Chung-Kyu (CK) Park

Richard M. Morgan

Kennerly H. Digges

National Crash Analysis Center (NCAC), The George Washington University
USA

Paper Number 11-0142

ABSTRACT

The new car assessment program (NCAP) conducted 95 frontal crashes with child dummies in child restraint systems (CRS) in the rear seat. In addition to the two mid-size male dummies in the front seat, there were one or two child dummies in the rear seat area. The child dummies were (1) 12-month-old, (2) 3-year-old, and (3) 6-year-old. The child dummies were restrained in a CRS or a booster. This research focused on comparing the response of the child dummies with the adult dummy. The study examined the dynamic readings of the head acceleration, chest acceleration, chest deflection, and upper neck loading.

In terms of the customary injury assessment reference values (IARVs) for the adult and child dummies, the adult dummy had an easier time going under the IARVs than the child dummies. The passing rate for the adult was almost 100% while the passing rate was 60 - 70% for the child dummies. In short, the different dummy sizes in their respective seating location do not show the same relative level of protection as measured by body motion and instrumentation inside the dummy occupant.

The 3-year-old and 6-year-old child dummies show relatively elevated head response because their heads are not restrained in the sense that the adult's head is cushioned by the airbag. Some device or concept is needed to reduce the rotational motion of the head for the forward-facing child. The child dummies do not take advantage of the ride down (connecting the occupant to the initial crushing of the vehicle structure to slow down the occupant) as capably as the adult dummy. Some device or concept - such as the pre-tensioner for the adult in the front seat - is needed to reduce the free motion of the forward-facing child. The motion and response of the 6-year-old child dummy appear to vary more than the other crash test dummies.

INTRODUCTION

Recent investigations (of frontal laboratory crashes) have found that adult-size dummies in the rear seat

had much higher head and neck injury-assessment values than adult-size dummies in the front seat. Generally, the rear seat dummy had higher chest acceleration readings than the front seat dummy. [1-3]

In investigating real-world field data in 2009, Kent *et al.* [5] observed that, "the relative effectiveness (to mitigate serious injury and death) of rear seats with respect to front seats for restrained adult occupants in newer vehicle models is less than it is in older models, presumably due to the advances in restraint technology that have been incorporated into the front seat position." Other studies have examined real-world data and suggested similar findings. [5-7]

A 2005 report by Starnes [8], which was based on the analysis of the fatality analysis reporting system (FARS) and the national automotive sampling system crashworthiness data system (NASS CDS) data, focused on child passenger injuries in different crash configurations. For all crash configurations, a child occupant, whether restrained or unrestrained, was safer when travelling in the second row of the vehicle as opposed to the front passenger seat. It was also found that in non-fatal crashes, unrestrained passengers were much more likely to have been injured than restrained passengers.

In 2008, Hong *et al.* [9,10] investigated frontal crashes conducted by NCAP. All crashes had two 50th % male Hybrid III dummies in the front-seat area and a total of twenty-eight 10-year-old (10YO) child Hybrid III dummies in the rear-seat area. Hong compared the 10YO Hybrid III dummy with the adult dummy in the front seat. In these NCAP tests, almost all the front-seat adults had low IARVs. In contrast, many of the rear-seat 10YO child dummies saw violent head motion, high head injury criterion (HIC), high tension or compression in the neck, and high chest accelerations. In a few vehicles, the 10YO child dummy saw much smoother head motion, lower HIC, lower tension, and lower chest acceleration.

In this paper, an analysis of child dummies (1 through 6-years-old) was conducted to determine crash conditions that involved rear-seat injuries that

are not currently being directly addressed by vehicle safety standards or by consumer information test protocols. Analysis of US NCAP tests were conducted to determine the relative safety provided by seating position and by vehicle model year. Opportunities for reducing IARVs [11] in the child dummies were determined by examining current laboratory safety testing. Areas of opportunities include improved occupant restraint to reduce the dynamic readings of the children relative to their IARVs.

METHODOLOGY

This study examines the responses of child dummies and the performance of CRS in frontal NCAP tests. There are 95 cases of the frontal NCAP test performed from 2001 to 2005 with child dummies on rear seats of a vehicle as shown in Table 1 [12]. The vehicles are classified into 3 types: a passenger car, a sport utility vehicle (SUV) and a van, and a light truck. Generally there are two adult dummies on a driver and a passenger seats, and one or two child dummies on the rear seat. The adult dummy is the Hybrid III 50th percentile male dummy. Three child dummies, such as the Hybrid III 6-year-old (6YO) child dummy, Hybrid III 3-year-old (3YO) child dummy, or child restraint airbag interaction (CRABI) 12-month-old (12MO) child dummy, are used. The child dummies are seated on the rear seat with a CRS or a booster. The 12MO child dummy is restrained by a 5 points belt on a rear facing CRS (RFCRS) and the RFCRS is affixed to the vehicle by using the 3 points seatbelt system. The 3YO child dummy is restrained by a 5 points belt on a forward facing CRS (FFCRS), which is affixed to the vehicle by using the 3 points seatbelt system and the top tether or the lower anchors and tethers for children (LATCH) system.

The 6YO child dummy is restrained by the 3 points seatbelt system on a booster.

Table 1. Cases of the frontal NCAP test with child dummies on rear seats of a vehicle (performed from 2001 to 2005)

Type of Vehicle	Number of Tests	Type of Child Dummy	Number of Dummies
Passenger Car	46	6YO Child	7
		3YO Child	56
		12MO Child	13
SUV & Van	39	6YO Child	6
		3YO Child	62
		12MO Child	9
Light Truck	10	6YO Child	2
		3YO Child	17
		12MO Child	1
Total	95	6YO Child	15
		3YO Child	135
		12MO Child	23

The pass rates of HIC15, maximum chest G's and peak chest deflection of dummies in frontal NCAP tests are summarized in Table 2. Table 2 shows that the pass rates of HIC15 and chest G's of adult dummies are almost 100%, which means that drivers will be well protected in frontal vehicle crash environment. The pass rates of HIC15 and chest G's of child dummies are not as good as the adult dummies even though they need to be. The injury pass rates of child dummies are around 50 – 70% and especially the pass rate of HIC15 of 6YO child dummies is as low as 21%. In other words, a child on rear seat might be expected to suffer much more severely from impact than an adult on driver seat during frontal vehicle collisions even though a child is supposed to be as well protected as an adult. Interestingly, the chest deflection of the adult and the child dummies is passed the injury criterion in all

Table 2. Pass Rates of HIC15, chest max G's and chest peak deflection of dummies

Type of dummy	Type of vehicle	Pass rate of HIC15	Pass rate of chest G's	Pass rate of chest deflection
50th Percentile (Driver) (HIC15 < 700) (Chest G's < 60 G's) (Chest Deflection < 52mm)	Passenger Car	100.0 % (45/45)	100.0 % (45/45)	100.0 % (45)
	SUV	100.0 % (39/39)	92.3 % (36/39)	100.0 % (38)
	Light Truck	100.0 % (10/10)	90.0 % (9/10)	100.0 % (10)
	Total	100.0 % (94/94)	95.7 % (90/94)	100.0 % (93)
6YO Child (HIC15 < 700) (Chest G's < 60 G's) (Chest Deflection < 40mm)	Passenger Car	0.0 % (0/6)	42.9 % (3/7)	100.0 % (6)
	SUV	33.3 % (2/6)	50.0 % (3/6)	100.0 % (5)
	Light Truck	50.0 % (1/2)	100.0 % (2/2)	100.0 % (1)
	Total	21.4 % (3/14)	53.3 % (8/15)	100.0 % (12)
3YO Child (HIC15 < 570) (Chest G's < 55 G's) (Chest Deflection < 34mm)	Passenger Car	74.5 % (41/55)	67.3 % (37/55)	100.0 % (56)
	SUV	69.5 % (41/59)	77.0 % (47/61)	100.0 % (62)
	Light Truck	64.7 % (11/17)	76.5 % (13/17)	100.0 % (17)
	Total	71.0 % (93/131)	72.9 % (97/133)	100.0 % (135)
12MO Child (HIC15 < 390) (Chest G's < 50 G's)	Passenger Car	50.0 % (6/12)	41.7 % (5/12)	N/A
	SUV	88.9 % (8/9)	100.0 % (7/7)	
	Light Truck	0.0 % (0/1)	0.0 % (0/1)	
	Total	63.6 % (14/22)	60.0 % (12/20)	

cases.

ANALYSIS OF HEAD ACCELERATION

In Table 2, the pass rate of HIC15 of adult dummies is 100%, but the passing of 12MO and 3YO child dummies is around 65-70% and the passing of 6YO child dummy is as low as 20%. To understand this, the head response of adult dummies is compared with one of child dummies. Table 3 summarizes the cases that HIC15 of the child dummies is higher than one of adult dummies. In the 76% of the cases, child dummies experience higher head acceleration than adult dummies during the vehicle crash. The data points of HIC15 of adult dummies vs. HIC15 of child dummies are plotted in Figure 1. It shows that the data points of the 12MO child dummies are distributed around a diagonal dot-line, but most of the data points of 6YO and 3YO child dummies are spread far over the diagonal dot-line. HIC15 of all adult dummies is less than 700, but one of many child dummies, especially 3YO and 6YO child dummies, are much greater than 700. In other words, child dummies experience higher HIC15 values relative to IARVs than adult dummy during crash.

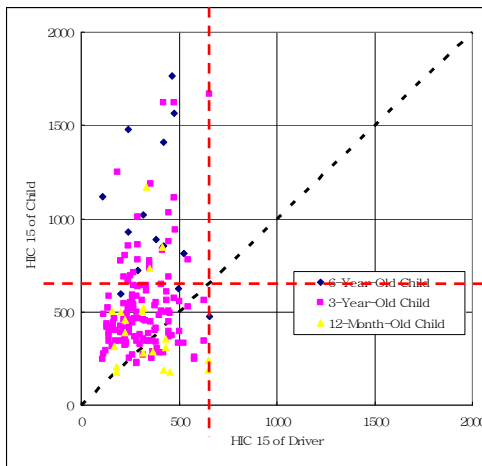


Figure 1. HIC15 of the driver vs. HIC15 of the child

Table 3. Cases of [(HIC15 of the child) > (HIC15 of the driver)]

Type of child dummy		Cases of [(HIC15 of child) > (HIC15 of driver)]		
6YO Child	Forward Facing	93% (13/14)	85% (131/145)	76% (123/165)
3YO Child		82% (108/131)		
12MO Child	Rear Facing	60% (12/20)		



(a) Adult dummy (Test 5130)



(b) 6YO child dummy (Test 5130)



(c) 3YO child dummy (Test 5130)



(d) 12MO child dummy (Test 4242)

Figure 2. Snapshots of the dummies' behavior

Figure 2 shows snapshots of the dummies' behavior during impact. After the vehicle impacts the barrier, the forward facing occupant starts moving forward. Since the torso of the occupant is restrained by the seatbelt, the head of the occupant starts rotating and then X- and Z- head accelerations occur as shown in Figure 3. In the case of the occupants in front seats, the rotational head motion is restrained by an airbag, like in Figure 2(a). Thus the airbag contributes to reduce the head acceleration of front occupants and leads the high pass rate of HIC15 in Table 2. However, in the rear seat, the occupant's head is not restrained. Therefore the heads of the forward facing 6YO and 3YO child dummies are fully rotated around the axis of the shoulder like Figure 2(b) and 2(c). Figure 3(a) shows that X- accelerations are not much different among all dummies, but Z- accelerations of the 6YO and 3YO child dummies are much higher than one of the adult dummy. The head of 12MO child, who is restrained with the RFCRS like Figure 2(d), does not rotate since the head is

supported by RFCRS. However, the RFCRS itself is rotating and produces considerable head accelerations as shown in Figure 3(b).

The head resultant accelerations of 6YO and the 3YO dummies in some tests are shown in Figure 4. It can be seen that there are two peaks in the head resultant acceleration. The 1st peak is due to the forward movement of the head like Figure 5(a) and the 2nd peak is due to the rear seat contact with the back of the head like Figure 5(b). In some cases, the 2nd peaks of the head acceleration are considerable high, or even higher than the 1st one of 3YO child dummies in Figure 4(b). In Table 4, the cases that the 2nd peak of head acceleration is higher than its 1st one are 28% in 3YO child dummies and 20% in 6YO child dummies. Also, the cases that HIC15 around the 2nd peak of head acceleration is higher than 570 G's, which is the head injury criteria of 3YO child, are 5%. It seems that the 2nd peak of head acceleration of 3YO child dummies is considerable.

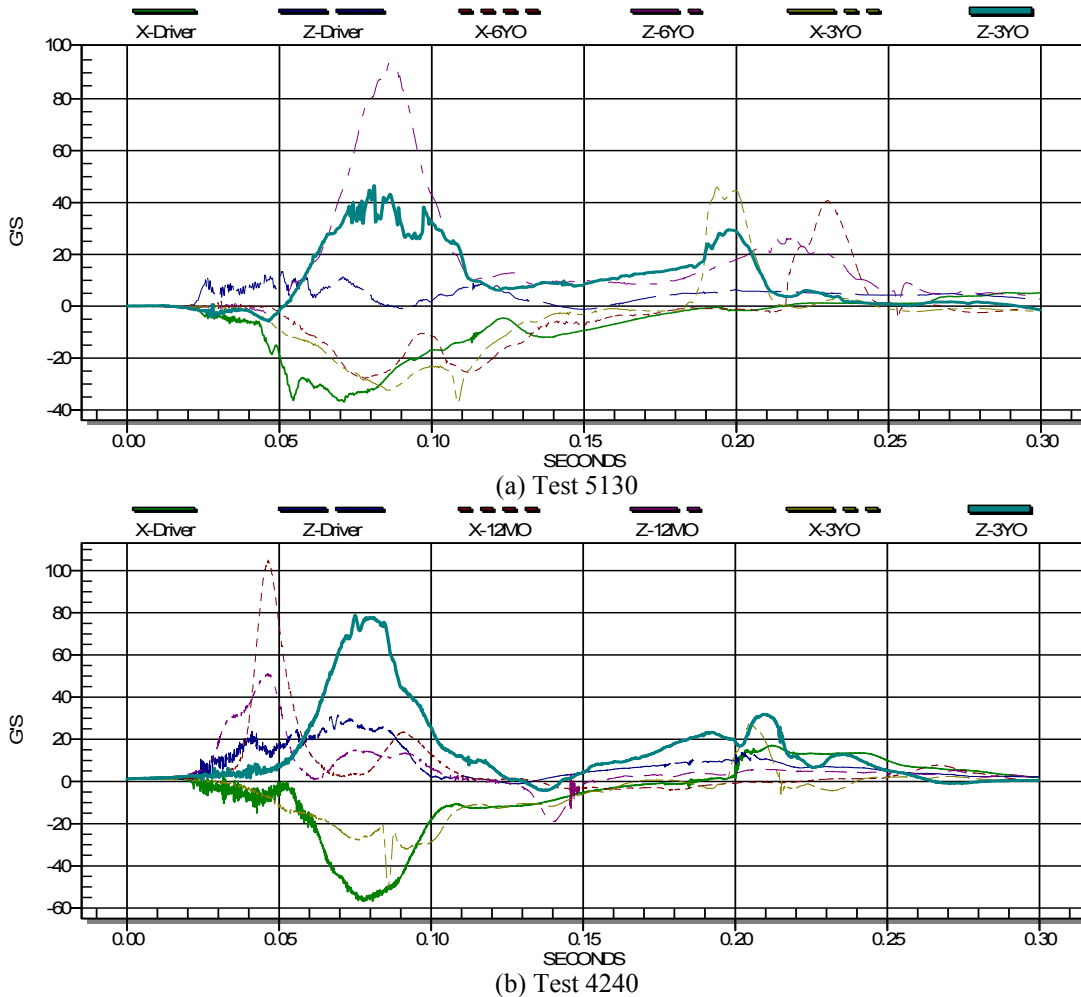
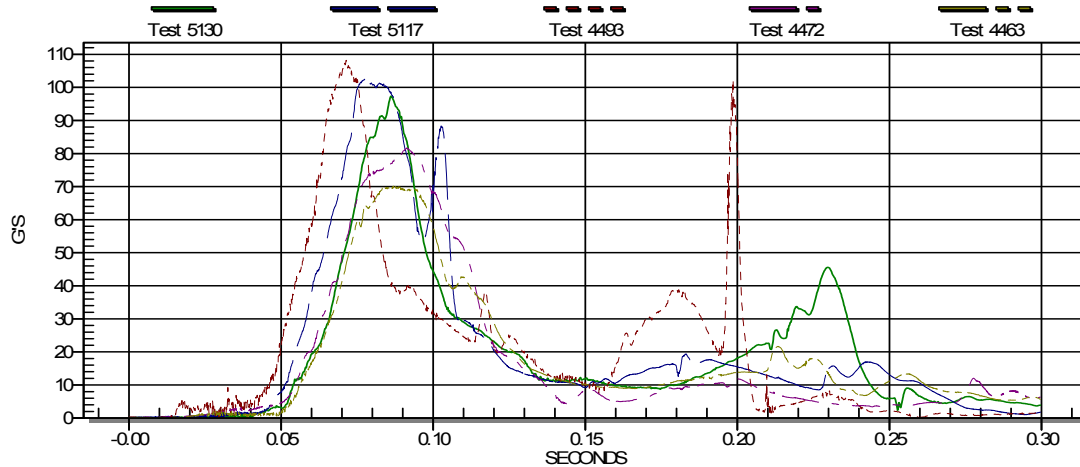
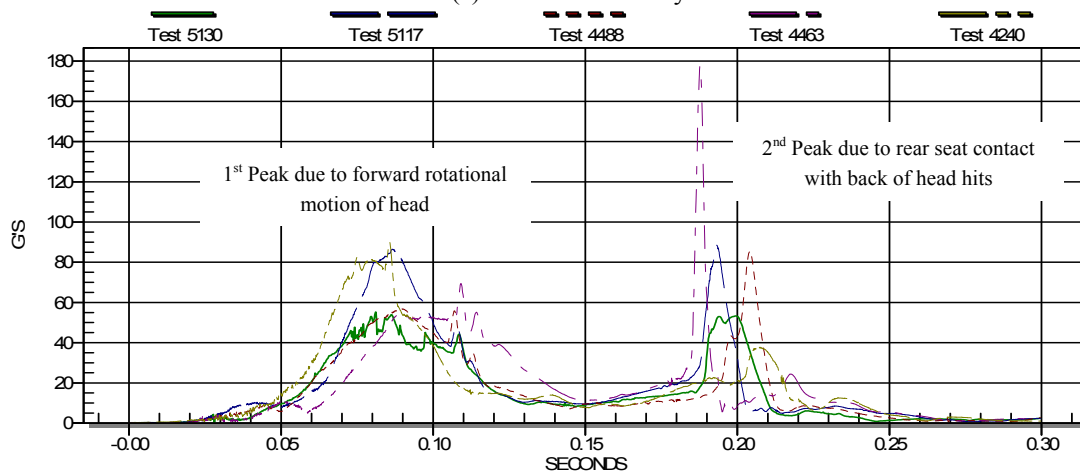


Figure 3. X- and Z- head accelerations of adult, 6YO child and 3YO child dummies



(a) 6YO child dummy



(b) 3YO child dummy

Figure 4. Resultant head acceleration curves

Table 4. Relationship between 1st Peak and 2nd Peak of Head Resultant Acceleration

		Cases of [2nd Peak > 1st Peak]	Cases of [HIC15 at 2nd Peak > 570 G's]
3YO Child	Passenger Car	19.6 % (9/46)	6.5 % (3/46)
	SUV	35.2 % (19/54)	5.6 % (3/54)
	Light Truck	28.6 % (4/14)	0.0 % (0/14)
	Total	28.1 % (32/114)	5.3 % (6/114)
6YO Child	Total	20.0 % (1/5)	0.0 % (0/5)



(a) at 1st peak time of head acceleration



(b) at 2nd peak time of head acceleration

Figure 5. Behavior of 3YO child dummy (Test 4901)

ANALYSIS OF HEAD VELOCITY

The velocity histories of dummies are helpful to understand the initial behavior of occupants and the interaction between the vehicle and the occupant during crash. The velocity curves are obtained by integrating the acceleration curves and only X-velocity (longitudinal) is utilized here. Figure 6 shows the typical X-velocity curves of a vehicle and dummy head in frontal NCAP test. In general, the vehicle velocity starts to decrease right after vehicle impact barrier, but the deceleration of occupant velocity is not occurred until time t_1 , which is the required time for the restraint system to fully work on occupants because of initial space between restraint and occupant. Figure 7, which is cited from reference [13], gives the good physical interpretation of the velocity profiles in frontal crash of vehicle. In Figure 7(a), the area under the vehicle velocity curve represents the crush of the vehicle. The area between the vehicle velocity curve and the occupant velocity curve, up to time t_1 , represents the initial restraint to occupant spacing (e.g., the spacing from occupant to an airbag or the longitudinal slack in a lap and shoulder belt). The area between the vehicle velocity curve and the occupant velocity curve, after time t_1 , represents the stroking of the restraint system. A lot of time (up to t_1) is wasted in bringing the occupant to rest. The area not wasted is the stroke of the restraint system and the vehicle crush after the restraint picks up the occupant in Figure 7(b). The area labeled “vehicle crush after the restraint picks up the occupant” in Figure 7(b) is commonly referred to as *ridedown*, which is the important part to reduce the stroke of the restraint system.

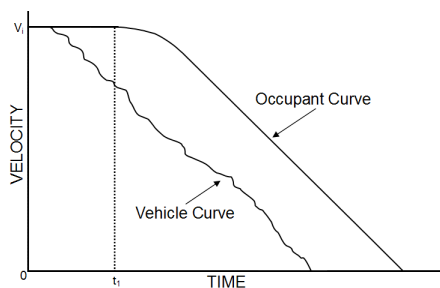


Figure 6. Typical head X-velocity curve

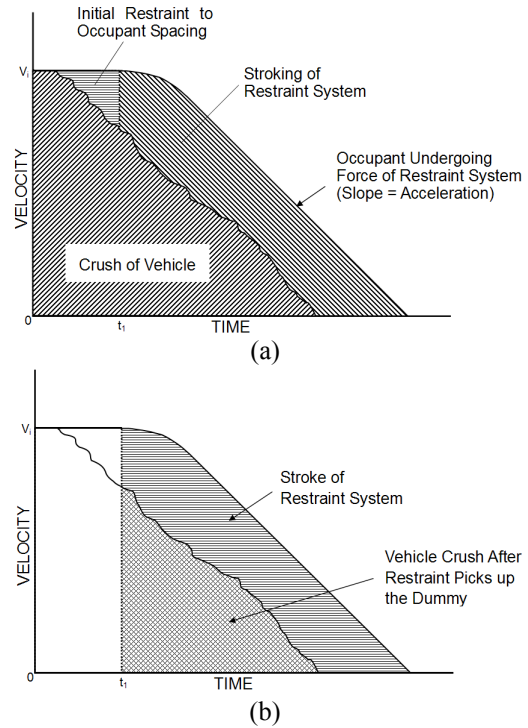


Figure 7. Interpretation of head X-velocity curve [13]

Figure 8 shows the X-velocity curves of some cases. It can be seen that the time t_2 , the initial restraint space of the 6YO and the 3YO child dummies in rear seat, is much longer than the time t_1 , the initial restraint space of the adult dummy in driver seat. This means that even though the child dummies are well seated and secured by CRS or booster with seatbelt, there is still a lot of initial space and slack between occupant and restraint system and between CRS or booster and rear seat. Therefore the child is supposed to have a small *ridedown*, which is unfavorable for the child.

Fundamentally, the *ridedown* contributes for occupants to reduce the stroke of the restraint system, which is the impact force on the head and chest. The *ridedown* is also related with the vehicle crush. Figure 9 shows the relationship between chest and head of dummy and vehicle. Statistical linear regression curves shows that the maximum chest acceleration and the maximum upper neck force of the 3YO and 6YO child dummies decrease respectively when the vehicle crush increases.

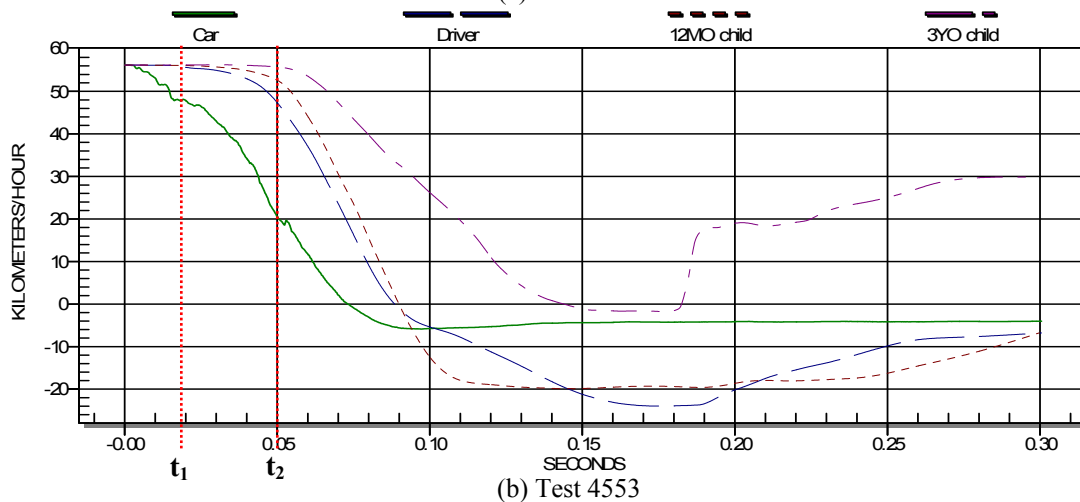
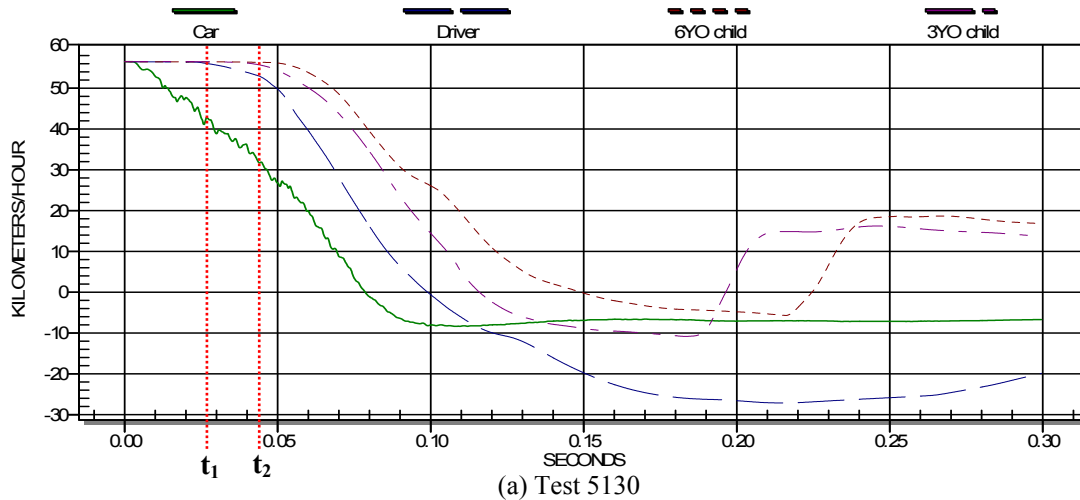


Figure 8. X-velocity curves

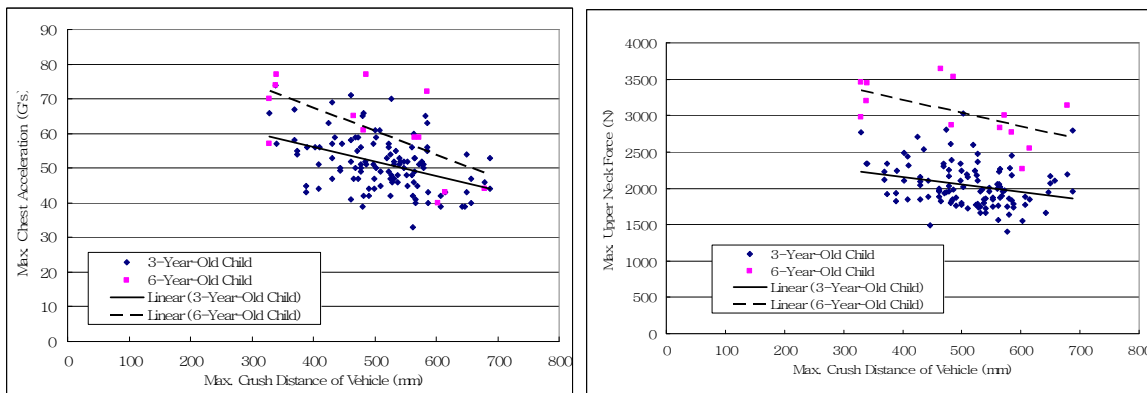


Figure 9. Vehicle crush vs. max. chest acceleration and max. upper neck force

ANALYSIS OF UPPER NECK FORCE

In general, the upper neck force (tension) is linked with the head acceleration. The data points of the upper neck force vs. the head acceleration are plotted in Figure 10. It shows that the upper neck force is

proportional to HIC15. In addition, it can be seen that the upper neck force and HIC15 of the 3YO and 6YO child dummies is much higher than the responses of adult dummies.

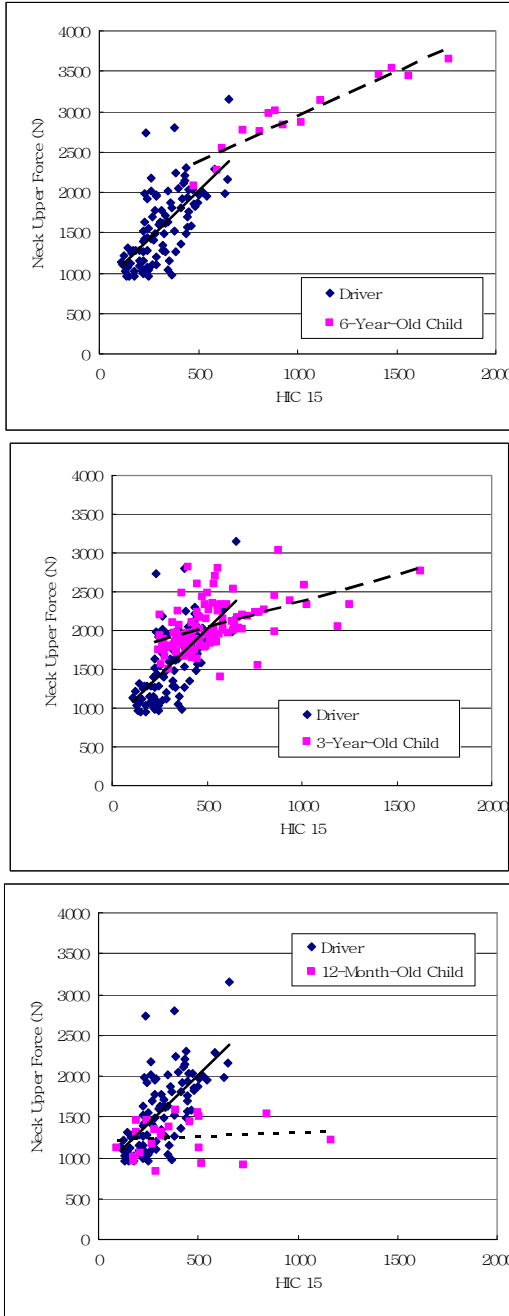


Figure 10. Data distribution plots of Neck Upper Force vs. HIC15

As mentioned in the previous section, the rotational motion of the dummy head during impact produces the Z-acceleration (a_z), the centripetal acceleration. According to Newton's law, multiplying the Z-acceleration by the mass of dummy head should equal to the Z-upper neck force (F_{neck}) if there is no external force ($F_{external}$), in other words,

$$F_{external} = ma_z - F_{neck} , \quad (1)$$

and $F_{external}$ is zero. Figure 11 shows the data points of maximum Z-upper neck force vs. maximum Z-head acceleration. The diagonal line indicates the $F_{neck} = ma_z$ line, where the masses of dummy head (m) are 3.47 kg in 6YO child dummy and 2.73 kg in 3YO child dummy [14]. The data points of 6YO child dummy in Figure 11(a) are distributed close to the diagonal line, which means that the external is zero, in other words, Eq (1) is zero. However, the data points of 3YO child dummy in Figure 11(b) are quite scattered over the diagonal line, which means any external force exists on dummy head during crash, in other words, Eq. (1) is not zero. Figure 12 is the snapshots of the behavior of the 3YO child dummy in test 3554. The child is restrained by FFCRS. Basically FFCRS has a chest clip, which is a stiff material and located on the middle of the dummy chest shown in Figure 12(a). Figure 12(b) shows that the chin of the child dummy hits the chest clip during crash. Thus $F_{external}$ is the force caused by that the chin of 3YO child dummy hits the chest clip or chest. Also, the reference [11] looks into the external force by dummy chin contact with chest clip. Probably, this external force produces a high reverse X-velocity of the head of 3YO child dummy and induces the high 2nd peak of head acceleration of 3YO child dummy in Figure 4(b). On the other hand, the 6YO child is restrained by 3-points rear seat belt on the booster. During crash, the head of 6YO child dummy is fully rotating without any external force as shown in Figure 2(b). This head motion of 6YO child dummy produces high acceleration and upper neck force and makes pass rate of HIC15 as low as 21.4% in Table 2.

According to references [11] and [15], real world crash analysis suggests that neck trauma corresponds to only a small fraction of the injuries found in children in passenger vehicles crashes. In Figure 10, however, the upper neck tensions exceed the injury criteria (6YO:1890N, 3YO:1430N, 12MO:780N [11]) in most of the cases, which suggests that there is a possibility that the neck force of child dummies is over-predicting neck injury and that further study is needed.

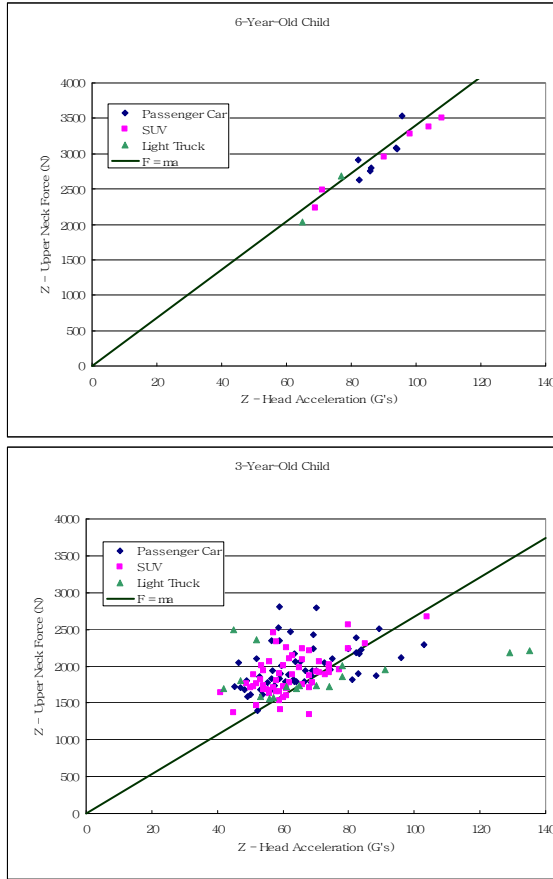


Figure 11. Max Z-upper neck force(F_{Neck}) vs. Max Z-head acceleration



(a) before impact



(b) moment that chin hits chest clip

Figure 12. Behavior of 3YO child dummy (Test 3554)

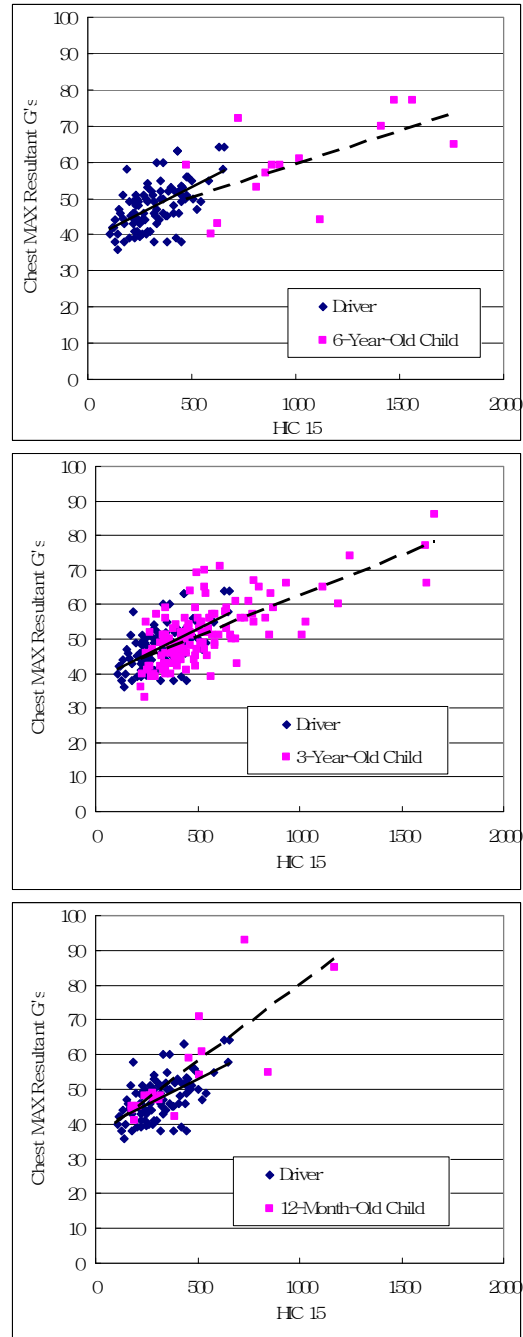


Figure 13. Maximum chest resultant G's vs. HIC15

ANALYSIS OF CHEST ACCELERATION AND DEFLECTION

In Table 2, the pass rate of chest G's of the child dummies is about 60%, while the pass rate of the adult dummies is 96%. The data distribution of the maximum chest resultant G's vs. HIC15 is plotted in Figure 13. It shows that the maximum chest G's is proportional to HIC15. In addition, Figure 9 shows

that the maximum chest acceleration is inversely proportional to the vehicle crush. The pass rate of the chest deflection is 100% for all dummies in Table 2. The data distribution of the maximum chest deflection vs. HIC15 is plotted in Figure 14. It shows that, in the cases of the 3YO child dummy, the chest deflection is much lower than the driver in spite of the fact that the chest acceleration is similar with the driver in Figure 13. It is because the 3YO child dummy is restrained by the 5-point CRS, which has two harnesses on the child chest like Figure 12(a). These two harnesses make the force be dispersed around the chest.

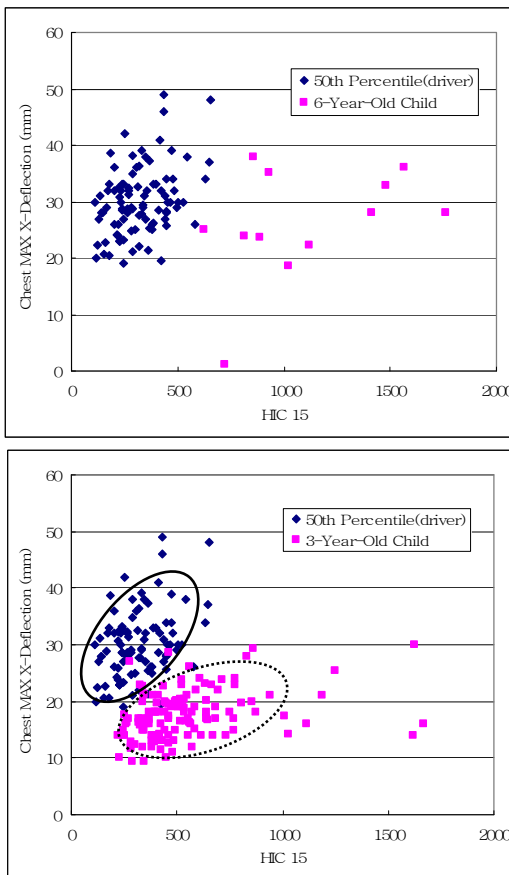


Figure 14. Maximum chest X-deflection vs. HIC15

CONCLUSIONS

The objective of this study is to examine the responses of child dummies and the performance of CRS in the frontal NCAP tests. The responses of head, upper neck and chest of adult and child dummies in 95 NCAP tests are analyzed.

Head Acceleration

- Pass rate of HIC15: Driver - 100%, 6YO child - 21.4%, 3YO child - 71%, and 12MO child - 63.6%
- Child dummies experience higher HIC15 values relative to IARVs than adult dummy during crash
- HIC15 around the 2nd peak of the head acceleration of the 3YO child is considerable.

Head Velocity

- The head X-velocity is helpful for understanding the initial occupant behavior and the relationship between the vehicle and the occupants during impact.
- The much space between the restraint systems and the child makes the “ridedown” area small, which is unfavorable for the child.

Upper Neck Force

- The upper neck tension forces of the child dummies are exceed the criteria in the most of the cases.
- As HIC15 increases, the upper neck force increases.

Chest Acceleration and Deflection

- Pass rate of chest maximum acceleration : Driver - 95.7%, 6YO child - 53.3%, 3YO child - 72.9%, and 12MO child - 60%
- Pass rate of chest maximum deflection : all occupants - 100%

This study suggests that the performance of the CRS could better protect the child in the rear seat during frontal crash. Based on the study, a couple of countermeasures can be recommended. Firstly, a forward facing child experiences severe head acceleration and neck force because of rotational head motion. Thus, during frontal crash, child head needs to be restrained by some means like airbags in front seats. Secondly, child on CRS or booster in rear seat has a lot of initial slack and gap between child and CRS and between CRS or booster and rear seat, which make ridedown small. The ideal countermeasure is to make the crash performance of vehicles improved. In practice, some devices are needed to reduce the initial slack, for example, a pretensioner or an air-belt in the rear-seat area.

REFERENCES

- [1] Tylko, S. and Dalmotas, D., Protection of rear seat occupants in frontal crashes, *Proceedings of the 19th Conference on the Enhanced Safety of*

- Vehicles (ESV)*, Washington DC, Paper No. 05-0258, June 2005.
- [2] Saunders, J., NHTSA's research program for adult rear occupants in frontal crashes, *SAE Industry/Government Meeting*, Washington DC, May 2006.
- [3] Mizuno, K., Ikari, T., Tomita, K., and Matsui, Y., Effectiveness of seatbelt for rear seat occupants in frontal crashes, *Proceedings of the 20th Conference on the Enhanced Safety of Vehicles (ESV)*, Lyon France, Paper No. 07-0224, June 2007.
- [4] Kent, R., Forman, J., Parent, D.P. and Kuppa, S., Rear seat occupant protection in frontal crashes and its feasibility, *Proceedings of the 20th Conference on the Enhanced Safety of Vehicles (ESV)*, Lyon France, Paper No. 07-0386, June 2007.
- [5] Smith, K. and Cummings, P., Passenger seating position and the risk of passenger death in traffic crashes: a matched cohort study, *Injury Prevention*, 2006;**12**(2):83, 2006.
- [6] Kuppa, S., Frontal crash protection for rear seat occupants, *SAE Industry/Government Meeting*, Washington, DC, May 2006.
- [7] Sahraei, E., Soudbakhsh, D., and Digges, D., Protection of rear seat occupants in frontal crashes, controlling for occupant and crash characteristics, *Stapp Car Crash Journal*, 2009;**53**:75-91.
- [8] Starnes, M., Child passenger fatalities and injuries, based on restraint use, vehicle type, seat position, and number of vehicles in the crash, *NHTSA Technical Report No. DOT HS 809 784*, U.S. Department of Transportation, July 2005.
- [9] Hong, S-W., Park, C-K., Morgan, R.M., Kan, C-D, Park, S., and Bae, H., A study of the rear seat occupant safety using a 10-year-old child dummy in the new car assessment program, *SAE International Journal of Passenger Cars- Mechanical Systems*, 2009;**1**(1):371-382.
- [10] Hong, S-W., Park, C-K., Morgan, R.M., Kan, C-D, Park, S., and Bae, H., Using consumer information testing to improve rear seat occupant protection, *SAE Industry/Government Meeting*, Washington DC, May 2008.
- [11] Maltese, M.R. and Eppinger, R.H., Development of improved injury criteria for the assessment of child restraint systems, *NHTSA Docket # 2002-11707-18*, April 2002.
- [12] *NHTSA* vehicle crash test database, <http://www-nrd.nhtsa.dot.gov/database/asp/vehdb/querytesttable.aspx>.
- [13] Strother, C.E. and Morgan, R.M., A fundamental look at side impact, *Proceedings of the American Association for Automotive Medicine (AAAM) 23th Annual Scientific Conference*, Louisville KY, October 1979.
- [14] Humanetics Innovative Solutions, <http://www.dentonatd.com/dentonatd/anthropomorphic.html>.
- [15] Morgan, R.M., Sled and vehicle crash testing with child restraints in the USA, *CRASH-TECH 2003 Conference*, Nuremberg, Germany, May 2003.

EVALUATION OF AN IMPROVED PERFORMANCE ANTI-SUBMARINING SEAT BELT SYSTEM

Tom Gibson

Amy Clarke

Human Impact Engineering

Australia

Lui Pisaniello

Marcel Stephan

Lino Fusco

Lifebelt

Australia

Robert Judd

Autoliv

Australia

Paper Number 11-0246

ABSTRACT

The objective of the present study is to evaluate a development of the conventional seat belt, offering improved control of anti-submarining and chest loads especially for smaller occupants.

The seat belt continues to be the prime safety system fitted to automobiles. Crash injury data indicates that performance improvements continue to be required, particularly in the rear seat and with smaller occupants in the areas of anti-submarining, adaptation to smaller occupants (such as children making the transition from using child restraints) and chest loads. World interest in simple low cost, lightweight vehicles for use in developing countries is emphasising this need.

The new belt system, the Lifebelt, retains similar belt geometry to current seat belt systems but with an extension of the seat belt webbing in a continuous loop around the upper thighs. It makes use of many available belt system components, and has the potential to allow a simple lightweight seat belt system with acceptable performance, without some of the complex add on systems now being used.

The evaluation began with static fit trials and then used dynamic sled testing under frontal crash test conditions similar to regulatory crash tests (50 km/h and 30g pulse). A number of sled tests (n=20) were carried out in front and rear seat configurations and with different seat structures reflecting current production as well as simplified seating. The new system was compared to conventional belt systems in typical seats and belt geometries. HIII 50M and HIII 5F dummies were used to assess the effect of occupant size, with the small female having the greater tendency to submarine. Anti-submarining effectiveness was assessed from video and with belt motion monitored by iliac spine force transducers, as used for Japan NCAP testing.

The enhanced system retains similar belt geometry and occupant use to current belt systems, with some changes to the seat structure for installation. The new belt with the extra continuous lap loop was shown to give a high level of anti-submarining performance while at the same time retaining good occupant kinetics and keeping the chest loads within acceptable limits. The system is able to reduce the need for add on components (such as the in seat anti-submarining ramp and pretensioners), which are required to give current, conventional seat belts acceptable performance.

INTRODUCTION

Currently, issues regarding the safety of smaller occupants in rear seats, and the effect of seatbelts during rollovers and side impacts are areas of vehicle safety research interest worldwide. Of specific recent concern has been the incidence of 'submarining' injuries to smaller seat occupants in frontal crashes, Tylko and Dalmotus (2005) and Kuppa et al. (2005).

In 2005, Kuppa et al reported that in the US 90% of rear seat occupants were seated in the second row of vehicles, with 78% seated in outboard seats. Of these occupants, 64% were restrained occupants in frontal crashes, 78% of which weighed less than 160lbs (72.5kgs), and 64% of which were 12 years of age or younger.

In 2008 an investigation of the US data found that although rear seat occupants accounted for 14% of all vehicle occupants, they accounted for 23% of occupants with injuries and 9% of fatalities, Bilston (2010).

Numerous studies have investigated the location and source of the rear seated occupant injuries, with an overwhelming consensus of a high prevalence of injury to the chest and abdomen due

to interaction with the seatbelt, Kuppa et al (2005), Tylko et al (2005), Zellmer et al (1998).

Cuerden et al (2007) established the lap belt as the cause of 85% of MAIS 1 abdominal injuries and 60% of MAIS 2+ abdominal injuries.

In the study performed by Tylko et al (2005) with HIII 5F and HIII 10YO dummies restrained with the shoulder/lap belt in the rear seat, all experienced abdominal penetration by the lap belt, or very high chest responses. Submarining was seen in all tests bar one exception.

These studies highlight the poor protection afforded to rear seat occupants by current rear seat restraints, particularly in comparison to the ever improving front seat restraint systems, Bilston et al (2010).

Following the work of Mizuno et al (2007), JNCAP from FY2009 assesses the safety of rear seat occupants JNCAP (2009). A group of measures including crash testing, usability evaluation, and seatbelt reminders have been introduced to drive improvements in the safety performance of rear seatbelt systems and to encourage users to wear the seatbelt. During the offset frontal crash test, a HIII 5F dummy is seated in the rear outboard seating position. The HIII 5F is used to assess rear seat occupant chest loads, and any lap belt penetration into the abdominal cavity (submarining) by means of load cells at the iliac crest.

The Lifebelt is a development of the existing conventional seat belt design. It is based on the lap sash seatbelt, with the lap portion of the belt forming a 'loop' around the thighs. See Figure 1. This loop around the upper thighs improves the capability of the seat belt restraint system by minimising the likelihood of 'submarining' in frontal crashes. The enhanced system is a simple and effective system for the safe restraint of occupants in front and rear seats without the need for complex seat structures with anti-submarining pans.

Lifebelt Iteration 1

The development version of the Lifebelt system, Iteration 1, was used in the following tests, comparisons and analyses. The Iteration 1 seatbelt system is shown in Figure 1. It consists of a vertical outboard emergency locking retractor (ELR) with upper D ring (#1), through which the sash belt passes to latch into the inboard buckle (#3) on a flexible stalk angled at 45° in a standard orientation. The slipping tongue (#2) forms the end of the upper lap belt which crosses the lap and

passes through a D ring (#4) on the outboard side. The belt continues along the femur on the outboard side of the seat to a D ring (#5) located approximately upper thigh. The lower lap portion runs under the upper thigh to an anchorage (#6) aligned with the D ring, on the inboard side of the seat base. The layout can be seen in Figure 2.



Figure 1. The Lifebelt system (Iteration 1) installed in a vehicle front seat.



Figure 2. Lifebelt Iteration 1 seatbelt system.

TEST SERIES

A total of 20 tests have been performed to date as a part of the proof of concept testing for Lifebelt. The testing was developmental and so includes some tests where component failures occurred. For the purposes of this report, 10 tests have been selected for inclusion. The 10 tests are grouped into four test series for clarity as follows:

- Rear Seat Control Tests,
- Lifebelt 5th % Female Tests,
- Front Seat Control Tests and
- Lifebelt 50th % Male Tests.

The test parameters for the four test series are summarised in Table 1.

Table 1.
Summary of the test parameters

Test (Number)	Seatbelt	Dummy (HIII)	Seat	Sash Load Limiter	Iliac Crest Load Cells	Knee Impact Cushion	Test Facility	Test Date
Series 1 Honda Rear Seat Control Tests								
Control 1 (S090258)	Autoliv	5F	Honda Rear	No	No	No	Crashlab	06/09
Control 2 (D1-4260)	Autoliv	5F	Foam Seat	No	No	Yes	Autoliv	05/10
Series 2 Lifebelt HIII 5th % Female Tests								
Lifebelt 1 (D1-4189)	Lifebelt Iteration 1	5F	Standard Honda	No	No	Yes	Autoliv	02/10
Lifebelt 2 (D1-4258)	Lifebelt Iteration 1	5F	Honda Foam Seat	No	No	Yes	Autoliv	05/10
Lifebelt 3 (D1-4309)	Lifebelt Iteration 1	5F	Honda Foam Seat	Yes	No	Yes	Autoliv	07/10
Lifebelt 4 (D1-4411)	Lifebelt Iteration 1	5F	Honda Foam Seat	Yes	Yes	Yes	Autoliv	10/10
Series 3 Ford Front Seat Control Tests								
Control 3 (D1-4306)	Autoliv	50M	Ford Front	No	No	Yes	Autoliv	07/10
Series 4 Lifebelt HIII 50th % Male Tests								
Lifebelt 5 (D1-4259)	Lifebelt Iteration 1	50M	Honda Foam Seat	No	No	Yes	Autoliv	05/10
Lifebelt 6 (D1-4307)	Lifebelt Iteration 1	50M	Honda Foam Seat	Yes	No	Yes	Autoliv	07/10

The sled testing was performed at two established test laboratories, Crashlab in Sydney, Australia and Autoliv in Melbourne, Australia.

Tests at Crashlab were performed according to the ADR4/03 'Seatbelts' frontal impact test pulse. The peak test acceleration was 27.5 g at 39.2 msec and the velocity change was 43.7 km/h. Tests at Autoliv were performed according to the ECE R16 'Safety Belts and Restraint Systems' frontal impact test pulse. The peak test acceleration was 28 g at 42 msec with a nominal 48 km/h velocity change. These are both severe dynamic test pulses used to certify the strength of seat belt systems fitted to current vehicles.

Anthropometric Test Devices

Hybrid III 5F and Hybrid III 50M anthropomorphic test devices (ATD) are used to represent the restrained occupants in the vehicle seat during the test series. These dummies are specified under the US regulations (the Federal Motor Vehicle Safety Standard FMVSS 208):

- Title 49 CFR Part 572 Subpart O – Hybrid III 5th percentile female test dummy (HIII 5F) and
- Title 49 CFR Part 572 Subpart E – Hybrid III 50th percentile male test dummy, (HIII 50M).

These parts describe the anthropomorphic test devices that are to be used for motor vehicle safety standard compliance testing of motor vehicles and motor vehicle equipment. During this project the dummy positioning was based on Subpart O/E of Part 572. The dummies were instrumented to acquire biomechanical injury data for the head, neck, thorax, pelvis and femur.

Test Seats and Seat Belts

Rear Seat Control Tests A Honda seat was chosen for control testing, as a split folding rear seat typical of those in vehicles currently on the market. The seat is secured to the vehicle at the base of the seatback, allowing for numerous folding adjustments necessary in small multi-purpose vehicles. The Honda seat has a standard 3 point lap sash ELR seatbelt. The seat base consists of a simple flat plywood base with padding. It does not incorporate any form of anti-submarining profile in the seat base.

The seat was mounted to the test sled using the original mounting brackets from the vehicle. The geometry of the seat as tested was as measured in the vehicle. The Honda belt geometry was replicated for the control tests. Standard 'off the shelf' Autoliv belts with vertical ELRs were used in all the control tests.

Front Seat Control Tests A current model Ford front seat was chosen as a production front seat typical of the range in vehicles currently on the market. It incorporates an anti submarining pan and the inboard seatbelt mount positioned on the seat frame.

Lifebelt Tests The Lifebelt Iteration 1 test seat belt components, including the ELR, webbing, D rings, buckle and stalk and anchors were standard 'off the shelf' Autoliv parts. The Lifebelt Iteration 1 tests, presented here, had the lower lap belt mounted to the sled as shown in Figure 3.

The Iteration 1 version of the Lifebelt, discussed here, is the first of the planned developments of the Lifebelt concept.



Figure 3. In board sled mounted anchorages for the Lifebelt Iteration 1 as used in the tests.

TEST RESULTS

Test Series 1 – Rear Seat Control Tests

Test Series 1 consisted of two tests using a HIII 5F dummy restrained in a standard Honda rear seat with the standard seat belt geometry by an Autoliv "off the shelf" seatbelt, Table 1. The Control Test 1 (S090258 – at Crashlab) was performed with the standard rear seat and seatbelt geometry. Control Test 2 (D1-4260 – at Autoliv) used a simple foam seat base, see Figure 4, and made use of an improved seatbelt geometry reflecting developments with the Lifebelt.

Inspection of the vehicle seat following these tests revealed no signs of deformation of the seat or seat anchorages. The seat base remained intact. There were no failures of the seatbelt components. The dummy was effectively restrained in the vehicle seat by the seatbelt in both tests. Seatbelt components were replaced between tests.

The peak response values for the HIII 5F dummies during the tests are included in Appendix A, along with the Injury Assessment Reference Values IARVs for the Hybrid III 5F dummy for comparison, Mertz (1984). An IARV is an industry accepted dummy response value where the risk of

significant injury (or AIS 3) to a vehicle occupant would be unlikely, less than 5% risk.

Control Test 1 resulted in the dummy submarining. This was shown by the lap belt riding above the right and left ASIS (or anterior superior iliac spine) and penetrating into the dummy's abdomen, see Figure 4. Control Test 1 showed high chest compression and neck flexion moments with respect to the IARVs plus submarining.



Figure 4. (left) Position of the lap belt in the dummy's abdomen (arrowed) following Control Test 1. (right) Position of the lap belt above the left ASIS (arrowed) following Control Test 2. Note the soft seat base (right) used in Control Test 2.

Control Test 2 also resulted in the dummy submarining, with the lap belt riding above the left ASIS and penetrating into the dummy's abdomen, see Figure 4. Control Test 2 again showed high chest compression and neck flexion moments with respect to the IARVs.

Note: Control Test 1 was run with no knee impact bolster and a slightly different sled pulse (Crashlab sled) to Control Test 2 (Autoliv sled).

Test Series 2 – Lifebelt HIII 5F Tests

Test Series 2 consisted of four tests with a HIII 5F dummy restrained by the Lifebelt Iteration 1 seatbelt configuration in a rear seat, Table 1. The first Lifebelt Test 1 (D1-4189) was performed with the standard Honda Rear seat. The remaining three tests (D1-4258, D1-4309 and D1-4411) used a simple foam seat base, similar to Control Test 2 (D1-4260).

An inspection of the seat post the Lifebelt tests revealed no signs of deformation of the seat or seat anchorages. The seat base and seat back remained in place. There were no signs of failure of the seatbelt or seatbelt components and the dummy and belt remained in place post crash. The dummy was effectively restrained in the vehicle seat by the Lifebelt seatbelt in all four tests. Seatbelt components were replaced after every test.

Appendix B compares the peak response values for the HIII 5F dummy tests with the IARVs for the Hybrid III 5F dummy.

Lifebelt Test 1 performed well in restraining the dummy in the seat, however the upper lap belt moved upwards to rest above the ASIS, see Figure 5. Although there was upward motion of the belt, there was no intrusion or penetration of the belt into the abdomen of the dummy (submarining). The areas of concern in terms of dummy loading during the tests included chest compression levels and upper neck forces.



Figure 5. Post Lifebelt Test 1. Note the final position of the upper lap belt was on the ASIS, but not penetrating into the abdomen.

The Lifebelt performed very well in Lifebelt Test 2, with no signs of submarining or dummy instability, see Figure 6. The areas of concern in terms of HIII 5F dummy loading during Lifebelt Test 2 were high chest compression and upper neck forces.

Lifebelt Test 3 was a repeat of Test 2 but with the addition of a sash belt load limiter, which reduced the peak sash belt load from 9.22kN to 5.21kN. The lifebelt performed very well in Lifebelt Test 3 with the lap belt positioned below the ASIS post test, see Figure 6. In Test 3, chest compression and acceleration levels were reduced, however the neck forces remained an area of concern in terms of dummy loading with respect to the IARVs.

Lifebelt Test 4 was a repeat of the Lifebelt Test 3 conditions with load limiter, but Denton ASIS load cells were included in the dummy instrumentation. The ASIS load cells were fitted to demonstrate quantitatively the anti submarine performance of the Lifebelt seatbelt and back up the post test visual inspection used for the earlier tests.

In Lifebelt Test 4, the HIII 5F dummy was stable with good dynamic and kinematic responses, showing no signs of submarining either visually



Figure 6. (left) HIII 5F post Lifebelt Test 2 (D1-4258). (right) HIII 5F post Lifebelt Test 3 (D1-4309).

post test or in the instrumentation responses and had lower chest compression. The loading to the ASIS load cells showed no signs that submarining or unstable belt positioning occurred.

Test Series 3 – Front Seat Control Test

Test Series 3 consisted of a single test (D1-4306) performed with a HIII 50M dummy restrained in a standard Ford front seat.

Inspection of the vehicle seat after the control test revealed no signs of deformation of the seat or seat anchorages. The seat base and seat back remained in place. There were no signs of failure of the seatbelt or seatbelt components on visual inspection with the dummy and belt in place post crash.

The dummy was effectively restrained in the vehicle seat by the seatbelt. There were no signs of instability and submarining did not occur during the test. Note that the seat had an inbuilt anti-submarining ramp and good belt geometry.

Appendix A shows the peak response values for the HIII 50M dummy during the test with the IARVs for the 50th percentile male for comparison. The HIC response and chest compression of the dummy were high in the test when compared with the IARVs.

Test Series 4 – Lifebelt HIII 50M Tests

Two Lifebelt tests (D1-4259 and D1-4307) formed Test Series 4 each with a Hybrid III 50M dummy restrained by the Lifebelt Iteration 1 seatbelt configuration with soft seat base.

Inspection of the vehicle seat after the HIII 50M Lifebelt tests revealed no signs of deformation of the seat or seat anchorages. The seat base and seat back remained in place. There were no signs of failure of the seatbelt or seatbelt components on quick visual inspection with the dummy and belt in

place post crash. The dummy was effectively restrained in the vehicle seat by the seatbelt.

Appendix C shows the peak response values for the dummy during the test with the IARVs for the 50th percentile male for comparison.

The Lifebelt Iteration 1 performed very well in Test 5, effectively restraining the 50th percentile male dummy with no signs of submarining or instability of the dummy, see Figure 7. The level of chest compression was an area of concern in terms of dummy loading with respect to the IARVs.



Figure 7. (left) HIII 50M Post Lifebelt Test 5. (right) HIII 50M post Lifebelt Test 6.

A chest load limiter was introduced into the sash portion of Lifebelt system for Test 6. The Lifebelt performed well in the Lifebelt 6 test, again effectively restraining the HIII 50M dummy with no signs of submarining or instability of the dummy, see Figure 7. The load limiter reduced the chest loading and compression, Appendix C, however these remained slightly above the IARV limit.

DISCUSSION

Anti-Submarining Performance of the Lifebelt

The anti-submarining performance of the Lifebelt is best assessed using the HIII 5F dummy as this smaller dummy is more susceptible to submarining than the larger 50M dummy. The HIII 5F has been used for this purpose as a rear seat occupant in Japan NCAP frontal offset testing since 2009, NASVA (2010).

Submarining, determined by inspection of the post test photographs and the shape of the lap belt load curve, occurred in the two 5F Control Tests, Tests 1 and 2. It did not occur in the Lifebelt Tests 1, 2, and 3 (standard rear seat with soft foam seat base and with or without load limiter).

In the Lifebelt 4 test (D1-4411), in addition to the visual inspection, Denton ASIS load cells were also used with the HIII 5F dummy to demonstrate

quantitatively the anti submarine performance of the Lifebelt seatbelt system. With this instrumentation the moment and force readings change to zero when submarining occurs and the belt slips upwards off the load cells. This was not seen during Lifebelt Test 4.

Effect of a Soft Seat Base on the Lifebelt

The effectiveness of the Lifebelt seatbelt system when used with a simple soft foam seat base is demonstrated by comparison of Lifebelt Iteration 1 Tests 1 (D1-4189) and 2 (D1-4258). The Lifebelt seatbelt system prevented submarining with the hard seat base, Figure 5, and the soft seat base, Figure 6. It did not need the seat base design to ensure that submarining did not occur.

The HIII 5F dummy responses for these tests are compared in Figure 8. The neck loads were reduced with the soft seat, Figure 8, and the head excursion increased, Figure 9.

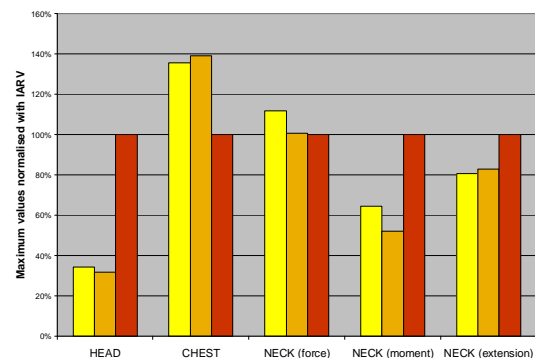


Figure 8. HIII 5F test results of the Lifebelt in a standard rear seat (D1-4189 yellow) and the Lifebelt with a soft seat base (D1-4258 brown). The IARV's for the HIII 5F are shown in red.

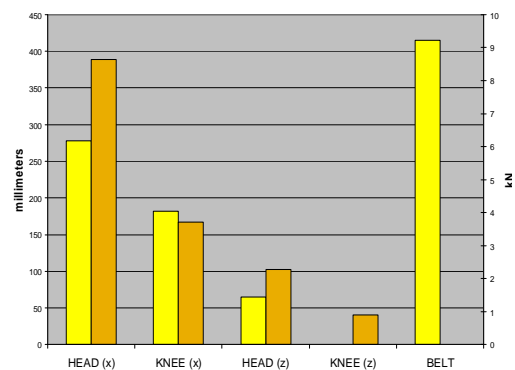


Figure 9. HIII 5F excursion and sash belt load results of the Lifebelt with a standard rear seat (D1-4189 yellow) and with a soft seat base (D1-4258 brown).

Effect of a Chest Load Limiter on the Lifebelt

A comparison of the HIII 5F dummy responses in Lifebelt Tests 2 (D1-4258), 3 (D1-4309) and 4 (D1-4411), demonstrates that including a force limiter in the sash remains an effective means for controlling the chest loads. In each test the Lifebelt seatbelt system was able to prevent submarining both without and with the load limiter, Figure 6. All three tests were with the soft seat base.

The HIII 5F dummy responses for these tests are compared in Figure 10. The chest load limiter reduced the sash belt load and the resultant chest compression to acceptable levels. The neck loads were slightly increased with the load limiter, Figure 10, and the head excursion increased, Figure 11. These effects can be seen in the trajectory of the dummy in the two tests, Figure 12.

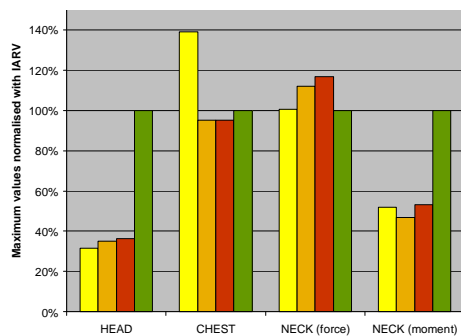


Figure 10. Comparison of HIII 5F performance with the Lifebelt (D1-4258 yellow) and Lifebelt with sash load limiter (D1-4309 brown and D1-4411 red). The IARV's for the HIII 5F are shown in green.

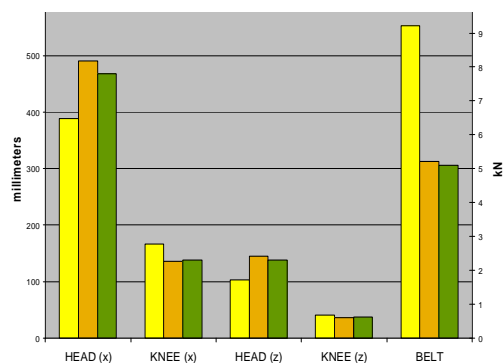


Figure 11. Excursion and sash belt load comparison of HIII 5F performance restrained by the Lifebelt (D1-4258 yellow) and Lifebelt with load limiter (D1-4309 brown and D1-4411 green).

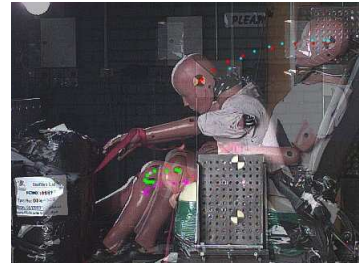


Figure 12. Excursion comparison of HIII 5F performance restrained by the Lifebelt (D1-4258 blue and pink) and Lifebelt with load limiter (D1-4309 red and green).

The HIII 5F Dummy in the Lifebelt

The HIII 5F dummy was fully restrained in the control tests (S090258 and D1-4260). There was no sign of dummy instability, but submarining occurred in both tests, Figure 4.

The HIII 5F dummy was well restrained in the Lifebelt Tests 1, 2, 3 and 4, with the lap belt remaining below the ASIS, see Figures 5 and 6. There was no sign of submarining or dummy instability during the tests.

The dummy responses in the Lifebelt Tests 1, 2, 3 and 4 were very good, especially with the use of the load limiter in Lifebelt Tests 3 and 4, as shown in Figure 13. The chest load limiter reduced the sash belt load and the resultant chest compression to acceptable levels. The neck moments were low with the load limiter, and in this size occupant the head excursion was increased.

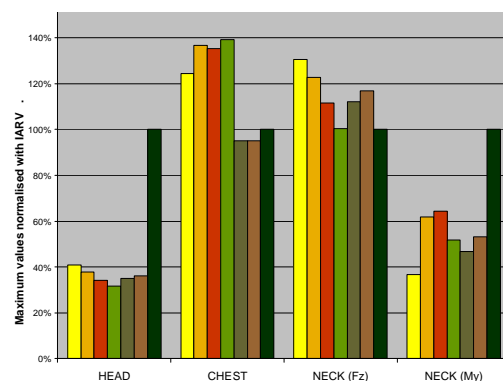


Figure 13. Comparison of HIII 5F performance in the standard rear seat Control Test 1 (S090258 yellow) and standard rear seat with soft seat base Control Test 2 (D1-4260 orange) with the Lifebelt Test 1 (D1-4189 red), Lifebelt soft seat base Test 2 (D1-4258 green) and Lifebelt with load limiter Tests 3 (D1-4309 grey) and 4 (D1-4411 brown). The IARV's for the HIII 5F are shown in dark green.

The HIII 50M Dummy in the Lifebelt

The HIII 50M dummy was fully restrained in the control test (D1-4306). There was no sign of dummy instability or submarining.

The HIII 50M dummy was well restrained in both the Lifebelt Tests 5 and 6, with the lap belt remaining below the ASIS, see Figure 7. There was no sign of submarining or dummy instability during the tests.

The dummy responses in the Lifebelt Tests were very good, especially with the use of the load limiter in Lifebelt Test 6, as shown in Figure 14. The chest limiter reduced the sash belt load and the resultant chest compression to acceptable levels. The neck loads were reduced with the load limiter, and in this size occupant the head excursion was reduced, Figure 15 and 16.

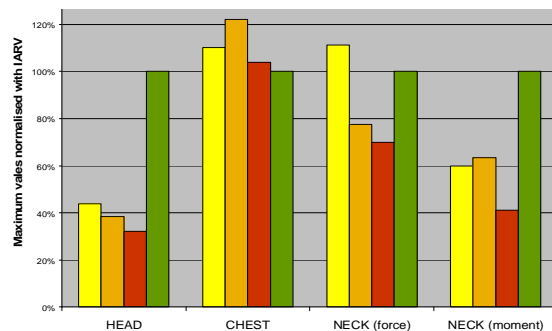


Figure 14. Comparison of HIII 50M performance in the standard front seat Control Test (D1-4306 yellow) and restrained by the Lifebelt Test 5 (D1-4259 brown) and Lifebelt Test 6 with load limiter (D1-4307 red). The IARV's for the HIII 50M are shown in green.

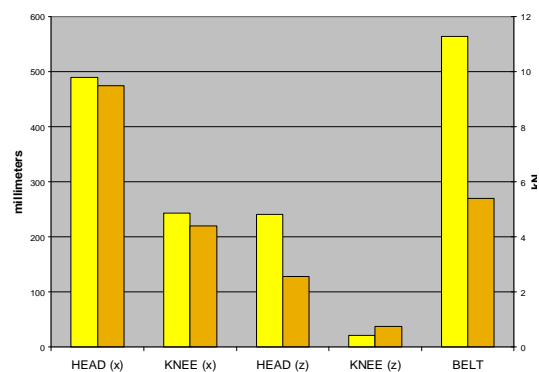


Figure 15. Excursion and sash belt load comparison of HIII 50M dummy performance in Lifebelt Test 5 (D1-4259 yellow) and Lifebelt Test 6 with load limiter (D1-4307 brown).

The test setup was not designed to measure the chest excursion, but based on the video results the Lifebelt HIII 50M tests remained within the ECE R16 chest excursion requirement of 300 mm with the load limiter.

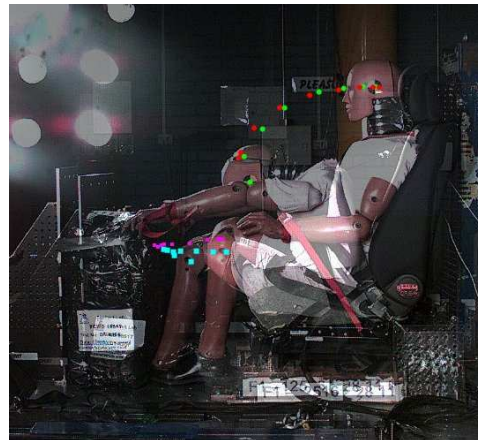


Figure 16. Excursion comparison of HIII 50M performance restrained by the standard front seat (D1-4306 red and pink) and by the Lifebelt with soft seat base (D1-4259 green and blue).

ANALYSIS OF THE FORCES IN THE LIFEBELT SEATBELT SYSTEM

The forces in the Lifebelt Iteration 1 seatbelt system were analysed to define the loading forces acting through the seatbelt, the belt system and on the anchorage points. The test chosen as the worst case loading was the Lifebelt system with a 50th HIII 50M dummy seated on the soft seat base with no load limiter (Test D1-4259).

The Lifebelt system has 6 anchorage points through which the belt loading is transmitted (see Figures 1, 17 and 18):

1. The **SG** (Shoulder D ring) is superior and posterior to the right shoulder of the dummy. Belt tensions T1 and T2 act on this anchor point.
2. The **ELR** (Emergency Locking Retractor) is inferior to the SG. Belt tension T1 acts on this anchor point.
3. The **IB** (In Board) is adjacent to the left hip of the dummy. Belt tensions T2 and T3 act on this anchor point.
4. The **OBA** (Out Board A) is adjacent to the right hip of the dummy. Belt tensions T3 and T4 act on this anchor point.
5. The **OB** (Out Board) is adjacent to the mid right thigh of the dummy. Belt tensions T4 and T5 act on this anchor point.
6. The **IBA** (In Board A) is adjacent to the mid left thigh of the dummy. Belt tension T5 acts on this anchor point.

Table 2.

Estimated forces acting on Lifebelt anchorage points, during worst case loading scenario Test 5 D1-4259.

Anchor point	Belt tensions	Belt tensions resolved to component forces			Anchorage force (kN)
		F _x (kN)	F _y (kN)	F _z (kN)	
SG	T1 & T2	9.01	4.36	-16.48	19.28
ELR	T1	0	0	11.28	11.28
OBA	T3 & T4	19.15	6.67	6.97	21.44
OB	T4 & T5	-10.60	11.28	-3.86	15.95
IB	T2 & T3	16.65	-10.60	9.91	22.08
IBA	T5	0	-11.28	0	11.28

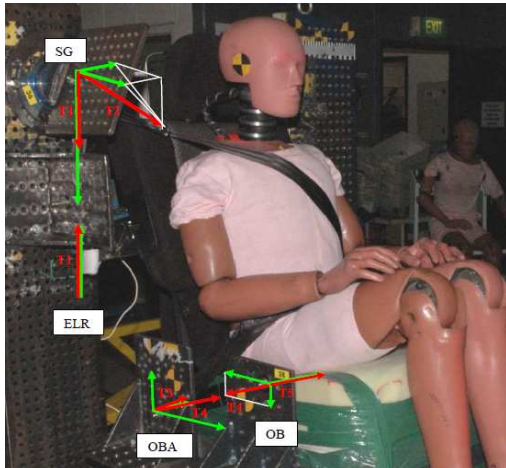


Figure 17. Forces acting on Lifebelt outboard anchor points. The red arrows indicate the applied loads due to belt tension and the green arrows the resultant force on the anchorage point in the local axis system.

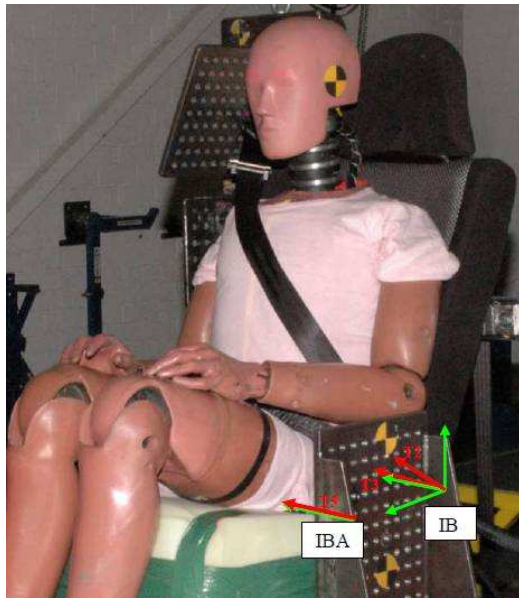


Figure 18. Forces acting on Lifebelt inboard anchor points. The red arrows indicate the applied loads due to belt tension and the green arrows the resultant force on the anchorage points in the local axis system.

The following assumptions were required to estimate loadings at each anchorage point:

- The D rings are frictionless;
- The belt system acts as a cable with uniform tension throughout, i.e. that T1, T2, T3, T4, T5 are equal;
- The belt forces on each D ring act in line with the belt webbing;
- Forces were estimated with the 3D geometry of belt as seen at the maximum excursion of the head of the dummy;
- Maximum excursion was assumed to occur at the same time ($t=0.071$ s for D1-4259) as the recorded peak sash belt load
- The maximum belt tension was 11.28kN, therefore it was assumed:
 $T1=T2=T3=T4=T5= 11.28$ kN.

The forces estimated for the D rings and anchorage points are shown in Table 2. In Figures 17 and 18, the red arrows (T1 to T5) indicate the applied loads due to the belt tension and the green arrows the resultant force on the anchorage in the local axis system.

SUMMARY

A new development of the traditional seat belt system has undergone proof of concept testing. The testing of the Lifebelt Seatbelt system presented here clearly demonstrates that it is an effective restraint system for both front and rear seat occupants.

The Lifebelt is able to be used with a simple soft foam seat base design without submarining.

The system makes use of existing seat belt components. To a user there is no change in the operation of the seat belt.

Throughout the tests reported here, the motion of the dummies was well controlled and both the HIII 5F and 50M dummies remained stable and with acceptable biomechanical responses when tested in the Lifebelt.

The high chest deflection readings noted for the tests with both the standard and the Lifebelt systems were able to be dealt with by means of load limiters. The introduction of the load limiters reduced the chest load to acceptable levels and had no negative effects with respect to dummy stability, submarining and other biomechanical responses.

LIMITATIONS

A limitation of the study was that it was based on early developmental systems and was intended to prove the concept only. The results obtained indicate that the enhanced belt system is worthy of further development.

REFERENCES

Bilston, L., Du, W. and Brown, J. 2010 "A matched-cohort analysis of belted front and rear seat occupants in newer and older model vehicles shows that gains in front occupant safety have outpaced gains for rear seat occupants." *Accident Analysis and Prevention* 42 p1974-1977

Cuerden, R., Scott, A., Hassan, A and Mackay, M. 1997 "The Injury Experience of Adult Rear Seat Car Passengers" In the Proceedings of the IRCOBI Conference, Hannover 1997.

Kuppa, S., Saunders, J. and Fessahaie, O. 2005 "Rear Seat Occupant Protection in Frontal

Crashes." Paper Number 05-0212, In the Proceedings of the ESV Conference.

Mertz H 1984 "Injury Assessment values used to evaluate Hybrid III response measurements. General Motors Submission.

Mizuno, K., Ikari, T., Tomita, K. and Matsui, Y. 2007 "Effectiveness Of Seatbelt For Rear Seat Occupants In Frontal Crashes." Paper Number 07-0224, In the Proceedings of the ESV Conference.

NASVA 2011 The National Agency for Automotive Safety and Victims Aid website. <http://www.nasva.go.jp/mamoru/en/>

NCSA, 2008. Fatal Accident Reporting Scheme. <http://www-fars.nhtsa.dot.gov/Main/index.aspx> (accessed August 20, 2009).

Tylko, S. and Dalmotas, D. 2005 "Protection of Rear Seat Occupants in Frontal Crashes." Paper Number 05-258, Proceedings of the ESV Conference.

Zellmer, H., Luhrs, S. and Bruggemann, K.. (1998) "Optimized Restraint Systems for Rear Seat Passengers." Paper Number 98-SI-W-23, Proceedings of the ESV Conference.

APPENDIX A

Standard Seat and Seatbelt Control Test - Peak Responses

Parameter	Unit	Control Test 1 (S090258)	Control Test 2 (D1-4260)	Control Test 3 (D1-4306)	IARV	IARV
		max / min	max / min	max/min		
Dummy		HIII 5F	HIII 5F	HIII 50M	HIII 5F	HIII 50M
resultant head acceleration	G	78.8	72.7	81.1	193	180
HIC15			598	699	779	700
upper neck force FX	kN	0.1/-1.7	0.0/-1.22	0.01/-1.57	1.9	3.1
upper neck force FY	kN	0.4/-0.3	0.51/-0.10	0.41/-0.14	1.9	3.1
upper neck force FZ	kN	2.7/-0.3	2.54/-0.03	3.66/-0.03	2.07	3.29
upper neck moment MY	Nm	60.0/-34.8	58.7/-39.4	114/-35.3	95 (flexion) 39 (extension)	190 (flexion) 77 (extension)
resultant chest acceleration (3ms)	G		52.4	50.7	73	60
chest compression	mm	-51.0	-56	-55	41	50
viscous criteria	V.C		-0.39	0.49/-0.26	1.0	1.0
upper sternum deflection rate	m/s		0.78/-3.59		8.2	8.2
lower sternum deflection rate	m/s		0.57/-3.59		8.2	8.2
femur force left FZ	kN	2.8/-0.6	2.0/-0.25	2.5/-0.31	6.19	9.07
femur force right FZ	kN	3.0/-1.1	1.49*/-2.27	2.24/-0.16	6.19	9.07
resultant pelvis acceleration (3ms)	G		55.4	58.7		
shoulder belt force	kN	6.6/-0.1	8.41	10.53		
head excursion x	mm		502.6	437.5		
knee excursion x	mm		155.7	63.6		
head excursion z	mm		219.4	318.8		
knee excursion z	mm		51.9	15.6		

Note: the peak dummy response values marked in red equal or exceed the corresponding IARV.

APPENDIX B

HIII 5F Tests - Peak Responses

Parameter	Unit	Lifebelt 1 (D1-4189)	Lifebelt 2 (D1-4258)	Lifebelt 3 (D1-4309)	Lifebelt 4 (D1-4411)	IARV
		max / min	max / min	max / min	max / min	
Dummy		HIII 5F				
resultant head acceleration	g	65.8	60.9	67.7	70.0	193
HIC15		423	367	511	467	779
upper neck force FX	kN	0.16/-1.15	0 /-1.04	0.01/-1.18	0.01/-1.08	1.9
upper neck force FY	kN	0.31/-0.02	0.28/-0.07	0.08/-0.11	0.15/-0.14	1.9
upper neck force FZ	kN	2.31/-0.02	2.08/-0.02	2.32/-0.03	2.42/-0.08	2.07
upper neck moment MY	Nm	61.2/-31.4	49.3/-32.3	44.4/-22.8	50.5/-21.2	95 (flexion)/ 39(extension)
resultant chest acceleration (3ms)	g	53.5	53.8	39.7	40.0	73
chest compression	mm	-55.5	-57	-39	-39	-41
viscous criteria	V.C	0.75	0.8/-0.3	0.64/-0.18	0.65/-0.17	1.0
upper sternum deflection rate	m/s		1.37/-3.73	0.37/-4.23	0.35/-3.93	8.2
lower sternum deflection rate	m/s		1.36 /- 3.49	0.61/-3.32	0.29/-3.36	8.2
femur force left FZ	kN	2.09/-0.30	1.79 /- 0.68	1.79/-0.32	1.99/-0.34	6.19
femur force right FZ	kN	2.51/-1.41	0.77 /- 3.45*	2.73* /- 1.17	2.29 /- 4.15*	6.19
resultant pelvis acceleration (3ms)	G	65	56.2	55.3	59.7	
Left Iliac force	kN				4.09	
Right iliac force	kN				2.64	
Left iliac moment	Nm				34.9/-5.0	
Right iliac moment	Nm				6.2/-26.5	
shoulder belt force	kN		9.22	5.21	5.1^	
head excursion x	mm	278.4	389	490.9	468	
knee excursion x	mm	181.8	167	135.5	138.3	
head excursion z	mm	65.4	102.6	144.6	138.3	
knee excursion z	mm	0	40.6	36.2	37.2	

Note: the peak dummy response values marked in red equal or exceed the corresponding IARV.

* noisy sensor

^ Damaged load cell

APPENDIX C

IIII 50M Tests - Peak Responses

Parameter	Unit	Lifebelt 5 (D1-4259)	Lifebelt 6 (D1-4307)	IARV
		max/min	max/min	
Dummy		IIII 50M	IIII 50M	IIII 50M
resultant head acceleration	g	69.3	58.1	180
HIC15		446	294	700
upper neck force FX	kN	0.06/-1.78	0.0/-1.16	3.1
upper neck force FY	kN	0.25/-0.11	0.13/-0.23	3.1
upper neck force FZ	kN	2.55/-0.02	2.3/-0.01	3.29
upper neck moment MY	Nm	120.6/-34.4	78.1/-37.9	190 (flexion) 77 (extension)
resultant chest acceleration (3ms)	g	45.1	46.6	60
chest compression	mm	-61	-52	-50
viscous criteria	V.C	0.47/-0.28	0.56/-0.26	1.0
femur force left FZ	kN	2.31/-0.79	2.67/-0.39	9.07
femur force right FZ	kN	2.65/-0.72	3.25/-0.41	9.07
resultant pelvis acceleration (3ms)	G	49.2	61.6	
shoulder belt force	kN	11.28	5.39	
head excursion x	mm	489.2	475	
knee excursion x	mm	243.4	220	
head excursion z	mm	241	128.1	
knee excursion z	mm	21.5	37.5	

Note: the peak dummy response values marked in red exceed the corresponding IARV.

INNOVATIVE BONNET ACTIVE ACTUATOR (B2A) FOR PEDESTRIAN PROTECTION

Evrard, Borg

SNPE Matériaux Energétiques

France

Paper Number : 11-0113

ABSTRACT

Since few years, appearance of front vehicles has changed progressively to become friendly towards pedestrians and to meet new regulatory and Euro NCAP queries.

In 2009, Pedestrian Protection received an additional weight with the second phase of the European regulation “Phase 2” and the new scheme of EuroNCAP rating. Requirements on head impact injuries mitigation have been reinforced and compel cars designers to make advised choices between passive and active solutions.

Car designers implement passive solutions with significant changes of the structure to provide a clearance between the bonnet and hard surfaces underneath, allowing free deformations of the bonnet and head energy absorption during the impact.

In parallel, more and more solutions named active hinge systems (or bonnet deployment mechanism) are selected with the aim to lift the bonnet in few milliseconds when a pedestrian knocks the bumper, and to create the saving space under the bonnet surface.

The choice of such active hinge systems is lead by relevant benefits because they allow for:

- car designers, greater freedom for the style;
- carmakers, to meet CO2 rate limitation by improving aerodynamic characteristics;
- consumers, to reduce gasoline consumption.

In January 2011, Euro NCAP working group on pedestrian protection has officially published a method for testing “pop-up” bonnets. As a consequence, active hinge systems can be from now assessed with an official and comprehensive document.

The Bonnet Active Actuator (B2A) designed by SNPE Matériaux Energétiques (SME) is a smart pyrotechnic piston lifter specially designed to operate Active Hinge Systems and to help

carmakers to increase the pedestrian score and so to get a satisfying Euro NCAP rating.

The Bonnet Active Actuator (B2A) has been tested in various cars environment and is ready for applications in cars programs.

AIM OF STUDY

This paper gives an overview of the features and a description of the B2A. It includes the following:

- Background,
- Active Bonnet System review,
- B2A physical content and functions,
- Components testing and simulation,
- Conclusion

BACKGROUND

Directive 2003/102/EC (2) allowed for the EU wide introduction of safety legislation aimed at the protection of pedestrian and other vulnerable road users. Vehicles were required to pass a number of performance tests in two phases in 2005 and 2010. The second phase has been approved in 2009 and came into force with the EC N° 78/2009 regulation (3).

The content of these regulations is based on individual component tests: a Legform test assesses the protection afforded to the lower leg by the bumper, an Upper Legform assesses the leading edge of the bonnet and child and adult Headforms are used to assess the bonnet top area.

The protection of vulnerable road users is also a critical concern for Euro NCAP since 1997. Euro NCAP released a separate star rating for pedestrian valid until 2009 and assesses vehicles with similar sub-systems tests. From 2009, pedestrian score has become integral part of the overall rating scheme with the aim to raise significantly the pedestrian safety area of assessment and to challenge vehicles manufacturers to find solutions for Pedestrian Protection improvement.

In January 2011, the Euro NCAP working group on pedestrian protection has officially published a new method for testing deployable bonnet systems through the updated pedestrian testing protocol version 5.2.1 – January 2011 (1).

In this paper, Euro NCAP requires that pedestrian protection is not compromised by the results of the deformation of the bonnet on impact due to the load of the body. So at the point of head impact, it is essential that the bonnet deflection in the deployed position is controlled and so doesn't exceed the total available clearance between deployed bonnet and engine hard points.

As a consequence, Active Hinge Systems must be able to:

- sustain pedestrians with controlled collapses of bonnets and not bottom out throughout head impact duration,
- retract and absorb energy of head impact in a reverse controlled motion,

Furthermore, Active Hinge Systems must be able to sustain the bonnet few hundreds milliseconds after T fire - 300 ms are generally requested by cars manufacturers - and to keep its head shock absorption capacity during all this period.

ACTIVE BONNET SYSTEM REVIEW

Main features

Bonnet Active Actuator (B2A) is designed to be adapted easily to various hinge kinematics, bonnet strengths, geometries and mass, and cars manufacturer's queries related to functions and performances to fulfil before, during and after pyro-triggering.

Bonnet Active Actuators (B2A) control the movement of the bonnet and the effort during the 3 functioning phases requested by Active Hinge Systems.

- They open quickly and simultaneously the 2 hinges located at each corner of the rear part of the bonnet with a controlled linear lift motion.
- They absorb pedestrian impact on the bonnet by a reverse controlled linear motion.
- They relax their efforts after few seconds and so allow bonnet re-closing manually in case a false deployments.

Bonnet Active Actuator (B2A) is a cost effective and highly reliable solution. It allows to meet the new Euro NCAP tests method and increase the score with its particular features and functionalities:

- easy adjustment for various models of hinges and kinematics;
- hinge unlocking and bonnet deployment time;
- bonnet support waiting for pedestrian impact until few hundred milliseconds after T fire;
- bonnet deflection control under body loading and head shock absorption particularly on hinges areas;
- bonnet reclosing without effort in case of false deployment.

Active Bonnet System overview

This section describes the basic structure and mechanisms of Active Bonnet System. So as it is illustrated in Figure 1., Active Bonnet System consists of the following components:

1. Bumper sensors. They are installed behind the front bumper fascia. They give information about the fact that an impact is occurring and also on the stiffness of the impacting object which can be pedestrian legs or anything else: pole, ball...
2. Electronic Control Unit (ECU): It is located inside the cabin of the car and judges the necessity to lift the bonnet after receiving and analysing bumper sensors signals and vehicle speed.
3. Active Hinge Systems (Hinge + B2A): As it is illustrated in Figure 2., they raise simultaneously the rear portion of the bonnet as soon as they receive the triggering signal send by ECU.

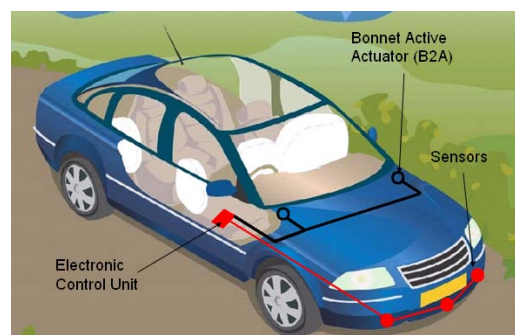


Figure 1. Active Bonnet System

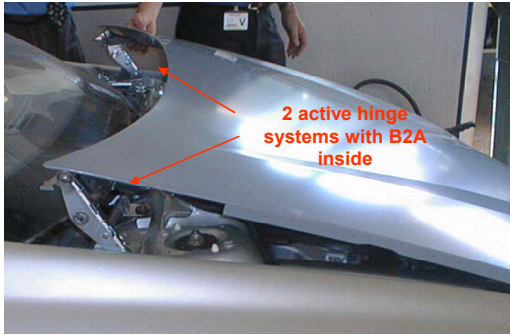


Figure 2. Bonnet and Active Hinge Systems in elevated position
(ready for head impact absorption)

Active Hinge System

Active Hinge System consists of 2 components:

1. Bonnet Active Actuator (B2A)

The pyro-actuator proposed and designed by SME is named Bonnet Active Actuator (B2A). It is constituted with a Micro Gas Generator (MGG) and a piston located in a tube as shown in Figure 3..

The piston move out under pyro-gas pressure when the MGG is triggered.



Figure 3. Bonnet Active Actuator (B2A) designed by SME

2. New hinges designs

Hinges are specifically designed to ensure an unusual function which is the lifting of the rear portion of the bonnet under a pushing force at approximately 100 mm high.

During normal operations, bonnets are currently open and close by upward and downward movements of their front parts which are controlled by hinges pivots.

When Active Hinge Systems are triggered, latching systems located currently at the vehicles front end become fixed pivots and as a result control the rotating movements of bonnets rear portions (Figure 2.).

New hinges designs gather the following components (Figures 4. & 5.):

- pivots for normal bonnets closing and opening operations,
- upper and a lower members for fixation on cars bodies and bonnets,
- locking devices to keep hinges mobile members folded for normal bonnets operations (shear pin, rivet or hook),
- intermediate ties arms and pivots to provide particular hinge kinematics and specific bonnets trajectory.

Figures 4. and 5. illustrate hinges designs examples with typical characteristics gathered in table 1. below.

	Figures 4 & 4bis	Figure 5
Hinge type	-Link hinge design type	-Free Pushing Force hinge design
B2A mounting	-B2A linked to the bonnet with a hinge mobile part	-No link between B2A and bonnet
Upraising controlled movement	-B2A pushing force applied horizontally (or almost) on the intermediate mobile part of the hinge. -Bonnet pivot vertical trajectory controlled with 2 intermediate ties arms	-B2A pushing force applied vertically on the bonnet.
Gear ratio between B2A and hinge strokes	3 (as an example)	1
Locking device		Shear pin

Table 1. Hinges designs characteristics

In both cases, hinges kinematics can be modified by the lengths and positions of intermediate ties arms.

During normal bonnets opening or closing, the locking devices (ex: shear pin, rivet or hook) keep hinges mobile parts in folded position, allowing only hinges upper member and bonnets to rotate around bonnets pivots.

Hinge gear ratio 3

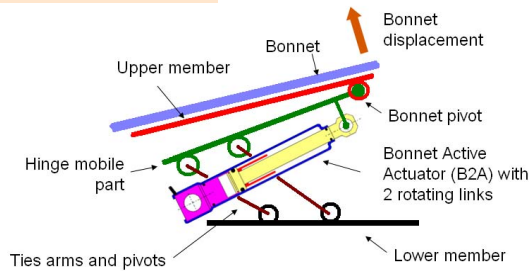


Figure 4. Link hinge design type
B2A end piston is linked to the hinge upper member

Hinge gear ratio 3

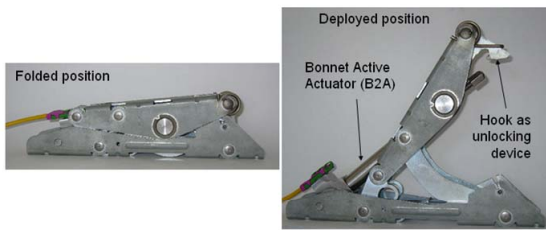


Figure 4bis: Link hinge design type
Prototype implementing a hook to unlock the hinge mobile parts

Hinge gear ratio 1

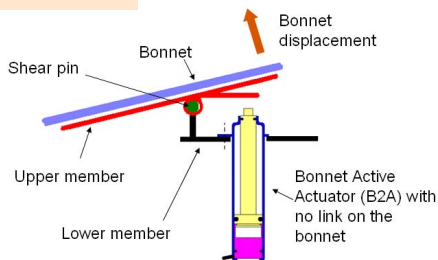


Figure 5. Free Pushing Force hinge design type
Piston is not linked to the hinge upper member

When B2A is triggered, its piston pushes the locking device until it breaks (shear pin or rivet) or opens (hook) allowing hinge upper member to move upward.

The piston deploys under pyro-gas pressure and extends the hinge. As the result, bonnet rear portion raises and provides the saving clearance under the bonnet surface.

Setting the times for the Bonnet Active Actuator operating phases

This section describes B2A operating phases, thresholds and durations for each of them.

Phase 1: Bonnet deployment

Active Bonnet System must provide assurance that bonnet always deploys before head impact and remains in elevated position when it happens.

Tests and simulations are carried out to evaluate typical head contact times in car to pedestrian collisions at a speed of 40 km/h. With AM50 dummy, it occurs at approximately 150 ms. The shorter is the height of the dummy, the shorter is the head contact time, so with the C6Y dummy, the contact time is estimated at 60 ms and the maximum value is given for 250 ms according to specific studies (4).

As a result and illustrated in Figure 6., the time for the bonnet deployment after T fire must be lower than the shortest head contact time and so is usually specified within 30 ms.

Phase 2: Bonnet support

After bonnet deployment, B2A must sustain a sufficient and constant effort (pyro-pressure) until pedestrian impact on bonnet, to ensure a deflection control under body loading and head shock absorption.

The time limit of this sustained force after T fire is usually specified at 300 ms Regarding the longest head contact times define above.

Phase 3: Bonnet reset ability

The sensing system could trigger a deployment even if no pedestrian is involved. In that case, B2A sustained force must be relaxed and cancelled after the 300 ms threshold, allowing a manual bonnet re-closing (few daN are generally requested).

Figure 6. presents threshold and times requested for B2A operating phases with the following parameters:

- T0 First contact leg-bumper
- T sensor Time for firing signal
- T sensor_max Largest value of T sensor
- T fire Time for firing

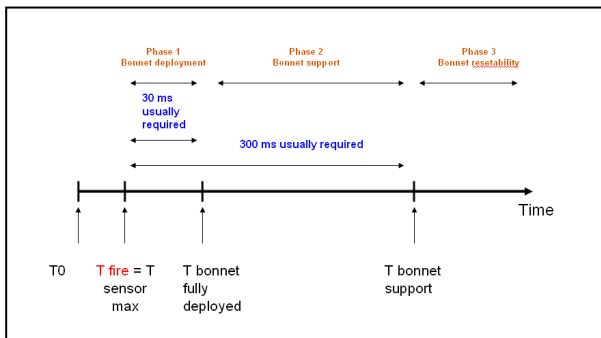


Figure 6. Times of B2A operating phases

B2A PHYSICAL CONTENT AND FUNCTIONS

B2A physical content

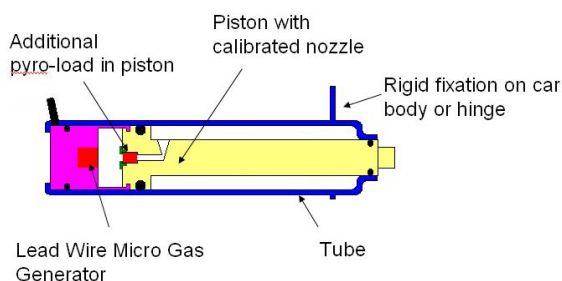


Figure 7. B2A general design

As shown in figure 7., B2A consists of:

- MGG (Micro Gas Generator),
- Additional pyro-load (in piston),
- Piston in tube with calibrated nozzle for pyro-pressure control,
- Casing/tube.

B2A is a fully tight actuator able of resisting the humidity and severe atmospheres which we find in engines compartments.

B2A functions

B2A design allows an easy sizing to achieve customers performances requirements illustrated in Figure 8. below.

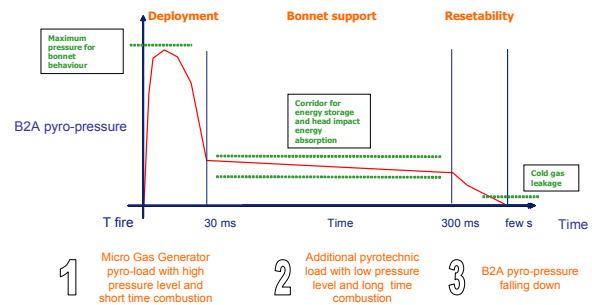


Figure 8. B2A operation phases vs pyro-gas effort (pressure)

Phase 1: Bonnet deployment - Controlled pyro-pressure and time with MGG pyro-load

B2A provides a controlled piston motion and effort upon receipt of an electric signal. This movement is started by the MGG ignition.

B2A piston extension occurs in a short time (within 30 milliseconds as requested by customers) under a quick pyro-pressure increase provided by the combustion of the MGG pyro-load. That creates a force which elevates the bonnet at the deployed position.

Combustion chamber pressures and resulting extension speeds can be sized and adapted to customers requirements without any modification of the B2A design.

The bonnet vertical trajectory is to be multiplied with the gear ratio of the hinge in order to define the stroke of the piston.

B2A design is able to fulfil a minimum stroke of around 10 mm to a maximum stroke of at least 120 mm depending on hinge kinematics and gear ratio (Figures 4. & 5.).

Phase 2: Bonnet support - Controlled energy storage for head impact absorption with the secondary pyro-load

When B2A is fully extended, it is able to store energy. The force level for this “work function” is achieved after the deployment phase and must remain constant until 300 ms after the T fire. The topic is to control the bonnet deflection under the body loading and to absorb the head shock which can occur during all this time.

The pressure of the additional pyro-load (Figures 7. & 8.) takes over the MGG pyro-pressure to provide longest time combustion at a lower level (Figure 11). Its combustion time is roughly multiply by 10 regarding MGG pyro-load combustion time. (30 ms for deployment to 300 ms for bonnet sustain).

This B2A force level is also easily tuneable. The value is define by the quantity and the composition of the additional pyro-load.

Phase 3: Bonnet reset ability – Bonnet closing if no pedestrian impact occurs, with pyro-pressure release

After a deployment event where no pedestrian impact occurs, bonnet has to be re-closed manually without any tool. The objective is for the driver to recover the visibility and to drive the car to a service facility.

For that topic, B2A provides a calibrated gas leakage whereby customer can move back the B2A to its initial un-deployed position through a manual force applied on the bonnet (Figure 12). Customer is likely to apply a few daN force at the rear portion of the bonnet just above hinges.

COMPONENTS TESTING AND SIMULATION

Objectives

Several simulations and tests has been done to check B2A operations:

- Bonnet deployment,
- Bonnet sustain and effort control,
- Bonnet reset ability.

Typical results

Figures 11. & 12 illustrate the typical curves coming from these simulations and tests.

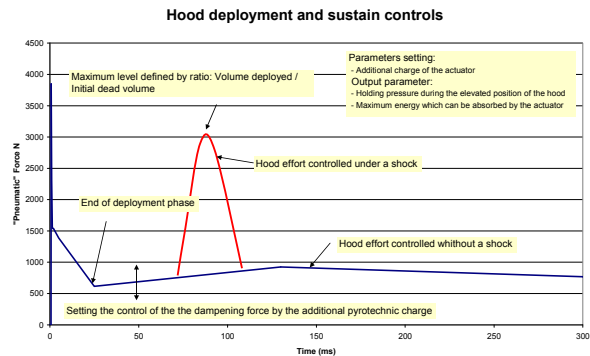


Figure 11. Simulation and test typical results

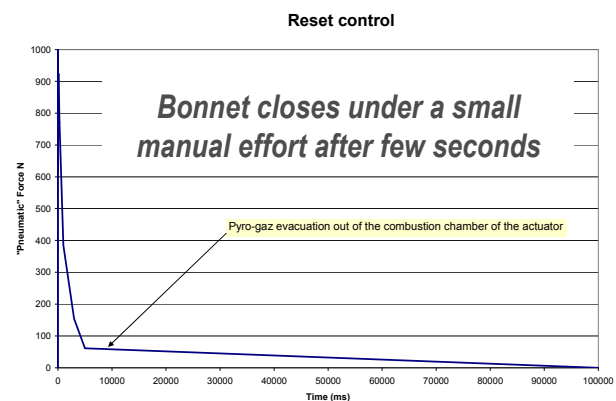


Figure 12. Piston force vs time after Tfire + 300 ms for bonnet re-closing

Comments

B2A allows specific tuning to meet customers requirements according to:

- Deployment time,
- Bonnet sustain effort for energy storage and time,
- Cold gas leakage to insure bonnet reset.

Tests are in accordance with simulation.

It has been so checked under impactors tests (Figure 11.) that :

- bonnets is fully lifted within 30 ms.
- Energy stored after deployment with pyro-gas allows to get good HIC values until 300 ms.

CONCLUSION

B2A is a simple pyro-piston lifter fulfilling carmakers and hinges designs requirements.

B2A design is easily tuneable with pyro-parameters without any change of the global design and main components, so:

- Micro Gaz Generator (MGG) pyro-load for bonnet deployment,
- Additional pyro-load for bonnet sustain and energy storage until 300 ms for pedestrian loading control and head impact energy absorption,
- Piston nozzle for cold gas leakage and bonnet reset ability.

Slots of time are significantly different and allow this easy tuning related to each environment:

- Deployment phase: ~ 30 ms
- Bonnet sustain : ~ 300 ms
- Bonnet reset : few seconds

B2A sizing is achieved with pyrotechnic and mechanic numerical models and tests. B2A is available for implementation in Active Hinge Systems and serial cars manufacturing.

REFERENCES

1. *European New Car Assessment Programme (EuroNCAP) – Pedestrian testing protocol – version 5.2.1 – January 2011..*
2. *Directive 2003/102/EC of the European Parliament and of the Council of 17 November 2003. Official Journal of the European Union L 321/15*
3. *Regulation (EC) N° 78/2009 of the European Parliament and of the Council of 14 January 2009. Official Journal of the European Union L 35/1*
4. *CLEPA European Association of Automotive suppliers - INF GR / PS /67 08.01.2004 – Pedestrian Protection Test method - Active hood/bonnet systems.*

NHTSA's Rear Seat Safety Research

Aloke Prasad

NHTSA
USA

Doug Weston

Transportation Research Center, Inc.
USA
Paper # 11-0348

ABSTRACT:

NHTSA has collected a series of rear seat occupant data from full-scale frontal vehicle tests. The data set encompasses Research and Development and New Car Assessment Program (NCAP) tests and a variety of dummies, including adults and children in child restraint systems. This paper examines the effect of the cushion characteristics (shape, stiffness, thickness) and crash pulse on a small adult and a child in a forward facing child restraint (CRS) using sled tests. A controlled dynamic test will help us better understand how these factors influence the CRS crash dynamics. The thickness of the cushions had the most effect on dummy injury assessment values (IAV). The crash pulse characterization Vehicle Pulse Index (VPI) was the best predictor for head and chest injuries in such occupants.

INTRODUCTION

Twelve percent of passenger vehicle occupants in police reported crashes are in the rear seat. In addition, approximately 10 percent of all passenger vehicle occupants killed are in rear seats. Sixty-four percent of outboard rear seat occupants involved in frontal crashes are belted, and among these restrained rear seat occupants, 64 percent are 12 years old and younger, and 78 percent weigh less than 160 lbs. Sixty-five percent of rear seat occupants killed are 16 years and older in age. Therefore, children and older occupants in the rear are of particular concern. [1]

NHTSA has collected a series of rear seat occupant data from full-scale frontal vehicle tests. The data set encompasses Research and Development and New Car Assessment Program (NCAP) tests and a variety of dummies, including adults and children in child restraint systems. The analysis of CRS testing showed that child occupant protection can not only be affected by the characteristic of the crash pulse, but also by other factors such as vehicle cushion stiffness, seat contour, and seat back angle.

1. Kuppa Shashi, et al. Rear Seat Occupant Protection in Frontal Crashes. Paper #. 05-212, 19th ESV Conference, Washington, DC.

SEAT PARAMETER EFFECTS

The study reported in this presentation examined the effects of rear seat cushion stiffness, seat top surface angle, cushion height at the front of the seat and seat support structure angle on a Hybrid III 3 year (3 YO) old child dummy in a forward-facing CRS and on a 5th percentile female (5th F) dummy in a 3-point seat belt. The crash simulation (sled) tests were conducted at a ΔV of 35 mph equivalent to a NCAP pulse for a 2006 Ford Taurus.

Seat Cushion Characterization

Twenty four vehicle rear seat cushions were measured and tested under static loads to measure their dimensions and stiffness. The vehicles and the cushion dimensions are listed in Appendix A. The static force-deflection test setup, using an 8-inch diameter indentation plate, is shown in Figure 1.



Figure 1. Static Test Setup

Stiffness measurement at the front of the cushion, where the cushion is most likely to bottom out in CRS sled tests, was considered for this study (Figure 2). The force-deflection characteristics of the vehicle rear seat cushions are in Appendix B.

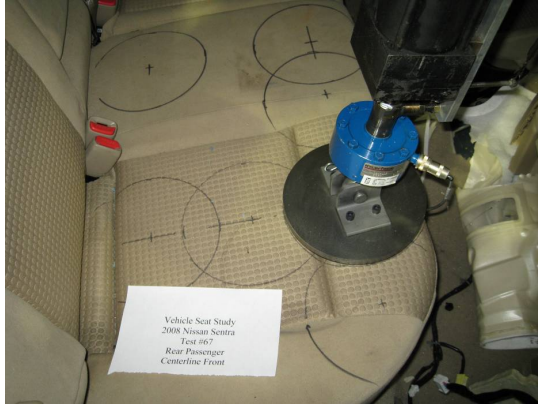


Figure 2. Cushion Test Location

Control Parameters for Rear Seats in Sled Tests

Based on the ranges of shapes, sizes, and stiffness recorded for the 24 vehicles, the following values were selected to characterize the rear seat in the sled tests:

- Cushion stiffness = soft, hard
- Cushion top surface angle = 7°, 16°
- Cushion height at front = 225 mm, 100 mm
- Seat frame support angles = 7°, 16°

Note that the seat support frame angle on the current FMVSS No. 213 seat is at 15° and the anti-submarining ramp below the seat cushion in the 2007 Ford 500 is 12°. The seat pan width (1372 mm), depth (508 mm), seat back angle, seat back shape and seat back foam were kept the same as in current FMVSS No. 213 seat. The four cushion shapes thus selected are shown in Appendix C.

Two different cushion stiffnesses (soft, hard) were obtained. They were both polyurethane foam, based on toluene diisocyanate (TDI), used in the North American market automobile seats. The foam characteristics, tested per ASTM D 3574 – 08 (15” x 15” x 4” block using a 8” diameter indenter) are shown in Figure 3.

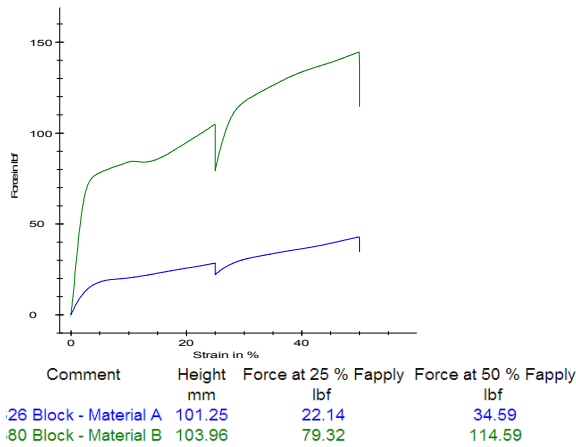


Figure 3. Cushion Foam Properties

The indentation forces at 25% and 50% deformation are 22.1 lbf and 34.6 lbf for the soft foam and 79.3 lbf and 114.6 lbf for the hard foam, respectively.

The selected sled seat cushions were tested under identical conditions as the vehicle seats (Figure 3). The results are overlaid and shown in Appendix B.



Figure 4. Sled Seat Static Test

Crash Pulse Used

The crash pulse selected for studying the cushion effects was representative of a high severity frontal impact of a mid-size passenger car. The frontal NCAP 35 mph crash pulses for the 2000 and 2004 Ford Taurus are shown in Figure 5. The representative sled pulse is also shown in Figure 5. The peak acceleration and ΔV of the sled pulse were 28.4 G and 36.0 mph (at 106.5 ms).

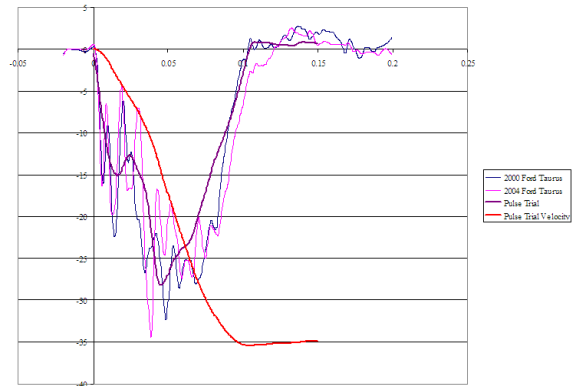


Figure 5. Sled Pulse

Test Matrix Summary

- The independent variables defining the seat were:
- Foam shapes: 4 (thick, thin; flat, wedge)
- Foam Stiffness: 2 (soft; hard)
- Base-Plate Angle: 2 (7°, 16°)

That resulted in 16 different rear seats tested in 16 sled tests. Each test had a belted 5th F and a 3 YO dummy in an Evenflo Titan Elite DLX Convertible forward facing CRS. The CRS was mounted to the seat by the lower anchors and top tether for children (LATCH) attachments. The sled pulse was an approximation of the 35 mph frontal NCAP crash pulse of a 2004 Ford Taurus.

The 5th F and the 3 YO dummies had instrumentation in the head, upper neck, and the chest.

Location of Seat Belt and LATCH Anchors

The ranges of cushion thicknesses and stiffnesses result in the occupant being seated at different heights on the sled for each of the cushion and seat angle combinations.

To ensure that the seat belt and LATCH anchors were at the same locations relative to the 5th F and 3YO respectively, belt anchor locations (Figure 6) were recorded in the 2004 Taurus relative to the H-point determined using the SAE J826 OSCAR H-point machine installed in the vehicle.



Figure 6. Seat Belt Attachment Locations

The OSCAR H-point machine was installed on each of the 16 combinations of cushion and seat angles (Figures 7-8).



Figure 7. OSCAR on a Thick Cushion



Figure 8. OSCAR on a Thin Cushion

Belt and LATCH anchor locations (at the same positions relative to the OSCAR H-point) were located for all 16 cushion-seat configurations. The CRS, belts, and retractors were changed after each sled test.

A typical test setup is shown in Figures 9 and 10. Each dummy was photographed by three high speed digital cameras. The position of the head and other landmarks on the dummies were calculated using 3D photogrammetry.



Figure 9. Sled Test Setup



Figure 10. Sled Test Setup

Test Results

The test matrix and IAV, normalized to the injury assessment reference values (IARV) are shown in Appendix D. The maximum head excursions are normalized to the highest value in all 16 tests. This provides a relative measure of head excursion to the worst case result .

5th Percentile Female

Test # 6 (thin, flat, soft cushion at 16 degrees) had the lowest maximum IAV (scaled head excursion of 0.93). Test # 13 (thick, flat, soft cushion at 16 degrees) had the highest maximum IAV (scaled neck tension of 1.53).

3YO Child

Test # 14 (thick, flat, soft cushion at 7 degrees) had the lowest maximum IAV (scaled neck tension of 1.62). Test # 16 (thick, flat, hard cushion at 16 degrees) had the highest maximum IAV (scaled neck tension of 1.88).

ANOVA Analysis

A one-way ANOVA analysis for the effect of cushion thickness, stiffness, shape, and angle on injury data is shown in Appendix E.

Variables that were at least 80% likely to be significant were analyzed using linear regression for each dummy individually and for scaled data analyzed jointly. Cushion thickness was the dominant variable.

Observations

Cushion thickness had the most effect on IAV. The maximum difference in head excursion was 2.3” for the 5th F, and 3.2” for the 3 YO child dummies. The thin cushion provided a more stable surface, while the thick cushion may have caused submarining in the 5th percentile female or slack in the CRS attachment. A different CRS may produce different results.

CRASH PULSE EFFECTS

Background

In response to the Transportation Recall Enhancement, Accountability, and Documentation (TREAD) Act, NHTSA evaluated various CRS in 193 MY 2001-2008 vehicle crash tests [2]. Eighty nine (89) vehicles were evaluated, equipped with a control CRS (Evenflo Vanguard). The vehicle pulse severity was found to affect the dummy performance. However, no solid correlation was found. (Peak chest acceleration somewhat correlated to the vehicle crush). For MY 2001 – 2004 tests, when controlling for the child restraint, vehicle make and model explained 64 percent of the variation in chest acceleration and 63 percent of the variation in HIC. One confounding factor was the presence of too many variables (CRS, pulse, vehicle seat) in these crash tests.

The test plan selected for this study presented below addressed some of those factors by keeping the same vehicle seat, CRS (Evenflo Titan Elite DLX), and ΔV , while changing the crash pulse.

Test Setup

Like the seat parameter effect tests, the pulse effect sled tests used two occupants (5th percentile female, 3 year old child Hybrid III dummies). The seat cushion was selected to be the New Programme for the Assessment of Child-restraint Systems (NPACS) foam, 5” thick and 19”

2. Evaluation of Child Occupant Protection In a 56 km/h (35 MPH) Frontal Barrier Crash, Docket Number NHTSA-2004-18682.

deep. The seat back was the same as used in the current FMVSS No. 213 seat. The seat cushion and seat back angles were set to the same values as in the FMVSS No. 213 (cushion at 15 deg, seat back at 20 deg.). The force-deflection characteristics of the NPACS foam as installed on the sled, is shown in Appendix F.



Figure 11. Sled Test Setup

The seat belt anchor locations (for the 5th F) and the LATCH anchor locations (for the 3 YO in FF CRS) were adjusted to be in the same relative location to the OSCAR H-point in the 2006 Ford Taurus rear seat.



Figure 12. Belt anchor Location

The CRS, belts and retractors were changed after each sled test. The 5th F and the 3 YO dummies had instrumentation in the head, upper neck, and the chest.

Crash Pulse Selection

To determine the characteristics of the sled pulses for use in this study, frontal NCAP crash pulses from 2003 to 2008 were examined. These are shown in Figure 13, along with the average of these crash pulses.

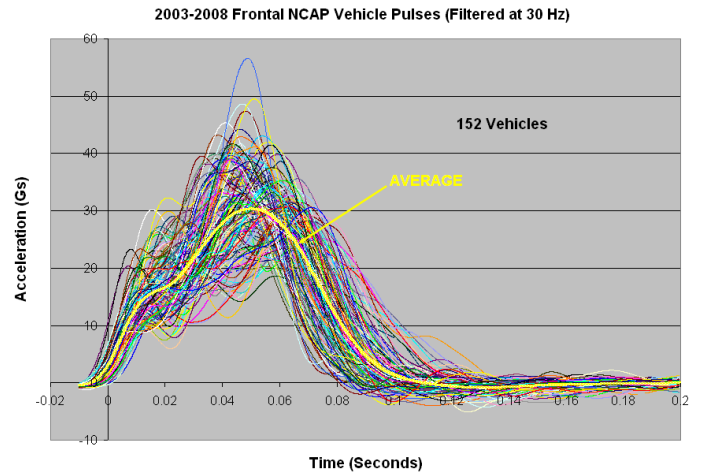


Figure 13 NCAP Crash Pulses

Based on the average NCAP crash pulse, the following criteria were used in selecting the sled pulses:

$$\Delta V = 35 \text{ mph}$$

$$\text{Pulse duration} = 100 \text{ ms} \pm 10 \text{ ms}$$

The sled pulses from existing HYGE sled pins available at the Transportation Research Center, Inc. (TRC) that satisfied these criteria, along with the current FMVSS No. 213 pulse (scaled to 35 mph), are shown in Fig. 14.

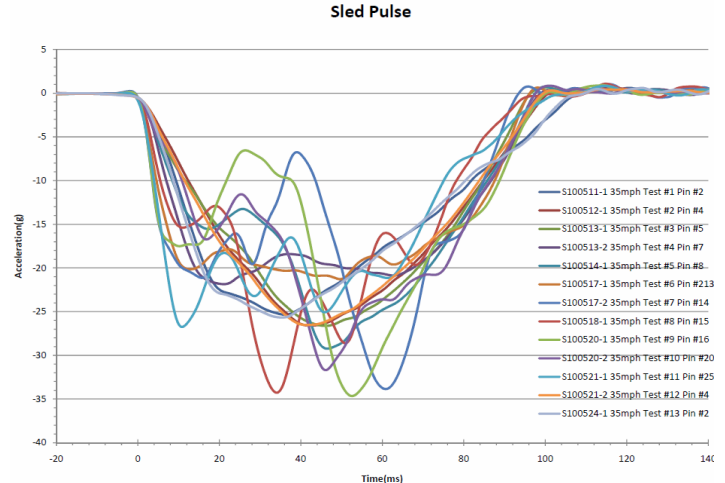


Figure 14 Sled Pulses Used for Pulse Effect

Sled Pulse Characterization

The selected sled pulses were characterized based on their acceleration values and their shapes. These would be used as independent control variables when examining the dummy IAV's from the sled tests.

The acceleration based pulse characteristics used were as follows (refer to Figure 15):

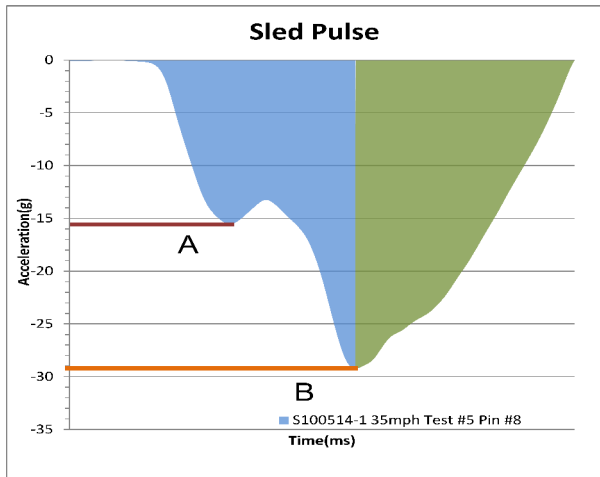


Figure 15. Acceleration-Based Pulse Characterization

Peak G's

Maximum acceleration

Average G's

Average acceleration from time zero to return to zero G's

Ratio of A/B

Ratio of relative maximum G's (A) to peak G's (B). If multiple relative maximums existed the most prominent curve was chosen.

Ratio of C/D

Ratio of the area (blue) before the maximum peak to area (green) after the maximum peak.

Front or Rear Loading

If the location of the peak is before the mid-point of the pulse, the pulse is front loaded. If it is after the mid-point, the pulse is rear loaded.

The shape of the sled pulse was characterized by the centroid of the acceleration vs. time plot (Figure 16).

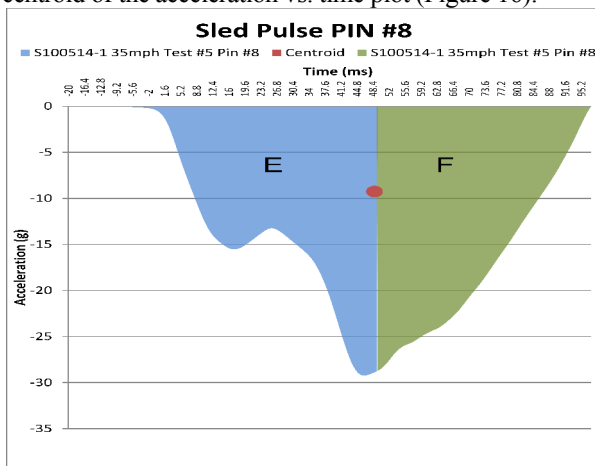


Figure 16. Shape Based Pulse Characterization

Value of Centroid (time, acceleration)

Ratio of E/F

Ratio of area under the curve before the centroid (E) to area under the curve after the centroid (F)
Vehicle Pulse Index (VPI)

Using 2-step pulse approximation, the peak acceleration of a belted occupant (estimated from a 1-D model) in a vehicle with seat belts and air bags. VPI is the "Vehicle Pulse Index." It is the peak acceleration on a unit mass representing the occupant, subject to the crash-pulse input and subject to a lumped-mass spring representing the restraint system (belt+bag stiffness). While VPI is calculated for the front seat occupant, it is still a useful measure when comparing crash pulses.

The pulse characteristics of the 13 sled pulses are shown in Appendix G. The dummy IAV's are in Appendix H.

Stepwise Linear Regression Model

The results of a stepwise linear regression model are shown in Appendix I. The models include all linear terms significant at the 15% level (i.e., there is at least an 85% probability that the term selected affects the results).

The results of the best fit models (predicted value vs. actual value) of the IAV's are in Appendix J and K.

Observations

For the 5th percentile female:

VPI was the best predictor of HIC and peak chest acceleration.

Peak sled acceleration was the best predictor of Nij. Pulse centroid acceleration value was correlated to head excursion.

Submarining was observed in some tests.

For the 3 year old child:

VPI was the best predictor of HIC and peak chest acceleration.

There was a weak correlation of VPI to the neck axial force and head excursion.

Pulse centroid acceleration value was correlated to the maximum chest deflection.

LIMITATION OF STUDY

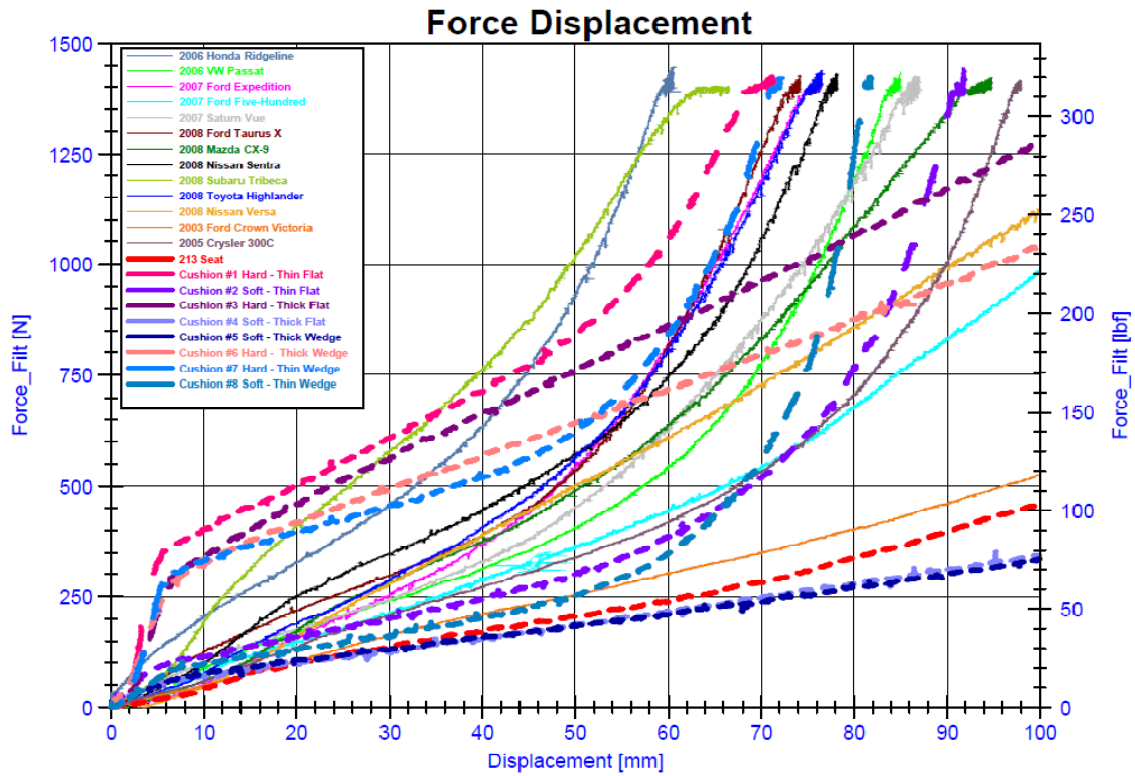
The cushion effect and pulse effect tests used a simplified rear seat design. The intent was to identify the effects of extreme values of seat parameters on dummy IAV's. Actual rear seats in vehicles use contoured shapes and cushion materials that may be very different from those used in the study. Some phenomena like submarining could be dependent on difference in the cushions used in this study compared to those used in vehicles. Also, the results for the 3year old in CRS may not be applicable to other CRS designs.

APPENDIX A Vehicle Seat Dimensions

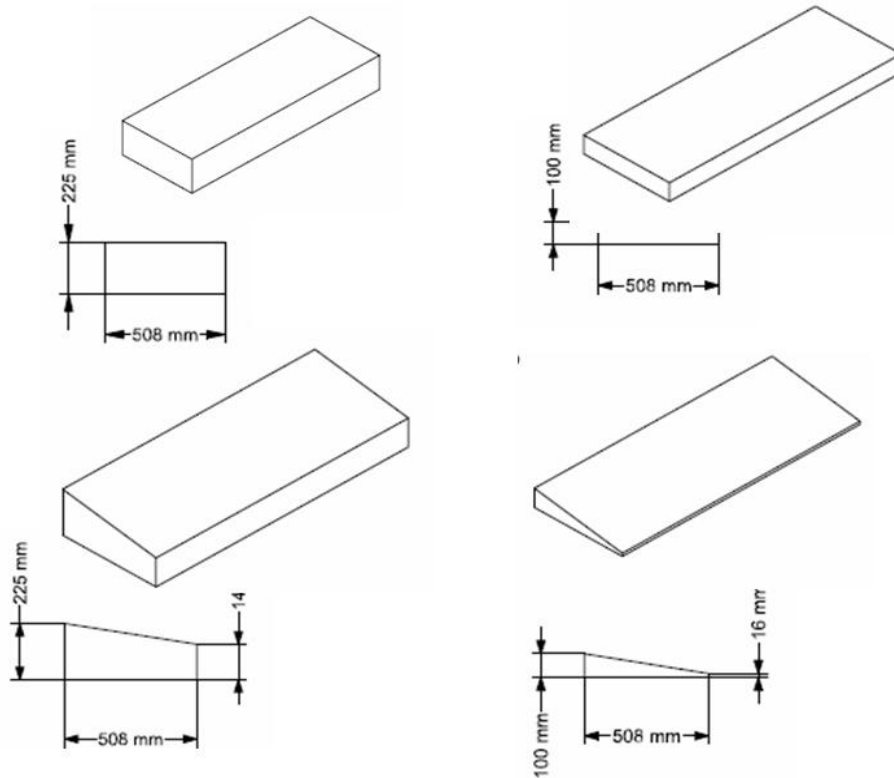
Vehicle Description	Front Seat Foam Thickness (A)	Seat Depth Front to Back (B)	Back Seat Foam Thickness (C)	Floor to Top of Seat	Seat Angle Degrees
2008 Ford Taurus X	100	510	90	380	6.7
1999 Volkswagen Beetle	100	450	95	340	8
1994 Honda Civic	105	500	70	275	12.9
2006 Volkswagen Passat	115	530	80	335	11
2002 Ford Focus	120	500	85	375	12.6
2007 Saturn Vue	130	520	80	302	8.6
2008 Subaru Tribeca	140	510	70	325	9
2002 Honda CRV	140	570	40	370	9.4
2007 Ford Expedition	140	520	65	340	10.2
2006 Dodge Durango	140	575	90	372	14.4
2007 Ford Edge	140	520	120	300	15.1
2008 Toyota Highlander	150	505	83	335	8.8
2005 Honda Odyssey	150	570	70	378	12.7
1996 Chevy Cavalier	160	490	60	320	8.2
2009 Chevy Equinox	160	690	60	365	10.8
2007 Jeep Commander	160	560	70	310	12.3
2006 Honda Ridgeline	165	500	50	375	11.4
2007 Mazda CX-9	170	515	50	295	11
2003 Honda Odyssey	170	520	90	373	13.4
1996 Chrysler Concord	170	620	28	330	18
1990 Honda Civic	190	480	90	315	9.3
2007 Ford 500	210	540	70	360	15
1996 Ford Taurus	215	545	40	348	16.8
2008 Nissan Sentra	225	555	48	365	10.3

APPENDIX B Vehicle Rear Seat and Sled Cushion Force-Deflection Plots

Rear Passenger Centerline Front Overlays



APPENDIX C Sled Cushion Shapes



APPENDIX D Test Results

Test#	Configuration	Independent variables				5th F						3 YO					
		thickness	Shape	stiffness	angle	HIC15	ChestG	ChestD	Nij	NeckT	HeadX	HIC15	ChestG	ChestD	Nij	NeckT	HeadX
S091006-1 Test 1	N	thin	wedge	hard	7	0.85	0.86	0.69	1.16	0.91	0.90	0.46	0.96	0.50	1.17	1.76	0.77
S091007-1 Test 2	H	thin	wedge	hard	16	1.12	0.74	0.59	1.03	1.00	0.88	0.49	0.84	0.50	1.05	1.81	0.85
S091008-1 Test 3	O	thin	wedge	soft	7	0.71	0.96	0.77	1.14	0.82	0.94	0.43	0.91	0.56	1.11	1.76	0.82
S091009-1 Test 4	G	thin	wedge	soft	16	0.92	0.81	0.62	1.14	1.05	0.88	0.40	0.89	0.59	1.04	1.67	0.81
S091009-2 Test 5	I	thin	flat	soft	7	0.70	0.80	0.80	0.82	0.98	0.96	0.45	0.90	0.53	1.21	1.83	0.81
S091014-1 Test 6	B	thin	flat	soft	16	0.82	0.75	0.72	0.86	0.91	0.93	0.48	0.88	0.55	1.11	1.69	0.78
S091014-2 Test 7	A	thin	flat	hard	16	0.83	0.74	0.73	0.90	0.91	0.95	0.50	0.89	0.59	1.16	1.75	0.84
S091015-1 Test 8	P	thin	flat	hard	7	1.14	0.86	0.72	1.33	1.44	0.92	0.45	0.86	0.54	1.20	1.76	0.89
S091015-2 Test 9	E	thick	wedge	soft	16	1.04	0.72	0.63	1.13	1.48	0.88	0.43	0.89	0.64	1.14	1.72	1.00
S091022-1 Test 10	L	thick	wedge	soft	7	1.04	0.75	0.74	1.16	1.28	0.99	0.45	0.92	0.63	1.12	1.69	0.94
S091015-3 Test 11	M	thick	wedge	hard	7	1.03	0.78	0.73	1.00	1.34	0.97	0.51	0.91	0.54	1.26	1.83	0.88
S091019-1 Test 12	F	thick	wedge	hard	16	0.79	0.75	0.60	1.00	1.14	0.96	0.48	0.94	0.64	1.14	1.70	0.98
S091019-2 Test 13	D	thick	flat	soft	16	1.13	0.73	0.74	1.26	1.53	0.91	0.65	0.98	0.65	1.21	1.84	0.91
S091023-1 Test 14	K	thick	flat	soft	7	0.94	0.80	0.77	1.19	1.29	0.92	0.43	0.96	0.69	1.03	1.62	0.96
S091021-1 Test 15	J	thick	flat	hard	7	0.81	0.80	0.72	1.12	1.28	0.94	0.51	0.93	0.62	1.13	1.73	0.92
S091021-2 Test 16	C	thick	flat	hard	16	0.66	0.86	0.61	0.92	0.96	1.00	0.54	0.92	0.56	1.21	1.88	0.91
S091023-2 Repeat of Test 1	N	thin	wedge	hard	7	1.07	0.73	0.65	1.11	1.40	0.92	0.51	0.95	0.62	1.15	1.84	0.86

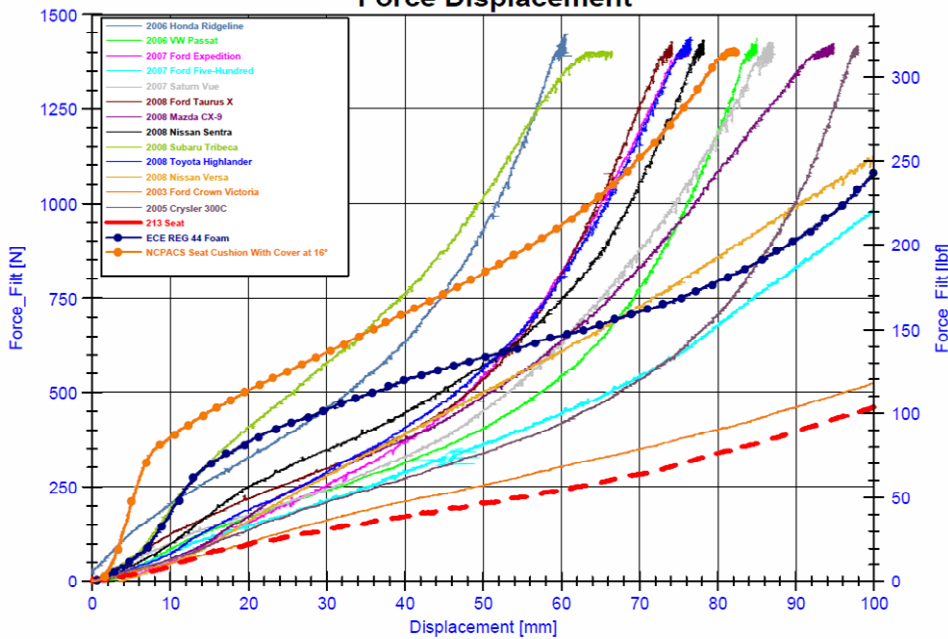
APPENDIX E ANOVA Analysis of Cushion Thickness Effect

Effect of Thickness, (95% Probability)			
Injury Criteria	Effect	Values	Statistically Different, $\alpha = 0.20$
Hic15_scaled	Thick > Thin	0.716 0.689	No
NIJ_scaled	Thick > Thin	1.126 1.085	No
Fz_scaled	Thick > Thin	1.520 1.412	No
Chdef_scaled	Thick > Thin	0.655 0.630	No
Ch3_scaled	Thick > Thin	0.852 0.843	No
Hdx_scaled	Thick > Thin	0.942 0.878	Yes

APPENDIX F NPACS Foam Cushion Stiffness

NPACS Foam Static Test

Rear Passenger Centerline Front Overlays Force Displacement



APPENDIX G Sled Pulse Characteristics

Independent variables

TEST #	PIN #	Peak Gs		Front or Rear Loading	Average Gs	Ratio A-B	Ratio C-D	Centroid		Ratio E-F (Centroid)	VPI
		Value (g)	Time (ms)		Value (g)	%	%	X Value (ms)	Y Value (g)	%	
1	2	25.36	36.16	Front	15.018	1.00	0.63	46.00	9.47	1.17	50.45
2	4	26.593	42.32	Front	15.81733	1.00	0.70	48.45	10.05	1.05	52.58
3	5	26.627	46.08	Front	16.49715	1.00	0.88	48.17	10.16	1.01	52.55
4	7	21.852	21.12	Front	15.90023	0.95	0.22	46.59	9.18	1.00	46.05
5	8	29.236	46.48	Front	16.33067	0.53	0.76	49.33	10.05	0.94	50.79
6	213	21.279	49.68	Rear	16.4112	0.95	1.28	45.43	9.09	1.02	46.06
7	14	33.854	60.8	Rear	17.00848	0.62	1.90	46.69	10.49	0.74	42.88
8	15	34.273	34.08	Front	16.39544	0.45	0.54	43.71	10.76	1.08	54.12
9	16	34.654	52.56	Rear	15.90221	0.51	0.95	50.08	10.57	0.76	46.23
10	20	31.69	46.08	Front	16.37635	0.53	0.71	50.13	10.20	0.97	51.13
11	25	26.752	10.88	Front	15.14911	0.87	0.11	41.41	9.77	1.00	48.70
12	4	26.517	41.52	Front	15.9318	1.00	0.70	47.61	10.04	1.06	52.54
13	2	25.673	35.44	Front	14.55039	1.00	0.62	45.45	9.62	1.17	51.21

APPENDIX H Pulse Effect Sled Test Results

Dependent variables

5th Female					
HIC 15	Chest G	Chest Deflection	NIJ	Neck Fz	Head Ex
700	60	52	1	2620	470
0.71	0.87	0.82	1.32	1.10	0.90
0.88	0.79	0.93	1.17	1.25	0.89
1.00	0.87	0.78	1.40	1.35	0.94
0.77	0.66	0.90	1.09	1.21	0.87
0.91	0.71	0.96	1.45	1.25	0.90
0.61	0.67	0.93	1.21	1.03	0.86
0.79	0.64	0.73	1.50	1.02	0.95
1.00	0.85	0.96	1.64	1.15	1.00
0.69	0.66	0.92	1.58	0.85	0.91
0.82	0.72	0.93	1.50	1.03	0.94
0.77	0.75	0.92	1.05	0.97	0.84

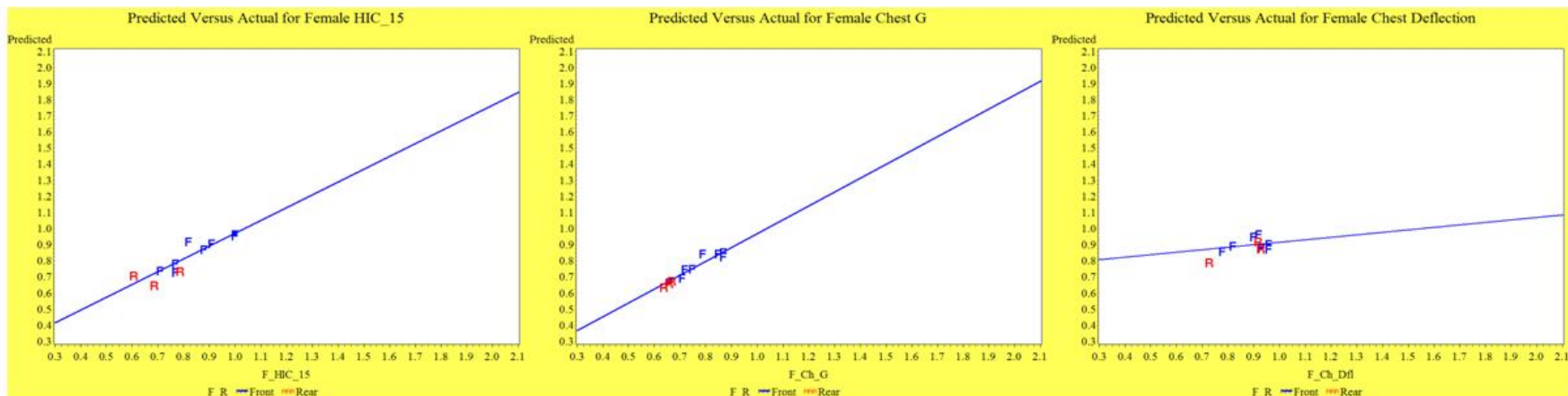
Three year old					
HIC 15	Chest G	Chest Deflection	NIJ	Neck Fz	Head Excursion
570	55	34	Value	1130	384.2
0.49	0.85	-	1.71	1.81	0.96
0.63	0.93	0.55	-	-	0.94
0.70	0.98	0.61	1.94	2.04	0.96
0.47	0.82	0.52	1.75	1.79	0.86
0.48	0.90	0.58	1.59	1.74	0.99
0.54	0.86	0.56	1.79	1.83	0.90
0.33	0.69	0.65	1.42	1.50	0.91
0.62	0.93	0.64	1.72	1.81	1.00
0.53	0.98	0.62	1.65	1.70	0.95
0.53	1.00	0.57	1.79	1.79	0.94
0.53	0.85	0.57	1.78	1.80	0.90
0.63	0.94	0.61	2.03	2.02	0.89
0.59	0.89	0.61	1.84	1.91	0.96

APPENDIX I Stepwise Linear Regression Models

5th Percentile Female Dummy				
<u>Injury Criteria</u>	<u>Input Term</u>	<u>Partial R²</u>	<u>Coefficient</u>	<u>Model R²</u>
HIC_15	VPI	0.51	+0.028	0.81
	Avg G	0.20	+0.096	
	Front_Rear	0.10	Front > Rear	
Chest G	VPI	0.69	+0.009	0.92
	A_B Ratio	0.08	+0.278	
	Peak G	0.08	+0.016	
	E_F Ratio	0.07	+0.426	
Chest Deflection	C_D Ratio	0.30	-0.085	0.37
	Front_Rear	0.07	Front > Rear	
NIJ	Peak G	0.71	+0.036	0.86
	Peak Time	0.09	+0.006	
	E_F Ratio	0.06	+0.539	
Neck Fz	VPI	0.31	+0.023	0.41
	Front_Rear	0.11	Front > Rear	
Head Excursion	Centroid G	0.60	+0.065	0.60

3 Year Old Dummy				
<u>Injury Criteria</u>	<u>Input Term</u>	<u>Partial R²</u>	<u>Coefficient</u>	<u>Model R²</u>
HIC_15	VPI	0.63	+0.030	0.68
	Front_Rear	0.05	Rear > Front	
Chest G	VPI	0.46	+0.023	0.65
	Centroid Time	0.18	+0.018	
Chest Deflection	Centroid G	0.56	+0.054	0.77
	C_D Ratio	0.10	+0.040	
	Centroid Time	0.10	-0.005	
NIJ	E_F Ratio	0.38	+0.615	0.52
			Front > Rear	
Neck Fz	VPI	0.31	+0.029	0.52
	Front_Rear	0.21	Front > Rear	
Head Excursion	VPI	0.31	+0.011	0.57
	A_B Ratio	0.26	-0.081	

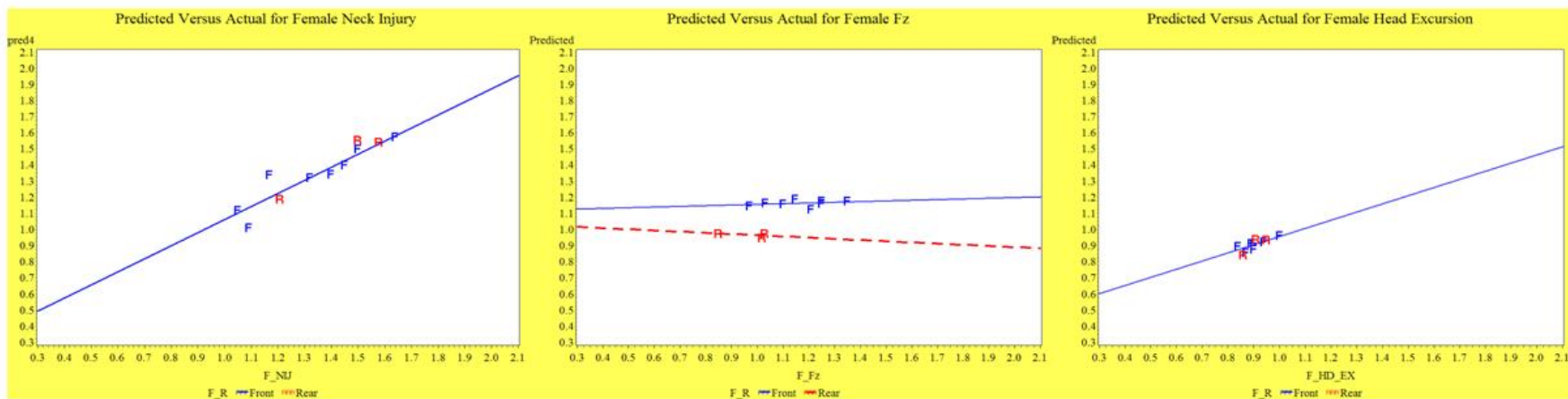
APPENDIX J Best Fit Models (5th Percentile Female)



HIC_15 0.81

Chest G 0.92

Chest D 0.37

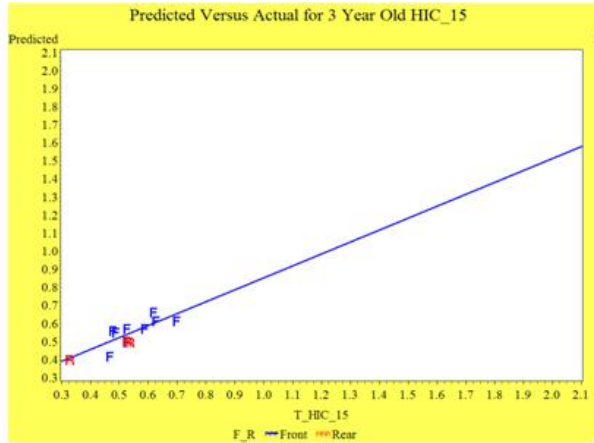


Nij 0.86

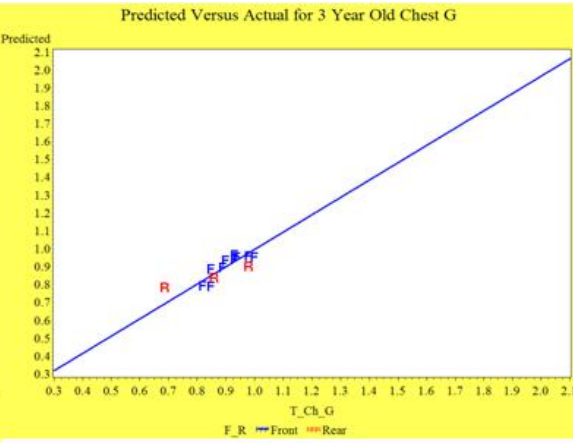
Neck Fz 0.41

Head Ex 0.60

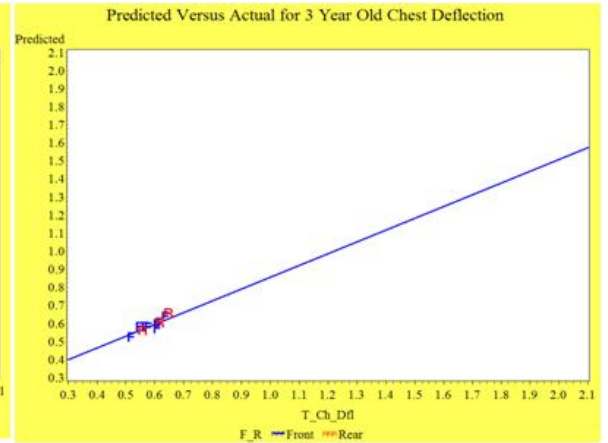
APPENDIX K Best Fit Models (3YO Child)



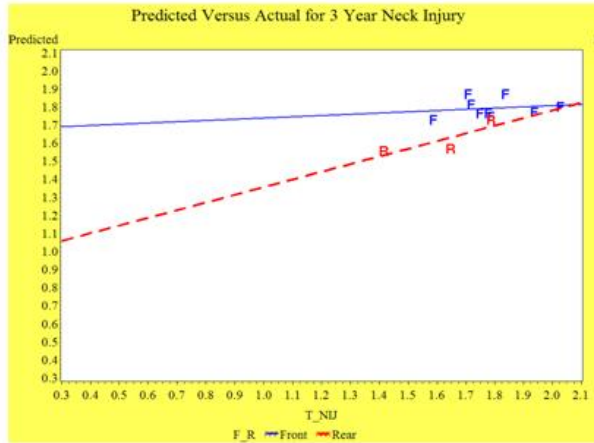
HIC_15 0.68



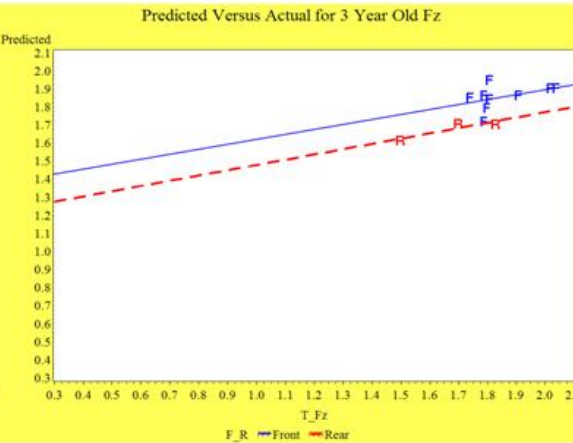
Chest G 0.65



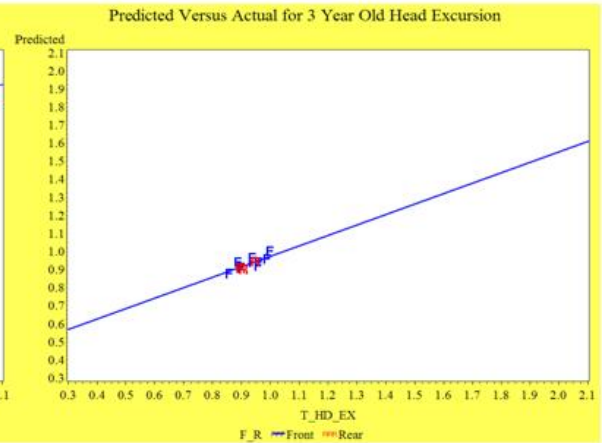
Chest D 0.77



Nij 0.52



Neck Fz 0.52



Head Ex 0.57

REAL WORLD ANALYSIS OF REAR SEAT OCCUPANT SAFETY IN FRONTAL CRASHES

Christopher Wiacek¹, Rodney Rudd¹, Lauren A. Collins²

¹National Highway Traffic Safety Administration

²Alpha Technology Associate, Inc.

USA

11- 0380

ABSTRACT

The National Highway Traffic Safety Administration's (NHTSA) Vehicle Safety Rulemaking and Research Priority Plan 2009 – 2011 describes the projects the agency plans to work on in the rulemaking and research areas in those calendar years. Specific programs identified in the plan included research to improve vehicle safety for rear seat occupants, children, and older people.

In support of the priority plan, an analysis of real-world crash data was conducted to determine the nature of the crash problem and examine the factors that contribute to rear seat occupant injury, including children and older people. A review of the National Automotive Sampling System Crashworthiness Data System (NASS-CDS) and Crash Injury Research and Engineering Network (CIREN) case data was conducted for restrained rear seat occupants in frontal crashes that sustained an Abbreviated Injury Scale (AIS) 3+ injury in 1998 model year and newer vehicles. For each occupant identified, a review of the accompanying investigation was conducted using a methodology similar to that described by Bean *et al.* [2009]. The authors were then able to identify occupant and crash characteristics associated with rear seat occupants commonly sustaining serious injuries in frontal crashes. For each occupant, a primary cause of the most severe injury was assigned and injury sources were identified. This review suggests that in the absence of overly severe frontal crash conditions and vulnerabilities due to advanced age, properly belted adults and children in age- and stature-appropriate child restraints are reasonably well-protected in the rear seat, although improvements could be achieved in some cases.

INTRODUCTION

Fatal crashes decreased by 9.9 percent from 2008 to 2009, and the fatality rate on U.S. roads has dropped to 1.13 per 100 million vehicle miles of travel. The injury rate per 100 million vehicle miles of travel decreased 6.3 percent from the previous year as well [NHTSA, 2010]. While many factors contribute to the reduction in the rate of injurious and fatal crashes, improvements in occupant protection are likely responsible for a sizeable portion of the long-term reduction. Front-row occupant protection in frontal crashes has benefited from recent developments in restraint performance and vehicle crashworthiness, which have been driven partly by manufacturers' efforts to improve vehicle scores in consumer information tests. Sherwood *et al.* reported in 2009 that 95% of the 2008 model year cars earned four or five stars in NHTSA's New Car Assessment Program and 91% earned the highest frontal crashworthiness rating from the Insurance Institute for Highway Safety. While much of the improvement in performance can be likely linked to improved frontal structures, the restraint systems for the occupants tested in those programs have improved as well. Kent *et al.* [2007] reported steadily increasing availability of seat belt pretensioner and force-limiting mechanisms, which, at the time, were nearing universal availability in the fleet. Since these advanced restraint technologies have typically been installed only in the first row, where their inclusion helps to improve test scores, occupants in the rear seating area have not seen the same benefits as their front seat counterparts.

Many recent studies have focused on the protection offered to rear seat occupants involved in frontal crashes. Some of these studies have found that, for some occupants, rear seating positions are associated with higher injury and fatality risk than front row

seating positions. Earlier studies, such as that by Evans and Frick [1988], suggested that rear seat occupants had 30 to 38 percent lower fatality risk compared to front seat occupants. When occupant age was considered, Kuppa *et al.* [2005] found that occupants younger than 50 years of age were more protected in the rear seat, but those above 50 years of age saw greater protection in the front seat. That same study included an analysis of frontal barrier crash data, which indicated that the rear seat dummies in 2004 model year vehicles experienced higher head and neck injury measures compared to the front seat dummies. An analysis of the 1991 through 1998 NASS-CDS by Parenteau and Viano [2003] identified teenage and adult occupants restrained by a lap and shoulder belt in the rear primarily experienced injuries of the thorax related to the shoulder belt. In a follow up study of the 1991 through 1999 NASS-CDS, Parenteau and Viano [2003b] identified head and extremity injuries were the body regions with the most frequent serious injuries (AIS 3+) from interior contact for 4-12 year old occupants in the rear restrained in a lap and shoulder belt.

More recently, Kent *et al.* [2007] concluded that rear seat occupants in newer vehicles were less effectively protected than front seat occupants, which they attributed to a relative decline based on increased effectiveness in the front seating positions due to the inclusion of advanced restraints in the newer vehicles. Bilston *et al.* [2010] explored this further by conducting a matched-cohort analysis of NASS-CDS data to examine the relative risk of AIS 3+ injury in the rear seat compared to the front seat. Their comparison divided the cases into vehicles of model year 1990-1996 and 1997-2007, and found that there was a significant difference in the AIS 3+ injury risk based on the model year with less relative protection in the rear seat of newer vehicles compared to the front seat. The findings echoed those from Kuppa *et al.* in 2005 that showed differences based on whether the occupant is a child or an adult over 50 years of age.

Using NASS-CDS data to calculate trends in injury risk for rear seat occupants, Esfahani and Digges [2009] found that belted and rear-seated adults between 16 and 50 years of age had a higher risk of

maximum AIS 2+ (MAIS) injuries in vehicles from the 2000s model years compared to the 1990s, although that risk was still lower than in the right front seat. Further investigating the effects of model year on rear seat occupant protection, Sahraei *et al.* [2009] performed logistic regression analysis on NASS-CDS data and found that newer model year vehicles were associated with a significantly higher AIS 2+ injury risk for belted rear seat occupants. Similar to some of their earlier work, Sahraei *et al.* [2010] conducted an analysis of model year segregated by occupant age group using Fatality Analysis Reporting System data. They found that the relative effectiveness of the rear seat compared to the front has decreased for belted children (less than 8 years of age) and belted adults (25 years and older) for the newer model years. None of the age groups of belted occupants demonstrated significantly better protection in the rear seats of newer vehicles, and of note was a negative effectiveness for belted adult occupants in the rear seat of newer vehicles.

The findings of several researchers presented above support further analysis of the rear seat occupant environment and injury causation problem. Many have concluded that improvements in the rear seat restraint environment would help to restore the rear seat advantage for all age groups in frontal crashes. The work presented in this paper represents one of the steps necessary to more completely understand the frontal crash experience of rear seat occupants.

METHODOLOGY

Using a technique similar to Bean *et al.* [2009], a detailed review of real-world frontal crashes with restrained, seriously injured rear seat occupants was conducted. The review focused on coded and non-coded data (photographs, summaries, crash diagrams, etc.), and resulted in the identification of critical factors contributing to the serious injuries of restrained rear seat occupants. The cases were selected from the NASS-CDS for the years 1997 through 2009 and the CIREN from 2000 to 2010. The following parameters were required for inclusion in the data set:

- 1998 and newer model year vehicles
- Frontal crash as primary injurious event where the general area of damage (GAD) and principle direction of force (PDOF)
 - GAD1='F'
 - GAD1='R' or 'L' and PDOF between 320 and 40 degrees
- Restrained rear seat (row 2 or higher) occupants
 - Lap and shoulder belts
 - Child restraints
- AIS level 3+ injury sustained

Fifty occupants in 45 vehicles were included in the final NASS-CDS data set. There were 29 occupants in 27 vehicles included in the final CIREN data set. For the NASS-CDS years examined, there were approximately 2,000 restrained rear seat occupants involved in frontal crashes prior to restricting the data set to only those occupants who sustained an AIS 3+ injury. Injured rear seat occupants included both sexes and affected a wide range of ages. The data was divided by age into occupants twelve years of age and under and those over twelve years of age. It was then determined whether the occupant was in an appropriate restraint condition for his or her stature and age. In effect, the data was divided into the following four major groups:

- 12 and under, properly restrained
- 12 and under, improperly restrained
- Over 12, properly restrained
- Over 12, improperly restrained

For ease of discussion, occupants 12 and under will be referred to as “children” while those over the age of twelve are designated “adults.”

In order to be classified as properly restrained, the occupant had to be in an age- and size-appropriate restraint that was installed and/or positioned properly during the event. Proper restraint for adult occupants meant a lap-and-shoulder belt was used and positioned properly. Proper restraint for child occupants was assessed according to NHTSA’s Car Seat Recommendations for Children [NHTSA, 2011a] along with the age, height, and weight guidelines set forth by the manufacturer of the child restraint system being used (if that information was

available in the case). For the purposes of this study, out-of-position occupants wearing their seat belts were still considered properly restrained.

Improperly restrained occupants were not in a restraint that was age- and/or size-appropriate, or the restraint was installed and/or positioned improperly during the event. Lap and shoulder belts, if used, may have been positioned improperly. An incorrect CRS based on the age and/or size of the child may have been used, or a child restraint, if one would have been appropriate, may not have been used at all. Figure 1 demonstrates the age and restraint condition distribution for the 79 total cases in the combined NASS-CDS and CIREN data set.

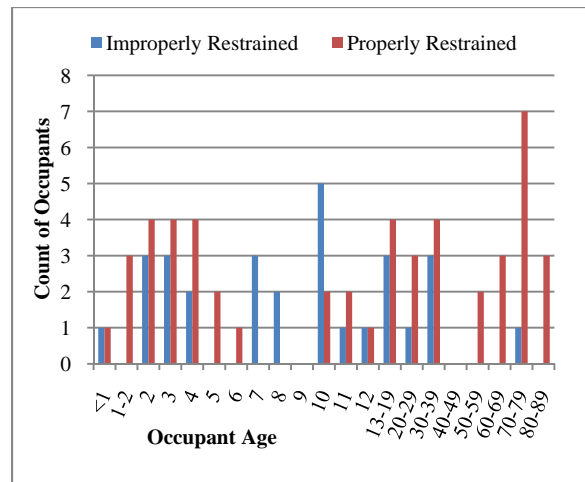


Figure 1. Age and restraint condition distribution for the combined NASS-CDS and CIREN data sets.

The cases were then divided amongst the authors, who then summarized each case using a standard format. The authors then assessed the primary and, if applicable, secondary factors associated with the MAIS injury sustained by the rear seat occupant. The distinction between primary and secondary factors is similar to what was described by Rudd *et al.* [2009].

The following section provides descriptions of the factors associated with injury causation assigned to the rear seat occupants in this data set:

Improper restraint system used: The restraint system (seat belt, child restraint, or combination

thereof) was not able to provide adequate protection for the occupant due to occupant size and restraint mismatch, incorrect belt routing, or other factors that interfered with the as-designed performance of the restraint. The type and severity of the occupant's injuries were directly associated with being improperly restrained.

Gross CRS misuse: Particular misuse of the child restraint is likely to result in injury to the occupant if involved in a crash [Decina, 2005]. Due to the general nature of field data collection, "critical" or "gross CRS misuse" was only attributed as a cause of injury in the most obvious of documented cases, and only when the restraint was appropriate for the child. For the purposes of this study, child restraints that were inappropriate for their occupant based on recommended best practices for child passenger safety did not fall under the designation of "gross misuse" but were simply categorized as "improper restraint."

High velocity change (delta-V): The deceleration of the vehicle during the event was of a severity that was believed to result in a delta-V near to or greater than the 56 km/h frontal impact test speeds in NHTSA's Federal Motor Vehicle Safety Standard No. 208 and the New Car Assessment Program consumer information program. There were no fatalities primarily attributed to high delta-Vs in this data set.

It should be noted that in many cases the delta-V was not estimated or the WinSMASH delta-V estimate was considered unreliable or underestimated due to the offset nature of the crash. In these cases, the barrier equivalent speed, crush measures, occupant compartment intrusion values and photos were used as a surrogate to estimate the severity of the crash. This method is consistent with Niehoff [2006]. The authors investigated the accuracy of WinSMASH as a function of crash mode, vehicle type, and vehicle stiffness and concluded WinSMASH underestimated longitudinal delta-V by 29 percent for crashes with a frontal overlap less than 50 percent.

Exceedingly severe: Similar to the description provided in Rudd *et al.* [2009], exceedingly severe crashes are those that meet any of the following:

- If known, the estimated delta-V crash for this crash was very high (over 64 km/h) and it is not likely the occupant could ride down crash forces and survive in the time and space available,
- All front seat belted occupants sustained incapacitating injuries or fatalities, and
- The occupant compartment at the position in question was compromised due to extensive intrusion.

Cases classified in this way were expected to be certain to produce moderate to severe injury even for a restrained rear occupant. All of the rear seat occupants in crashes classified as exceedingly severe sustained fatal injuries.

Contact with another occupant: The primary source of the occupant's severe injury was from contact with another occupant (restrained or unrestrained) in the vehicle.

Interior contact: The severe injury was sustained due to contact with hard interior surfaces adjacent to the occupant's seating position. In most cases, the direction and/or magnitude of the crash forces produced an occupant trajectory that resulted in contact with hard interior surfaces that led to serious injury. In others, this was due to occupant stature with respect to the rear compartment space.

Rear compartment intrusion: Severe intrusion occurred at the occupant's seating position leading to a reduction in ride-down space. These cases were occasionally characterized by restrained (and in certain cases, unrestrained) occupants in other vehicle seating locations sustaining minor or no injuries.

Occupant out of position: The coding or narrative in the case indicated that the occupant was not in a normal, upright seating position at the time of the event, and likely would not have sustained the same type or level of injury had they been seated properly during the crash.

Cargo intrusion: The primary source of injury was attributed to cargo intrusion into the rear seat as a result of being improperly secured in the trunk or cargo area of a vehicle.

Vulnerable occupant: The occupant was thought to be at higher risk of injury based on their elevated age or poor health condition. There was no specific minimum age for this factor, though typically these occupants were over the age of 65. These occupants' injury patterns and severities were more extensive than what would be expected with a younger occupant in similar crash conditions.

Given the case-review nature of this work, the NASS-CDS and CIREN cases have been combined for analysis and presentation purposes. No statistical analyses have been performed on the combined data, and no assessment of injury risk can be performed since case weights were not used.

RESULTS

The cases were grouped by age and whether the occupant was properly or improperly restrained at the time of the crash. For each grouping, the frequency of the primary and secondary causes of the injuries is tallied and presented below.

Occupants 12 and Under

Of the 79 occupants involved in the study, 24 involved children that were properly restrained (Table 1). The most frequently occurring cause of severe injuries was attributed to a high delta-V crash. There were four cases where none of the factors stood out, and the primary cause was listed as undetermined based on all of the available evidence. These four occupants sustained primarily abdominal injuries, but there were no reasons to expect improper restraint use resulting in poor belt fit or increased risk due to crash severity. A full assessment summary for each case reviewed in the study is available in the Appendix including the type of restraint in use such as lap and should belt, forward facing child seat or booster seat.

Table 1.
Causes of Injury to Properly Restrained Occupants 12 and Under

Cause	Primary	Secondary
High delta-V	8	2
Interior contact	7	1
Exceedingly severe	2	0
Cargo intrusion	1	0
Occupant out of position	1	0
Rear compartment intrusion	1	0
Undetermined	4	0
Total	24	3

The two most frequently occurring sources of injury in the properly restrained child occupants was the belt restraint and the front seat back support. In general, abdomen and torso injuries were associated with the belt restraint and head and extremity injuries were associated with the back of the front seats. The third most common source of injury was induced tension due to torso restraint, which is when the head pulls on the cervical spine and restrained torso due to deceleration and produces injurious tension and flexion. Injuries due to this mechanism are coded differently in CDS and CIREN, but have been combined for this study. CDS lists the source as "Other noncontact injury," though there is a contact between the occupant's torso and the restraint that leads to the injury. CIREN codes the belt as the injury producing component acting on the thorax, and specifies the tension mechanism in the cervical spine caused by the inertial loading from the head. This mechanism is more common in higher delta-V crashes. It should be noted that if there was evidence suggesting the source of the injury was different from what was coded in the investigation, the authors reassessed the source of injury for that case.

Table 2.
Source of Primary Injury to Properly Restrained Occupants 12 and Under

Source of Primary Injury	No. of Cases
Belt restraint webbing/buckle	8
Seat back support	8
Induced tension due to torso restraint	5
Undercarriage	1
Unknown	1
Unknown (likely driver's seat encroachment)	1
Total	24

There were 21 children classified as improperly restrained. The most frequently occurring cause of injury for improperly restrained children was an improper child restraint system being used (according to NHTSA's 4 Steps for Kids campaign). For older children, the vehicle seat belt may have been worn incorrectly (Table 3). Of interest, an improper restraint system being used was also determined to be a secondary cause of injury in six cases. In three cases it was assessed that the child seat was incorrectly installed.

Table 3.
Causes of Injury to Improperly Restrained Occupants 12 and Under

Cause	Primary	Secondary
Improper restraint system	12	6
Gross CRS misuse	3	0
Rear compartment intrusion	2	0
Interior contact	1	4
Cargo intrusion	1	0
Contact with another occupant	1	0
Occupant out of position	1	0
High delta-V	0	3
Total	21	13

The seat back support (i.e., the front seat back) was attributed as the primary source of injury for eight occupants (Table 4). In most cases, the occupant was not properly restrained or in an improper child seat and slipped out of the restraint system during the crash, making contact with the seat back. In the majority of the cases the occupant sustained head or

neck injuries, though, as with the properly restrained children, extremity injuries occurred as well.

Table 4.
Source of Primary Injury to Improperly Restrained Occupants 12 and Under

Source of Primary Injury	No. of Injuries
Seat back support	8
Belt restraint webbing/buckle	5
Hardware or armrest	2
B-pillar	1
CRS	1
Ground	1
Other occupants	1
Interior surface, excluding hardware or armrest	1
Floor or front center console	1
Total	21

For presentation purposes, Figure 2 combines data for the properly and improperly restrained children 12 and younger by primary injury cause and body region experiencing most severe injury. The data shows that the extremities are the most frequent maximum injured body region for children, occurring in 16 of the 45. Extremity injuries were typically associated with interior contact. Head injuries were the most significant injury for 11 of the child occupants, and occurred most often in crashes where the primary cause was improper restraint system used; they also occurred in cases of CRS misuse and in exceedingly severe crashes.

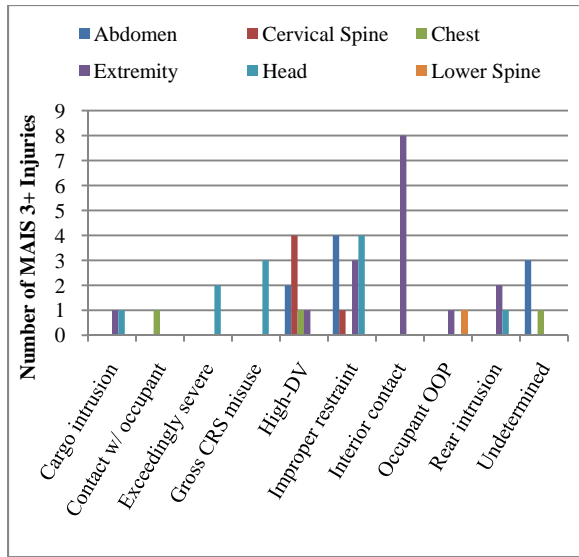


Figure 2. Injury Distribution by Primary Injury Cause for All Occupants 12 and Under.

Occupants Over 12

Twenty-six adult occupants were in the properly restrained category. The most prominent factor (present in ten of the cases) for adults who were properly restrained, was occupant vulnerability due to elevated age (Table 5). Crash severity (seven cases) and interior contact (five cases) were also common factors. It should be noted that high delta-V was identified as a secondary contributory factor to injury in four cases.

Table 5. Causes of Injury to Properly Restrained Occupants Over 12

Cause	Primary	Secondary
Vulnerable occupant	10	1
High delta-V	7	4
Interior contact	5	0
Rear compartment intrusion	2	0
Exceedingly severe	1	0
Occupant out-of-position	1	0
Cargo intrusion	0	3
Total	26	8

For the properly restrained category, the restraint system itself was the most frequent source of the severe injuries, in 16 of the 26 cases (Table 6). Considering that induced tension injuries due to the

torso restraint are also caused by the belt restraint, the total number becomes 18. The right side door (three cases) along with various other hard contact points were also noted as injury sources.

Table 6. Source of Primary Injury to Properly Restrained Occupants Over 12

Source of Primary Injury	No. of Injuries
Belt restraint webbing/buckle	16
Right side door	3
Induced tension due to torso restraint	2
Seat back support	2
Fold down armrest left	1
Interior B-Pillar	1
Unknown	1
Total	26

For improperly restrained adult occupants, the improper restraint condition was noted as the primary factor in four cases and a high delta-V was attributed as the cause in four of the eight cases reviewed (Table 7). In three of the cases, an improper restraint system was the secondary cause of the injury.

Table 7. Causes of Injury to Improperly Restrained Occupants Over 12

Cause	Primary	Secondary
Improper restraint system used	4	3
High delta-V	4	1
Interior contact	0	1
Vulnerable occupant	0	1
Total	8	6

For improperly restrained occupants, the source of the injury was attributed to the restraint system in five cases (Table 8). As further discussed in the paper, generally these were high delta-V crashes associated with injuries exclusive to the abdomen from the lap belt portion of the belt system.

Table 8.
Source of Primary Injury to Improperly
Restrained Occupants Over 12

Source of Injury	No. of Injuries
Belt restraint webbing/buckle	5
Seat back support	3
Total	8

For presentation purposes Figure 3 combines the data for the properly and improperly restrained adults by primary injury cause and injured body region. The most injured body region was the chest with fourteen cases; eight of those were related to occupant vulnerability. The second most common cause of chest injury was a high delta-V crash. In six cases, the occupant sustained abdominal injuries because of a high delta-V crash or being improperly restrained. Interior contact was primarily responsible for the extremity injuries. The findings are consistent with Parenteau and Viano [2003].

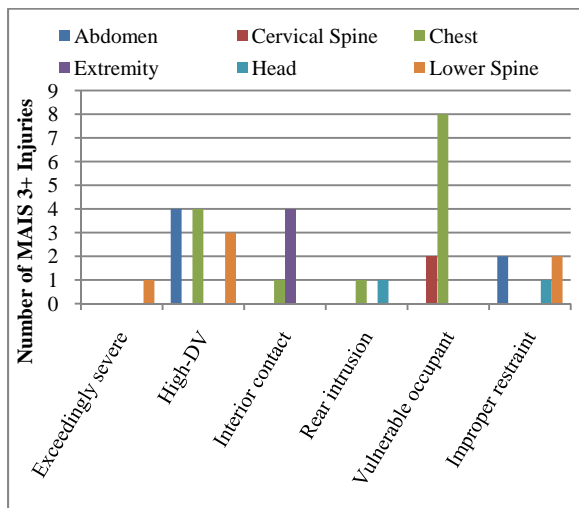


Figure 3. Injury Distribution by Primary Injury Cause for All Occupants Over 12.

DISCUSSION

The objective of this study was to identify specific factors that lead to injuries for restrained rear seat occupants in frontal crashes in order to better understand some of the recent statistical analyses that have suggested decreased protection in the second and third rows of newer vehicles. The following sections offer insight to some of the specific issues

that were found in the combined NASS-CDS and CIREN data set.

Improper Restraint

Though this data set was limited to restrained occupants, closer inspection revealed that the coded restraint status for some of the occupants did not reflect their actual status at the time of the crash. This was especially the case with occupants twelve and under: 21 out of 45 had their injuries attributed to being improperly restrained in some way. Premature graduation, as discussed in NHTSA [2001], was responsible for 18 of these 21 cases, while the remaining three were attributed to gross misuse of the child restraint. The most common type of premature graduation was booster-aged children being restrained only by the vehicle seat belt (as demonstrated in CDS case 2000-13-222 or CIREN 286006919).

The most common serious injuries for improperly restrained children were brain injuries, which occurred in seven of the 21 cases where the children were improperly restrained. Two of the properly restrained children sustained severe head injury, but they were in what was considered exceedingly severe crashes. In addition, a skull fracture and a facial fracture were also observed for improperly restrained children. The next most common injury for improperly restrained children were extremity fractures. These findings are also consistent with Paranteau [2003].

Of the three cases of injury assigned to gross CRS misuse, two of these children were seated in child restraints secured by a seat belt whose retractor was never properly locked. The third child in question (CDS No. 2006-12-161) was an infant restrained rear-facing (RF) in an infant-style CRS that did not receive the proper recall repair (per NHTSA recall No. 03C005000). The carrier separated from the base without this repair in place. The child was subsequently ejected from the vehicle and sustained fatal injuries.

Improper restraint was also observed for seven of the 34 adult occupants. For teenagers and adults, improper positioning of the vehicle seat belt was considered as such, if at the time of the event the

harness was not worn properly across the chest or there was potential slack in the shoulder harness. Though poor belt fitment or discomfort due to restraint routing geometry is usually thought of as a problem for smaller-statured occupants, individuals of a wide range of ages and statures were noted placing the shoulder belt portion under their arm or allowing the lap belt to sit too high on their abdomen (CDS No. 2009-11-113). Furthermore, slack in the shoulder harness may allow the occupant to slip out of the shoulder harness and sustain abdominal injuries from the lap belt especially in oblique or offset frontal impacts (CDS No. 2008-75-08). Although it cannot be conclusively determined from the data, the seated posture of the occupant at the time of the crash event may have contributed to the inadequate restraint of the upper body. Generally, these occupants sustained either abdominal injuries from the lap portion of the restraint or cervical spine injuries from impacting the front seat back because the upper torso was not properly used.

As a result of improper positioning or seat belt misuse during the event, injuries to both children and adults occurred. When improper seat belt positioning was observed in this data set, occupants may have sustained more serious injuries than if their seat belt had been positioned correctly, and especially experienced a high frequency of injuries to the soft tissues and organs of the lower abdomen. Improper positioning or intentional misuse of the shoulder belt portion of the seat belt puts a greater reliance on the lap belt to distribute loading, hence the propagation of injury to the areas of the body the lap belt covers. Occupants improperly using the shoulder belt also rarely sustained even minor upper torso injuries. The injury patterns were also similar to those occupants in a vehicle equipped with a lap only belt [Paranteau 2003b]. It is a reasonable assumption that if their seat belts were positioned properly, their injury patterns would have been different, even if they eventually sustained similar levels of injury.

Poorly installed CRS: Given known rates of poor CRS installation at 72.6 percent [Decina, 2005], this data implies that CRS being installed with minor misuses are still offering some level of protection to children. It is also of interest to note that there were only three cases containing a Lower Anchors and

Tethers for Children (LATCH) installed CRS in this data set. This may be due to the relatively recent introduction of the system in vehicles and on CRS, or it also may be a real-world indicator that there is a reduced chance of gross misuse with LATCH installations and therefore reduced chances of serious injuries occurring [Decina, 2006].

Booster-aged children in seat belts alone:

Though not recommended by NHTSA or other child passenger safety groups, the small number of fatal injuries seen in this data set for children of booster age may be evidence that lap and shoulder belts have the ability to offer some protection to children who would be best restrained by a booster seat. This is encouraging given that children between the ages of four and seven are only using booster seats and other CRS 55 percent of the time, with another 32 percent using seat belts only and thirteen percent completely unrestrained [NHTSA, 2010]. The children in this study that had prematurely graduated out of a booster seat typically sustained abdomen injuries due to poor lap belt fit and interaction with the pelvis.

Child passenger safety best practices: There was one case in this data set (CDS No. 2007-12-122) where two properly restrained children in the same vehicle suffered tension-based spinal injuries due to restraint of the torso and motion of the head. For each occupant, there is the possibility that they may not have experienced these injuries had they been in more “optimal” restraints. In the left rear seat of the vehicle in question (a 2006 Dodge Caravan), a 11 kg (24 lb), 86 cm (34”) tall 18 month-old female was properly restrained in a forward-facing convertible seat, but suffered an AIS 3 cervical spine fracture attributed to a high delta-V. Though she met the minimum requirements to ride forward facing, she would likely have benefitted from remaining rear-facing in that convertible, as NHTSA’s Car Seat Recommendations for Children state, “[c]onvertible and 3-in-1 car seats typically have higher height and weight limits for the rear-facing position, allowing you to keep your child rear-facing for a longer period of time.” Though the make and model of her CRS was unknown, according to NHTSA (Ease of Use Ratings, 2011) the majority of convertibles in the U.S. market would have continued to accommodate a child of her size rear-facing for some time.

In the right rear of the same vehicle, a 109 cm (43”), 20 kg (44 lb) three year-old male was restrained in a booster of unknown make and model and similarly suffered an AIS 3 cervical spine fracture. By most recommended child passenger safety best practices, he was too young for a booster seat; however, it is possible that he met the height and weight requirements of the booster seat he was using. He would likely have benefitted from being restrained in a five-point harness and may not have suffered the cervical spinal fracture if he had been.

Another similar case, CIREN 286037005, was a crash with a two year-old female seated in a five-point harness forward-facing seat who was 97 cm (38”) tall and 14 kg (31 lb). Next to her, in the right seat position, was a three year-old male of 104 cm (41”) height weighing 17 kg (37 lb) seated also in a five-point harness forward-facing seat (CIREN No. 286036859). She sustained upper cervical spine fractures and dislocations in a moderate severity crash, while the three year-old male in the next seat sustained only upper extremity fractures due to front seat back contact. Her tension-related neck injury may have been prevented had she been seated rear-facing (as long as her CRS could have accommodated her).

Interior Contact

Another common cause of injury in both the child and adult cases was interior contact. The cases in this study demonstrate that the most common maximum injuries for restrained occupants 12 and under were upper and lower extremity fractures, most commonly sourced to the seat back. As demonstrated in Parenteau [2003], the majority of injuries to properly restrained (lap-shoulder belted) children in the rear seat are upper and lower extremity injuries.

Properly restrained adults also sustained injuries due to interior contact, with four sustaining extremity fractures associated with seat back or door panel contact. Though the extremity injuries seen in this study are AIS 3, many of the occupants sustaining these injuries were not injured significantly otherwise. Given that the restraint of extremities is difficult in the rear seat environment, efforts to address the stiffness of various contact points may help to ameliorate some of these injuries.

Vulnerable Occupants

Twelve of the 34 adult occupants in this data set experienced injury due in some way to physical vulnerabilities as a result of age. They included eight women and four men, and ranged in age from 64 to 86 years. Eleven were properly restrained, and most sustained their highest AIS injury as a result of seat belt loading on the thorax, which led to rib fractures, lung contusions, other thoracic cavity injuries, and in three cases fatal heart lacerations. The two CIREN cases in which occupant vulnerability was a primary cause involved occupants who had been clinically diagnosed with osteoporosis, which was a critical factor in their injury. Of the five fatalities to adult occupants observed in this data set, four were attributed directly to the occupant’s vulnerability and the fifth was to a 75 year old female in an exceedingly severe crash due to the intrusion (CDS No. 2001-73-141). It should be noted that there was a 22 year old male seated next to the 75 year old female who sustained abdominal injuries sourced to improper restraint. This occupant was not exposed to the significant intrusion and for his position the event was not considered exceedingly severe. CDS case 2004-3-096 was fairly benign, with an estimated 32 km/h (20 mph) delta-V; however, the 72 year-old rear seat occupant sustained fatal thoracic injuries sourced to the seat belt. CDS case 2007-08-118 is another example where the risk of injury to older rear seat occupants is seen. Though the event was relatively severe, with an estimated 53 km/h (33 mph) delta-V, the front seat occupants suffered moderate belt-related injuries while the 86 year-old occupant in the right rear sustained a fatal heart laceration along with numerous rib fractures, a basilar skull fracture, and brain injuries. This occupant’s chest, because of age-related vulnerabilities, was not able to handle the severe loading from the shoulder belt. The elevated risk for older occupants in the front versus the rear seat has been documented in many recent studies [Kuppa *et al.*, 2005; Sahraei *et al.*, 2010; Bilston *et al.*, 2010] and the review of these field crashes affirms those findings.

Efforts to address the increased risk to vulnerable occupants in all seating positions are underway and further justified by these findings. Based on the earlier findings in the statistical analyses by Kuppa *et*

al. [2007] and Sahraei *et al.* [2010], there may be a need to encourage older, and potentially more vulnerable, adult occupants to occupy first row seats whenever possible so they may benefit from features of advanced restraint systems.

High Delta-V and Exceedingly Severity Crashes

Twenty-nine of the 79 rear seat occupants' maximum injuries were due either primarily or secondarily to a high level of compartment deceleration during the crash, which was based on delta-V or crush. Five were sourced to intrusion of the rear seat compartment at the occupant's location, which caused injury due to a reduction in the occupant's ride-down space. Another three were deemed exceedingly severe, or close to unsurvivable as was described by Bean *et al.* [2009].

Due to limitations associated with comparing delta-V in field crashes to those in laboratory tests, the extent to which some of these crashes were more severe than consumer information or regulatory tests could not be determined. The crashes in which occupant injuries were attributed to a high delta-V were potentially of a similar severity as that present in NCAP or IIHS frontal tests. There is potential for rear occupant crash protection improvements in some of these crashes, since some of them had front occupants who sustained less severe injuries. The injuries in these crashes were typically sourced to the belt restraint, suggesting that attention should be paid to fit or energy management of rear seat belts in order to increase rear occupant protection.

Exceedingly severe crashes where properly restrained rear seat occupants suffer a fatality are likely to show corresponding front seat fatalities. For example, the rear seat injuries in CDS case 2002-12-186 were attributed to the exceedingly severe nature of the crash. In this case, all three occupants (driver, right front passenger, and right rear passenger) sustained fatal injuries.

Undetermined Cause

A few of the cases included in this study did not exhibit any of the other factors previously discussed, and were therefore not categorized with the other cases. All of the cases involved properly restrained

child occupants, and the severity levels of these crashes were not believed to be high. CIREN cases 286000006 and 608090285 involved ten year-old males wearing the three-point lap and shoulder belt (both were at or above the recommended height of 145 cm for graduation out of a booster) who sustained abdominal injuries attributed to the lap belt. CIREN cases 377037363 and 608063219 involved four and five year-old females who were properly restrained in booster seats. CIREN case 377037363 was borderline high severity in an underride situation, but the restrained driver sustained very minor injuries while the booster-seated four year-old female sustained multiple rib fractures and lung contusions from belt loading. CIREN case 608063219 involved a five year-old female who sustained a bladder rupture in a very minor crash in which all of the other properly restrained occupants were not injured. She exhibited abrasions over her waistline from lap belt contact. The CIREN center noted that the belt fit may have been sub-optimal, but the child was in an appropriate restraint. Regardless, these four cases suggest that even properly restrained children in moderate severity crashes are sustaining injuries due to the restraints.

CONCLUSION

Given the relatively large number of occupants injured as a result of perceived improper restraint use, there is a potential need to reinforce NHTSA's CRS use recommendations as well as increase awareness of proper belt use by adults seated in the rear seat. While proper restraint use may not have protected the occupant from all injuries, the conditions of the cases in this study did suggest that many of the injuries were directly related to a failure to use the restraint system appropriately.

Of the adult occupants in this dataset, physical vulnerabilities due to advanced age were responsible for a large number of the major injuries. Injuries from interior contact, typically involving the extremities, were also common when crash severity was not considered an issue. The majority of the remaining adult cases were attributed to crash severity, which was considered high enough that the level of injury sustained was not unexpected. Many

children were also considered to be injured due to high delta-V and exceedingly severe crashes.

While many of the crashes were considered to be a higher severity, this does not, however, suggest there is no room for improvement in the area of rear seat occupant protection. As suggested by the data shown by prior researchers, the relative protection in the rear seat has decreased in newer model year vehicles. Furthermore, there is concern that as vehicle front structures become stiffer to manage intrusion in the occupant compartment, the vehicle crash pulse will also increase in magnitude. This may increase the risk of serious injury to rear seat occupants whose primary protection is only the seat belt. Incorporation of enhanced occupant energy management features to improve ride-down and better distribute the loading across the chest, along with improved fitment of the restraints to reduce slack and improved belt positioning across the torso, may have mitigated the serious injury sustained by some of the occupants in these crashes.

REFERENCES

75FR70670, Docket NHTSA-2009-0108

Bean James D., *et al.* (2009) Fatalities in Frontal Crashes Despite Seat Belts and Air Bags. DOT HS 811 202, National Highway Traffic Safety Administration, Washington, DC.

Bilston, L.E., *et al.* (2010) "A matched-cohort analysis of belted front and rear seat occupant in newer and older model vehicles shows that gains in front occupant safety have outpaced gains for rear seat occupants." *Accident Analysis and Prevention*, doi:10.1016/j.aap.2010.06.002.

Decina L.E., *et al.* (2005) Misuse of Child Restraints: Results of a Workshop to Review Field Data Results. DOT HS 809 851, National Highway Traffic Safety Administration, Washington, DC.

Decina, L.E., *et al.* (2006) Child Restraint Use Survey: LATCH Use and Misuse. DOT HS 810 679, National Highway Traffic Safety Administration, Washinton, DC.

Esfahani, E.S. and Digges, K. (2009) "Trend of rear occupant protection in frontal crashes over model years of vehicles." SAE World Congress, paper no. 2009-01-0377.

Evans, L. and Frick, M. (1988) "Seating position in cars and fatality risk." *American Journal of Public Health*, 78(11), 1456-1458.

Kent, R., Forman, J. Parent, D.P and Kuppa, S. (2007) "Rear seat occupant protection in frontal crashes and its feasibility." 20th International Technical Conference on the Enhanced Safety of Vehicles, paper 07-0386.

Kuppa, S., Saunders, J. and Fessahaie, O. (2005) "Rear seat occupant protection in frontal crashes." 19th International Technical Conference on the Enhanced Safety of Vehicles, paper 05-212.

National Highway Traffic Safety Administration (2001) *Premature Graduation of Children to Seat Belts*. Traffic Tech: Technology Transfer Series, Number 253, Washington, DC.

National Highway Traffic Safety Administration (2010) *The 2009 National Survey of the Use of Booster Seats*. DOT HS 811 377 National Center for Statistics and Analysis, Washington, DC.

National Highway Traffic Safety Administration (2010) "Traffic Safety Facts – Early Edition." DOT HS 811 402.

National Highway Traffic Safety Administration (2011a) *Car Seat Recommendations for Children*, <http://www.nhtsa.gov/Safety/CPS>. Accessed March 22, 2011.

National Highway Traffic Safety Administration (2011b) *Ease-of-Use Ratings*, <http://www.nhtsa.gov/Safety/Ease-of-Use>. Accessed January 6, 2011.

Niehoff, P., & Gabler, H. (2006). *The Accuracy of WinSMASH Delta-V Estimates: The Influence of Vehicle Type, Stiffness, and Impact Mode*. Paper No. 06B-306, Society of Automotive Engineers, Warrendale, PA.

Parenteau, C. and Viano, D.C. (2003a) "Field Analysis of Rear Occupant Injuries Part I: Adults and Teenagers." SAE World Congress, paper no. 2003-01-153.

Parenteau, C. and Viano, D.C. (2003b) "Field Analysis of Rear Occupant Injuries Part II: Children, Toddlers, and Infants." SAE World Congress, paper no. 2003-01-154.

Rudd, R.W., Bean, J., Cuentas, C., Kahane, C.J., Mynatt, M. and Wiacek, C. (2009) "A Study of the factors affecting fatalities of air bag and belt-restrained occupants in frontal crashes." 21st International Technical Conference on the Enhanced Safety of Vehicles, paper number 09-0555.

Sahraei, E., Soudbakhsh, D. and Digges, K. (2009) "Protection of rear seat occupants in frontal crashes, controlling for occupant and crash characteristics." Stapp Car Crash Journal, vol. 53, pp. 75-91.

Sahraei, E., Digges, K. and Marzougui, D. (2010) "Reduced protection for belted occupants in rear seats relative to front seats of new model year vehicles." Annals of Advances in Automotive Medicine, vol. 54.

Sherwood, C.P., Nolan, J.M. and Zubay, D.S. (2009) "Characteristics of small overlap crashes." 21st International Technical Conference on the Enhanced Safety of Vehicles, paper 09-0423.

Appendix

CAUSE OF INJURY	PROPERLY RESTRAINED OCCUPANTS	
	UNDER 12	OVER 12
Cargo intrusion	<i>Primary</i> <ul style="list-style-type: none"> • NASS 2007-75-146 (2L, UE, FF) 	<i>Secondary</i> <ul style="list-style-type: none"> • NASS 2000-12-086 (2R, AB) • NASS 2008-13-134 (2R, TH) • CIREN 459042257 (2L, LS)
Exceedingly severe	<i>Primary</i> <ul style="list-style-type: none"> • NASS 2000-11-130 (2L, H, RF) • NASS 2002-12-186 (2R, H, L&S) 	<i>Primary</i> <ul style="list-style-type: none"> • 2001-73-141 (2R, LS)
High severity delta-V	<i>Primary</i> <ul style="list-style-type: none"> • NASS 2007-41-218 (2L, LE, RF) • NASS 2007-12-122 (2L, CS, FF) • NASS 2007-12-122 (2R, CS, B) • NASS 2008-13-222 (2R, TH, B) • CIREN 286037005 (2L, CS, FF) • CIREN 554089295 (3L, AB, L&S) • CIREN 842003310 (2R, AB, L&S) • CIREN 842023821 (2C, CS, B) <i>Secondary</i> <ul style="list-style-type: none"> • NASS 2006-12-161 (2L, LE, FF) • CIREN 286036859 (2R, UE, FF) 	<i>Primary</i> <ul style="list-style-type: none"> • NASS 2008-73-176 (2L, TH) • NASS 2000-12-086 (2R, AB) • NASS 2004-43-036 (2R, TH) • CIREN 100121436 (2L, AB) • CIREN 459042257 (2L, LS) • CIREN 830069711 (2R, LS) • CIREN 852174467 (2L, TH) <i>Secondary</i> <ul style="list-style-type: none"> • NASS 2000-12-091 (2R, TH) • NASS 2009-81-70 (2C, TH) • NASS 2006-48-261 (2L, CS) • CIREN 591142661 (2L, AB)
Interior contact	<i>Primary</i> <ul style="list-style-type: none"> • NASS 2007-78-102 (2R, LE, B) • CIREN 160139577 (2L, UE, B) • CIREN 286008946 (2L, LE, FF) • CIREN 286035771 (2L, LE, B) • CIREN 286036859 (2R, UE, FF) • CIREN 558020414 (2L, LE, FF) • CIREN 608042073 (2L, UE, FF) <i>Secondary</i> <ul style="list-style-type: none"> • NASS 2007-41-218 (2L, LE, RF) 	<i>Primary</i> <ul style="list-style-type: none"> • NASS 2002-43-095 (2R, UE) • NASS 2005-09-028 (2R, UE) • NASS 2004-48-059 (2R, UE) • NASS 2003-75-031 (2L, TH) • CIREN 551091328 (2R, UE)
Occupant out of position	<i>Primary</i> <ul style="list-style-type: none"> • NASS 2006-48-19 (2L, UE, FF) 	<i>Primary</i> <ul style="list-style-type: none"> • CIREN 591142661 (2L, AB)
Rear compartment intrusion	<i>Primary</i> <ul style="list-style-type: none"> • NASS 2006-12-161 (2L, LE, FF) 	<i>Primary</i> <ul style="list-style-type: none"> • NASS 2005-02-011 (2L, H) • NASS 2004-45-227 (2R, TH)
Undetermined	<i>Primary</i> <ul style="list-style-type: none"> • CIREN 286000006 (2R, AB, L&S) • CIREN 377037363 (2L, TH, B) • CIREN 608063219 (2C, AB, B) • CIREN 608090285 (2R, AB, L&S) 	
Vulnerable occupant		<i>Primary</i> <ul style="list-style-type: none"> • NASS 2009-82-163 (2L, TH) • NASS 2000-12-091 (2R, TH) • NASS 2004-03-096 (2L, TH) • NASS 2009-81-70 (2C, TH) • NASS 2006-48-261 (2L, CS) • NASS 1999-45-809 (2L, TH) • NASS 2008-13-134 (2R, TH) • NASS 2007-08-118 (2R, TH) • CIREN 165428 (2L, CS) • CIREN 591139732 (2R, TH) <i>Secondary</i> <ul style="list-style-type: none"> • CIREN 551091328 (2R, UE)

IMPROPERLY RESTRAINED OCCUPANTS		
CAUSE OF INJURY	UNDER 12	OVER 12
Cargo intrusion	<i>Primary</i> • NASS 2006-12-070 (2R, H, L&S)	
Contact with another occupant	<i>Primary</i> • NASS 2004-79-188 (2L, TH, L&S)	
Gross CRS misuse	<i>Primary</i> • NASS 2006-12-161 (2L, H, RF) • NASS 2001-04-065 (2L, H, FF) • NASS 2005-48-125 (2L, H, B)	
High severity delta-V	<i>Secondary</i> • NASS 2008-13-222 (2R, H, B) • NASS 2004-04-069 (2L, H, B) • CIREN 591152151 (2R, AB, L&S)	<i>Primary</i> • NASS 2008-75-08 (2R, AB) • NASS 2002-79-016 (2R, LS) • NASS 2002-79-016 (2L, AB) • NASS 2001-73-141 (2L, TH) <i>Secondary</i> • NASS 2000-81-053 (2L, AB)
Improper restraint system	<i>Primary</i> • NASS 2008-13-222 (2R, H, B) • NASS 2004-04-069 (2L, H, B) • NASS 1999-45-190 (2C, CS, L&S) • NASS 2000-13-222 (2L, AB, L&S) • NASS 2002-43-127 (2L, H, L&S) • NASS 2006-13-117 (2R, UE, L&S) • CIREN 286006919 (2R, AB, L&S) • CIREN 286016523 (2L, H, L&S) • CIREN 286021930 (2L, LE, L&S) • CIREN 286021946 (2R, LE, L&S) • CIREN 377044044 (2L, AB, B) • CIREN 591152151 (2R, AB, L&S) <i>Secondary</i> • NASS 2000-12-157 (2R, LE, L&S) • NASS 2004-79-188 (2L, TH, L&S) • NASS 2002-78-151 (2R, H, L&S) • NASS 2004-48-94 (2R, OS, L&S) • NASS 2004-73-122 (2L, LE, L&S) • NASS 2006-12-070 (2R, H, L&S)	<i>Primary</i> • NASS 2009-11-113 (2R, LS) • NASS 2000-81-053 (2L, AB) • NASS 1999-73-062 (2L, LS) • CIREN 286020311 (2R, H) <i>Secondary</i> • NASS 2008-75-08 (2R, AB) • NASS 2002-79-016 (2R, LS) • NASS 2002-79-016 (2L, AB)
Interior contact	<i>Primary</i> • NASS 2000-12-157 (2R, LE, L&S) <i>Secondary</i> • NASS 2002-43-127 (2L, H, L&S) • CIREN 286016523 (2L, H, L&S) • CIREN 286021930 (2L, LE, L&S) • CIREN 286021946 (2R, LE, L&S)	<i>Secondary</i> • CIREN 286020311 (2R, H)
Occupant out of position	<i>Primary</i> • NASS 2004-48-94 (2R, LS, L&S)	
Rear compartment intrusion	<i>Primary</i> • NASS 2002-78-151 (2R, H, L&S) • NASS 2004-73-122 (2L, LE, L&S)	
Vulnerable occupant		<i>Secondary</i> • NASS 2001-73-141 (2L, TH)

2 - Second row, 3 - Third row, L – Left side position, C - Center position, R - Right side position, UE - Upper extremity injury, H - Head injury, LE - Lower extremity injury, CS - Cervical spine injury, TH - Thorax injury
 AB - Abdomen injury, LS - Lower spine injury, RF – Rear-facing restraint, FF – Forward-facing restraint, B – Booster, L&S – Lap and shoulder

DEVELOPMENT OF A TEST TOOL TO ANALYSE AIRBAG INDUCED INJURIES

Arturo, Dávila

Mario, Nombela

IDIADA Automotive Technology SA

Spain

Paper number 11-0345

ABSTRACT

Currently, the airbag is the most important and effective restraint system available on the market. Nevertheless, its activation is related to some facial, ocular and auditory injuries. The principal objective of this project was to develop an evaluation tool capable of predicting injuries to the face.

The project was designed because previous research shows that the above-mentioned injuries occur under velocities that vary in the limits of activation/no activation set by each manufacturer ($\Delta V < 48$ km/h). The majority of these injuries occur in frontal impacts where the interaction between driver and airbag is the greatest.

Furthermore, shorter occupants (<1.60 m) tend to receive the most severe injuries due to their proximity to the airbag. The most common injuries are facial, ocular and skin abrasion. The noise produced by an activating airbag is generally over the safe limit for a person, and can cause permanent damage to the internal ear. The explosion is generated by the chemical reaction of gases that may produce intoxication or skin injury.

Therefore, the first task of this project was to evaluate the injury map related to airbag activation in frontal impact, although other configurations were considered. A revision of the state of the art and the direct relation with possible facial, ocular and auditory injuries and intoxication was also performed. The next task was to develop a set of testing procedures for the evaluation of the established injuries that airbag deployment causes to the occupants. To finalize, an assessment of the developed tools and protocols was made.

The project activities focussed on the development of a measuring system designed to predict facial and ocular injuries resulting from blunt impacts during contact with the airbag, estimating the risk of suffering facial bone fractures or severe ocular injury. This was accomplished through a special mask that measures the pressure applied at specific points of the head, such as nose tip, eyes, eyebrows, jaw, etc.

To estimate the risk of auditory injury, a specially designed dummy head made use of special microphones to measure the sound and pressure levels found in the cabin during airbag activation. This head can be used both in static and dynamic tests.

For intoxication and skin abrasion injuries, a protocol and a tool to measure the amount of toxic gases released from the explosion of the airbag was developed. In this particular case, the most relevant toxic gases were selected and the adequate instrumentation established for the development of the test.

With the three elements combined, an overall evaluation on the severity of the airbag system to be assessed can be made, allowing manufacturers and designers to create more effective yet non-injurious systems.

The results of the project are in line with the proposed objectives, and the developed tools and the protocols are good enough to provide a more stringent evaluation of restraint systems and will also help in research regarding injury mechanisms in various accident configurations.

INTRODUCTION

Airbags, in spite of being perhaps the most effective safety restraint system in combination with the seat belt, are also associated with facial and hearing injuries. They have been linked to numerous nonfatal injuries of different severities which include eye, face, upper extremities, aortic rupture, lung contusions and thoracic abdominal injuries. The most frequent are injuries to the head, including audition.

Research has shown that the injuries induced by the airbag deployment are mostly minor, although some occupants did suffer more serious injuries, according to the Abbreviated Injury Scale (AIS) (Otte, 1995). Nevertheless, the use of airbags has led to an overall reduction in AIS 2+ injuries (Kuhn, Morris and Witherspoon, 1995). Another study conducted with European and Japanese airbag deployed vehicles (Morris, 1996) examined 186 frontal crashes, and the majority of the drivers

sustained AIS 1 injuries, being the head and the face the most commonly injured body region. From the analysed injuries involving airbag deployment, Kuhn, Morris and Witherspoon (1993) found that half of them were attributed to the airbag itself.

One of the reasons for sustaining airbag induced injuries is the proximity of body regions to the deploying airbag. Drivers who must sit close to the steering wheel to drive because of their height or any medical reason are more susceptible to being injured in case of accident. Sixteen of the 38 adult drivers whose deaths have been attributed to airbags were 160 cm tall or shorter, and all but one with fatal neck injuries were women.

Adams and Petri (1996) have suggested that the airbag induced injuries may be associated with specific design features, such as the amount of released energy, the speed of inflation, the volume, shape or folding pattern of the bag, etc. Also chemicals involved in inflating the bag have been implicated in injuries, so as the utilized pyrotechnic device. Some of the injuries come from the non-deployment, spontaneous deployment, airbag slap and bottom out.

We can state that airbags have a net injurious effect when activated in low severity crashes whereas they have a net protective effect in high severity accidents, meaning that the generality of the provoked injuries arise from low severity collisions or misfire situations. Also, the crash severity level at which airbags are protective is relatively higher for women than for men.

Vehicle speed at the time of the impact has been analyzed, showing that severe injuries such as orbital fractures, traumatic cataract and vitreous or retinal haemorrhage are found for speeds over 48 km/h. Meanwhile, below this velocity threshold, other severe injuries occur such as retinal detachment, ruptured globe, and worsened vision. In the case of hearing loss or auditory injury, the injurious mechanism is due to the elevated sound level of the explosion, the vehicle deformation and the pressure generated inside the cabin. These produce different effects inside the human ear, which can translate into temporal loss of hearing or permanent ear damage.

One important aspect to mention is that an airbag increases the amount of energy being released during an accident, which in turn increases the frequency of injuries sustained by the driver, yet they drastically reduce the probabilities of severe and fatal injuries to the body. This means that an airbag exerts distributed restraining forces over the head, face and upper chest region of the passenger, acting as a cushioning system and minimizing the

most severe scenarios for serious injuries but remains as an added system that, in certain cases, can cause more damage than the damage it was intended to avoid.

In this paper, three approaches to analyse injuries caused by deploying airbags have been carried out: the injuries to the face and eyes, the injuries to the hearing system and the toxicity of the chemicals found in the cabin after airbag explosion. The objective was to develop a system that was able to measure the amount of injury suffered by the passengers in the case of an accident in the nearby threshold of 50 km/h, where the effectiveness of airbags is questioned due to the injury potential they also represent. To achieve the objective, a special force measuring mask, a microphone adapted dummy head and a toxicity analysis procedure were evaluated.

DEVELOPMENT

Facial Injury Analysis

Facial injury analysis was set to obtain the amount of force or pressure that the occupant receives when interacting with the airbag. By design, the airbag is intended to act as a cushion between the user's head and upper chest and the steering wheel, dashboard and other components. To achieve this, a very fast chemical reaction inflates the airbag in less than 50 milliseconds, time when the occupant is about to reach the contact point with the airbag and provide energy absorption of the user dynamic movement. Generally, the energy exerted by the airbag is in the same range as that of the user, eliminating some of the negative effects on the user. In some cases, especially when the crash is under 50 km/h and the airbag activates, the energy of the passenger is not enough to offset the energy from the airbag, leading to face injuries.

In order to measure the amount of damage produced to the face of an occupant, a special vinyl dummy mask was developed. This mask is equipped with a series of force sensors that are distributed throughout the face in specific locations where injury can occur. The mask comes from a Hybrid III 50th percentile male dummy, which is the most widely used crash test dummy in the world for the evaluation of automotive safety restraint systems in frontal crash testing. The dummy is a regulated test device in the European ECE regulations and in the US safety standards. The skull and cap of Hybrid III 50th percentile male dummy are one piece cast aluminium parts with removable vinyl skins. The head skin of the dummy offers high bio-fidelity with its anthropomorphic structure.

To develop and improve the prototype, the required instrumentation had to comply with certain criteria, such as reliability, robustness, repeatability, ease of mounting, time response and functionality. All of these capable of being mounted over a vinyl dummy skin. The time response of the sensor was of special importance since the airbag inflates and starts deflating in about 0.2 seconds after the impact. For this task, Flexiforce sensors were selected because they can measure both static and dynamic forces of up to 4500 N and are thin enough to enable non-intrusive measurement. The sensors do not interfere with the dummy head profile and bio-fidelity. They use a resistive-based technology in which resistance is inversely proportional to applied force. Their flexibility enables them to be placed on non-planar surfaces such as a dummy face. The sensing area is a circle with a diameter of 9.53 mm, which is very adequate for positioning on critical points for precise measurement.



Figure 1. Modified dummy mask.

To validate the prototype and the latter evaluation of facial damage, three types of tests were established:

- Static tests with airbag deployment
- Dynamic tests on sled using UNECE 16 Standard pulse
- Full vehicle dynamic test (Full frontal with rigid barrier at 50 km/h)

To carry out all the tests, the same model of airbag was used. In this way a greater homogeneity and representativity of the tests and the performance is achieved. The selected airbag has the following characteristics:

- Airbag: Driver airbag.
- Vent hole diameter: 25 mm.
- Series mounted

Static tests The main objectives of the static tests were to verify that the mask and the sensors were working correctly and to obtain a basic reference value of the force exerted on the dummy

face, since all the dynamic energy of the test is eliminated from the system. The system was tested and evaluated for correct functionality, with admissible levels of repeatability and reproducibility.

The test was carried out with the dummy having a 20° incline to the front, achieving a close to the steering wheel position. This is required because the airbag volume is designed to fit between the dummy and the steering wheel, and without any dynamic activity, it would not contact the dummy face at all. With this inclined position, the airbag has full face contact at mid distance.



Figure 2. Dummy positioning.

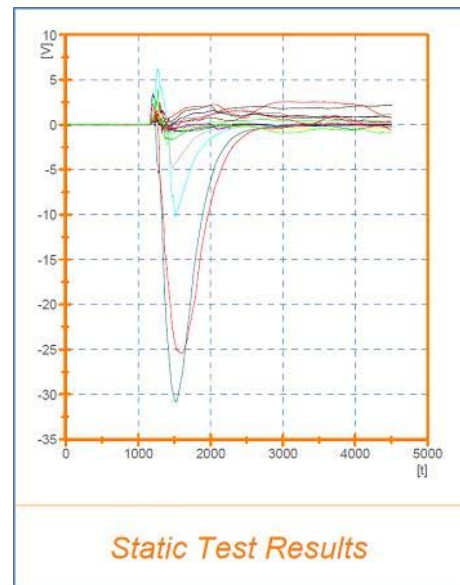


Figure 3. Static test results.

The results from these tests show the mask functionality and are a base measurement for the airbag forces. The signals shown in the graphs are the ones obtained from the mask sensors. The larger curves are the ones for the sensors located in

the most critical zones, that is, the front and centre of the face. With this test, we could be able to know the damage caused exclusively by the exploding airbag.

Dynamic tests The next step was to perform dynamic tests using a sled. The main objectives were to obtain the forces received on the face with a typical accident pulse and to be able to analyse the possible injuries caused. The tests were performed according to the following criteria:

- Type of test: Frontal impact
- Velocity: 50 ± 1 km/h
- Pulse: Standard UNECE 16

The required instrumentation to carry out these tests can be classified into three groups: mask, dummy and sled.

Mask instrumentation The mask is made out of 18 load cells. When installing the mask on the dummy, these cells are located on different points where the most typical injuries occur.

Dummy instrumentation The dummy instrumentation is comprised of three accelerometers located on the head's centre of gravity, one for each direction X, Y and Z.

Sled instrumentation The sled includes two accelerometers installed in the X direction (redundancy)

Prior to carrying out the test, the dummy must be correctly positioned. For this reason, a number of requirements for seating the dummy were established. This allows having a reference initial position in all the tests.

Seat position

- The seat must be located in mid position. In case there are no position slots at the mid point, the seat should be located in the slot immediately after.
- The seat must be in the lowest position.
- The seat back may be located according to the manufacturer. If such requirement is not available, the seat back must be reclined 25° to the back with respect to the vertical line.
- The headrest will be in the highest possible position.
- The headrest angle may be set according to the manufacturer. If such measure is not available, it should be in the mid position.
- The seat's lumbar support will be set according to the manufacturer. If this is

not available, then it should be fully retracted.

- The seat arms will be set to their functional position, as long as they allow for correct dummy positioning.
- The seat belt will be set according to the manufacturer.

Dummy positioning The dummy must be seated according to the EuroNCAP test protocols for frontal impact.



Figure 4. Sled test positioning.

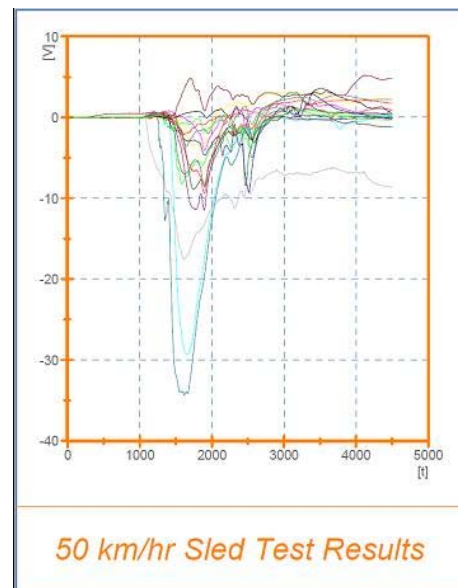


Figure 5. Sled test results.



Figure 6. Sled pulse.

The results from the dynamic tests clearly show an increase in the overall pressure exerted over the mask sensors, accompanied by higher head acceleration provoked by the higher energy of the tests. It is important to say that the readings from the sensors become more precise when the energy of the test increases. In this scenario, the force received by the central part of the face is much more than in the static tests.

Full vehicle test To complete the validation of the system, a full scale vehicle test was performed. This test helped us to verify that the mask can be used in more aggressive environments. Also, this test allows a comparison amongst the sled test values and the crash scenario test. The latter data shows the existing relation between the laboratory results and the ones observed and defined during the accidentology study phase. With these tests we have closed the Laboratory – full vehicle – real life scenario circle, defining a simplified methodology for the validation of the protocol (using the sled with the UNECE 16 standard) and comparing the results obtained with a full scale vehicle crash.

General test parameters:

- Type of test: Full frontal impact.
- Impact velocity: 50 ± 1 km/h
- Barrier: rigid

The required instrumentation to carry out these tests can be classified into three groups: mask, dummy and vehicle.

Mask instrumentation The mask is made out of 18 load cells. When installing the mask on the dummy, these cells are located on different points where the most typical injuries occur.

Dummy instrumentation The dummy instrumentation is comprised of three accelerometers located on the head's centre of gravity, one for each direction X, Y and Z.

Vehicle instrumentation The vehicle includes two accelerometers installed in the X direction (redundancy). They must be located in the tunnel, at halfway in the longitudinal direction.

Prior to carrying out the test, the dummy must be correctly positioned. For this reason, a number of requirements for seating the dummy were established. This allows having a reference initial position.

Seat position

- The seat must be located in mid position. In case there are no position slots at the

mid point, the seat should be located in the slot immediately after.

- The seat base must be inclined according to the manufacturer's data up to the mid position as maximum.
- The seat must be in the lowest position.
- The seat back may be located according to the manufacturer. If such requirement is not available, the seat back must be reclined 25° to the back with respect to the vertical line.
- The headrest will be in the highest possible position.
- The headrest angle may be set according to the manufacturer. If such measure is not available, it should be in the mid position.
- The seat's lumbar support will be set according to the manufacturer. If this is not available, then it should be fully retracted.
- The seat arms will be set to their functional position, as long as they allow for correct dummy positioning.
- The seat belt will be set according to the manufacturer. If the data is unavailable, it should be set to the middle position or the slot right above the middle.
- The steering wheel must be located in the mid position, horizontally and vertically.
- All vehicle windows must be in the lowest position.
- The gear change lever must be in neutral position.
- The pedals must be at resting position.
- Vehicle doors must be closed and unlocked.
- Rear-view mirrors should be in normal use position.

Dummy positioning The dummy must be seated according to the EuroNCAP test protocols for frontal impact.



Figure 7. Vehicle test setup.

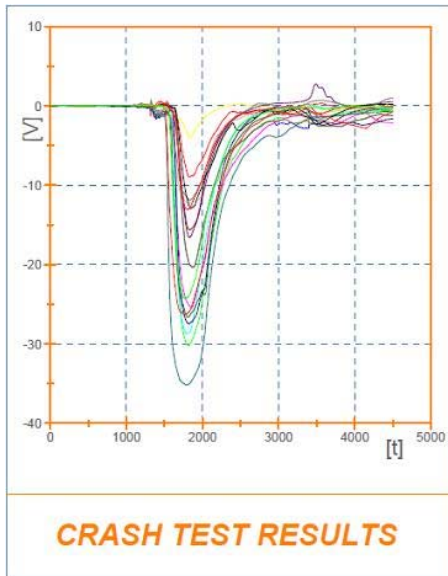


Figure 8. Crash test results.

Results from this impact show that the mask is still receiving the sensor data correctly, maintaining an adequate repeatability level. The forces found in this test are similar to those obtained from the sled test. A few slight differences are found regarding the head acceleration, mainly due to the fact that the pulse in the vehicle impact is different, and which will vary from case to case. Nevertheless, the vehicle has a greater energy absorption capacity, which makes the sled test more representative since the pulses can be repeated in an easier way and sets a worse case scenario for the dummy in terms of energy absorption.

Auditory system injuries

Another important step was the generation and validation of a tool to measure the sound level and pressure generated inside the vehicle's cabin during airbag activation. This is with the aim of evaluating the risk of suffering injuries, either temporal or permanent, to the hearing system. Generally, these injuries occur due to the high level of the sound generated by the airbag explosion and the accident noise itself and also because of the sudden increase in cabin pressure that occurs when the airbag inflates and displaces an extra amount of air equal to the volume of the airbag.

As mentioned earlier, the system designed to measure the sound level and pressure is also based on Hybrid III 50th percentile dummy heads. In this case, the heads have been modified to receive a couple of special microphones to measure the right and left side sound and pressure of the occupants. Two versions of the head exist: one in which the microphones are set in place through a special attachment harness and another one where the microphones were built in. The position of the

microphones was established considering that they must be the same place as the average human ear.

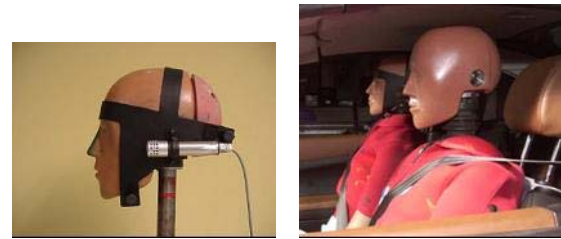


Figure 9. Microphones in dummy heads.

The microphones are protected in such a way that during the tests, these do not receive any damage and maintain their listening capability. To validate the protective device, a couple of tests were carried out. The system proved effective in protecting the device and maintaining its functionality.



Figure 10. Protected microphone.

The following equipment was used

- Microphones Bruel & Kjaer 4938 modified according to WB 1418
- Microphone preamplifiers Bruel & Kjaer 2670 modified according to WB 1419
- Microphone conditioners Bruel & Kjaer 2690-OS4
- Multichannel acquisition system LMS Pimento
- TMON software from the LMS CADA-X Package
- Workstation Hewlett Packard C360

Apart from the microphones installed in the dummy heads, an additional microphone is installed in the rear part of the vehicle, in the central position. This microphone allows measuring the sound and pressure levels from a further position and compares the data from the front (closer to the users) and the rear, where a passenger may also receive some of the effects.



Figure 11. Rear seat microphone.

The data obtained from the microphones of the heads and rear seat are used to calculate the amount of noise generated in the cabin. Two times are selected to make the calculation of acoustic pressure and sound level: 1 ms and 0,2 ms.

Calculation of the moving average of the squared acoustic pressure, with the following expression (Equation 1):

$$p_{AV}^2(t) = \frac{1}{T} \int_{t-T}^t p^2(t) dt \quad (1).$$

Where $p_{AV}^2(t)$ is the moving average of the squared acoustic pressure in squared pascals, T is the time window (1 ms or 0,2 ms were used), $p(t)$ is the acoustic pressure in pascals.

Calculation of the sound pressure level of the moving average with the following expression (Equation 2):

$$SPL(t) = 10 \log \frac{p_{AV}^2(t)}{p_0^2} \quad (2).$$

Where $SPL(t)$ is the sound pressure level in dB, $p_{AV}^2(t)$ is the moving average of the squared acoustic pressure in squared pascals, p_0 is the reference pressure equal to $20 \cdot 10^{-6}$ pascals.

With the idea of quantifying the noise and pressure values inside the cabin during an accident and airbag deployment, static and dynamic tests are performed. This is done in order to compare the difference in the level of sound and pressure with the airbags only and then with the added noise coming from the vehicle while crashing (deformation, breaking parts, other systems).

The system allows measuring the sound and pressure levels from the lateral and head airbags too. As the microphones act as the human ear, and are in the same location, the amount of noise perceived by them is the same in all accident configurations. All these tests can be carried out with the windows up or down, and that will also make a difference in the pressure levels. It is important to mention that front and lateral airbag tests must be carried out separately, since these systems never activate at the same time in a real accident. The last test should be the dynamic test, since in this case, the test is destructive.

Shown next are the main configurations for tests to measure sound and pressure levels inside a car:

Static

- Driver and/or passenger airbag, windows up.
- Driver and/or passenger airbag, windows down.
- Lateral airbags, windows up.
- Lateral airbags, windows down.

Dynamic

- Frontal impact with driver and/or passenger airbag activation, windows up.
- Frontal impact with driver and/or passenger airbag activation, windows down.
- Lateral and curtain airbag activation, windows up.
- Lateral and curtain airbag activation, windows down.
- Pole impact with lateral and curtain airbag activation, windows up.
- Pole impact with lateral and curtain airbag activation, windows down.

Reference values The reference values that are considered for the evaluation correspond to the intensity which the human ear is able to withstand for a certain period of time. If the intensity is low, the human ear can tolerate the sound for a longer period of time. If the intensity is high, then a short period of exposure could result in temporal or permanent injuries, especially to the inner ear.

A sound that exceeds 125 dB is considered to be above the human pain threshold and has a large probability of permanently damaging the ear, even in short time exposures. It is not recommended to be exposed to sounds that exceed 140 dB, even if the threshold time is in the range of 50 ms. Since the airbag explosion takes place in less than 1 ms, a person could theoretically withstand a sound in the range between 157 dB and 160 dB.



Figure 12. IDIADA's FTIR machine.

Table 1.

Sound level time exposures

Continuous dB	seconds
85	28800,000000
100	900,000000
115	28,125000
124	3,515625
130	0,878906
142	0,054932
145	0,027466
151	0,006866
157	0,001717
160	0,000858
166	0,000215
172	0,000054
184	0,000003

For the tests, the pressure and sound levels were recorded in the following positions:

- Driver left ear
- Driver right ear
- Passenger right ear
- Rear central area

Finally, ten tests were considered, which included eight with airbag deployment only, the ninth is an impact test with airbag deployment and the tenth is an impact with no airbag deployment.

Table 2.
Test setup

Kind of crash	Vehicle	Description of the test
Static front	1	Deployment of steering wheel and dashboard airbags and seat belt Pyrotechnic. Windows closed.
Static front	1	Deployment of steering wheel and dashboard airbags and seat belt Pyrotechnic. Windows closed. Dashboard not changed.
Static front	1	Deployment of steering wheel and dashboard airbags and seat belt Pyrotechnic. Windows open. Dashboard not changed.
Static side	1	Deployment of curtain and side airbags. Windows closed.
Static side	1	Deployment of curtain and side airbags. Windows closed. Side airbag cover and roof not changed.
Static side	1	Deployment of curtain and side airbags. Windows open. Side airbag cover and roof not changed.
Static front + side	2	Deployment of all the airbags. Windows closed.
Static front + side	2	Deployment of all the airbags. Windows open. Dashboard, side airbag cover and roof not changed.
Dynamic front	1	Deployment of steering wheel and dashboard airbags and seat belt Pyrotechnic. Windows closed.
Dynamic front	2	NO airbag deployment. Windows closed.

Table 3.
Test results

	Test Number									
	1	2	3*	4	5	6*	7	8*	9	10
Driver left ear (dB)	163,7	163,6	157,7	160,6	161,8	160,1	164,6	161,8	166,2	149,1
Driver right ear (dB)	165,2	164,2	159,3	156,8	157,2	155,3	164,7	157,9	168,5	149,6
Passenger left ear (dB)	167,2	165,2	156,0	157,6	157,8	153,8	164,5	156,9	165,9	150,0
Center rear (dB)	163,0	162,7	153,4	155,6	157,7	155,7	163,0	156,2	162,8	150,7

The results show that the most critical configuration is test number 9, which is the dynamic test with frontal airbags deployment, pyrotechnic seatbelt retractor and windows closed.

This test passed the threshold of the 168 dB. According to the risk exposition timetable, this sound is enough to cause permanent damage to the human ear, even with very low exposure time. Comparatively, the three tests made with the windows open reveal lower sound and pressure levels; nevertheless, the difference is not much and the sound level is still over the 140 dB maximum recommended limit.

Toxicity analysis

The airbags while deploying expel gases that result from the detonation used to inflate. This explosion needs to be controlled and extremely quick. Some manufacturers measure the resultant gases expelled through the vent holes and the effects they have on persons.

The following list of gases, which may represent a risk to the health of people, are taken from the Standard AK-ZV 01 “Pyrotechnic Retention Systems in Vehicles” used by: Volkswagen AG, Audi AG, Bayerische Motoren Werke AG (BMW), Daimler AG (Mercedes-Benz) and Porsche AG. This standard is applicable to different types of airbag available on the market and establishes the tests and limits of gas concentration that can be present after airbag deployment.

The list of gases and the limits are shown next:

Table 4.
Dangerous gases list

Cl ₂	5 ppm
CO	500 ppm
CO ₂	20.000 ppm
COCl ₂	1 ppm
NO	50 ppm
NO ₂	10 ppm
NH ₃	150 ppm
HCl	25 ppm
SO ₂	50 ppm
H ₂ S	50 ppm
HCN	25 ppm
HCHO	10 ppm

The established values are considerably under the IDLH (Immediate Danger for Live and Health)

These limits are considered as the TLV (Threshold Limit Value) – TWA (Time Weighted Average) for a person within an 8 hour exposure time. According to the substance, the TLV – STEL (Threshold Limit Value Short Term Exposure Limit) or the TLV – C (Threshold Limit Value Ceiling) is used. The TLV – STEL is the total amount of gas to which a person can be exposed during a maximum period of 15 minutes, and up to 4 times in one day. The TLV – C is the maximum value that should never be exceeded.

On international material safety data sheets, the value can be given in any of these three categories. These limits have been established by the ACGIH (American Conference of Governmental Industrial Hygienists). Parallel to the ACGIH, the MAK from the Federal Republic of Germany considers some different values for each gas.

To determine the quantity and concentration of the gases present in the cabin of a car after airbag deployment, a test in a sealed chamber must be carried out. To correctly obtain the data, measurements should be taken for the following 30 minutes after explosion. All the installed modules in the vehicle must comply with the requirements established in the AK-ZV 01 "Pyrotechnic Retention Systems in Vehicles".

The chamber must have an approximate volume of 2,5 m³ with a cubic form. The modules must be detonated in a controlled manner. There are two different configurations to measure the released gases:

Measuring setup 1 For Cl₂ (Chlorine) y HCl (Hydrogen Chloride) Dräger tubes must be used.

To measure NO (Nitrogen Oxide) and NO₂ (Nitrogen Dioxide), CLD (Chemical Luminescence Detection) or an infrared system can be used. An infrared system must be used to determine the other toxic gases in the list.

All the measurements shall be taken in parallel in a 30 minute range.

Measuring setup 2 A mass spectrometer, which is able to measure all gases simultaneously.

Measuring lines

For measuring setup 1: fluoropolymers (e.g. Viton, Teflon etc.)

For measuring setup 2: heated stainless steel pipe of TTL quality

Inside diameter: max. 5 mm

Length: max. 5 m

Dust filter CLD does not involve a filter, all other devices require a filter with 5 mm pore width. The NO and NO₂ measurements shall be performed without a filter.

Test point Test point: Centre of the sidewall in the unfolding direction

Test conditions Test temperatures: Room temperature

Test procedure

Preparation To prepare for measurement, the measuring setup is stabilized by means of room air measurements 5 minutes before module detonation; the module does not need to be in the chamber at this point. The airbag module is mounted on a fixture in as-installed position or optionally rigidly mounted with vertical airbag unfolding (Figure 1) in a 2.5 m³ chamber. Ambient air is present in the 2.5 m³ chamber. The module is detonated in the pressure-tight chamber using a suitable power source.

Samples for further analyses, if necessary, shall be taken from this chamber. The interior chamber temperature and the ambient temperature around the chamber shall equal room temperature immediately prior to detonation.

Gas analysis The tests must occur (60 ± 5) sec. after detonation of the module in the 2.5 m³ chamber, whereby the airbag must not be pressed out after module detonation and the gases that occur during or after detonation must not be agitated (as with a ventilator, for example). The measurements must be taken over a period of 30 minutes. The average must then be calculated.

Measuring setup 1 When measuring using Dräger Tubes, measurements are carried out in 5 minute intervals, whereby the cross sensitivities must be taken into consideration. The sample is removed directly from the chamber using a bypass, for example. When using CLD, the volume removal is in the order of □1.2 l/min.; when using FTIR, a flow rate of 0.5 to 2.5 l/min must be selected.

Measuring setup 2 When using a mass spectrometer, a flow rate of approximately 10 l/min shall be selected.

For all the installed modules in the vehicle (front, lateral, pyrotechnic) the following distribution is proposed:

- 50% frontal protection systems (driver, passenger and knee airbags)
- 25% lateral protection systems (head, thorax and window airbags)
- 25% seatbelt pyrotechnic retractor

The manufacturer establishes the value distribution in between the different components in the condition statement. The tests are carried out with a fully-equipped vehicle. These tests must be carried out as mentioned before in setups 1 and 2.

Measurement location The measurement of the gases is to be done in the front seat, in the dummy head area, on the side of the deployed airbags.

Test conditions

Temperature inside vehicle: 23°C ± 5°C
Atmospheric humidity: 40-60% relative humidity.

To determine the generated gases after airbag deployment, we have an infrared spectroscopy gas measurement machine (FTIR). Our equipment is designed to calculate the gases from the exhaust pipe from combustion engines; however some of the gases released from airbag activation are the same as those produced in the combustion of fuel.

The components we can analyse with our FTIR machine are:

Carbon monoxide	CO	listed
Carbon dioxide	CO₂	listed
Nitrogen oxide	NO	listed
Nitrogen dioxide	NO₂	listed
Nitrous oxide	N ₂ O	
Water	H ₂ O	
Ammonia	NH₃	listed
Sulphur dioxide	SO₂	listed
Formaldehyde	HCHO	listed
Formic acid	HCOOH	
Methane	CH ₄	
Ethylene	C ₂ H ₄	
Ethane	C ₂ H ₆	
Propylene	C ₃ H ₆	
1,3-Butadiene	1,3-C ₄ H ₆	
Isobutylene	iso-C ₄ H ₈	
Benzene	C ₆ H ₆	
Toluene	C ₇ H ₈	
Ethanol	C ₂ H ₅ OH	
Acetaldehyde	CH ₃ CHO	
Acetone	CH ₃ COCH ₃	
Xylene	C ₈ H ₁₀	
Ethyl benzene	C ₆ H ₅ C ₂ H ₅	
HFC-134a	CH ₂ FCF ₃	

The gas measurement can be done directly inside the vehicle or in a special chamber dedicated to the test.

The gases that we cannot measure with the FTIR machine are: Cl₂ (Chlorine), COCl₂ (Phosgene), HCl (Hydrogen chloride), H₂S (Hydrogen Sulphide), HCN (Hydrogen Cyanide).

The equipment readily available at IDIADA for this study was not capable of measuring all required gases, Consequently we will not be able to perform the tests established in the protocol. To this end, we need to use instrumentation or similar equipment, which indeed has the capabilities.

CONCLUSION

The work carried out during this project showed that airbags are very useful in reducing fatalities and serious injuries in road accidents. Nonetheless, their activation in near-threshold situations, where the dynamic requirements are not always met, may cause injuries to the occupants.

The most common injuries are directly to the face, to hearing and skin abrasion and possible inhalation or contact with toxic substances. During this project, we developed a set of tools that allowed us to investigate more deeply the effects of airbags and their interaction with the passengers. The designed tools aim at helping airbag designers and manufacturers along with automobile manufacturers to analyse the specific situations in which their product may or may not meet safety requirements in near-threshold situations.

The special dummy mask modified with pressure sensors showed very good results in measuring forces during accidents, these tests being carried out statically and dynamically in a sled and full frontal vehicle crash. The dynamic data were very well correlated and the difference between static tests and dynamic tests (both sled and car) showed a slight difference in pressure.

Regarding hearing damage, the installed microphones in the dummy heads were able to withstand the energy and dynamics of a crash and still provide accurate measurement of sound level and pressure. This fact makes them ideal for analysing the behaviour of sound waves and pressure distribution throughout the cockpit.

In the toxicity analysis, we discovered that important amounts of several gases are released, and each gas has a different toxicity level on the human being. In our special case, we were not able to measure all the required gases for the study. However, we now know what we need to measure and are searching for suitable equipment to do this. If possible, we will try to use equipment that can be fitted into vehicles and tested in the same run.

Further work needs to be done, and we are aiming to combine the pressure mask with the microphones to generate single test measurement equipment. We will also optimize the mask sensors, since not all of them may be required in the future.

REFERENCES

- [1] Adams S. L., Petri R. W. 1996. "Injury with spontaneous deployment of an automobile air bag". *Journal of Accident and Emergency Medicine*, Vol. 3, pp. 179–180.
- [2] Barrios, J.M. "Desarrollo del Procedimiento de Certificación de las Lentes Correctoras de Visión para la Protección de los Ocupantes en Relación con las Lesiones Oculares y Faciales producidas por los Airbags Frontales durante un Choque". 2006.
- [3] Dundar, S. 2007. "The Mask Project. Airbag Induced Facial and Ocular Injury Test Device".
- [4] Kuhn F., Morris R., Witherspoon C. D. 1993. "Air bag: Friend or Foe?" *Archives of Ophthalmology*, Vol. 111, pp. 1333-1334.
- [5] Kuhn F., Morris R., Witherspoon C. D. 1995. "Eye injury and the air bag. Current Opinion in Ophthalmology", Vol. 6, pp. 38-44.
- [6] Morris A., Thomas P., Brett M., Bruno-Foret J., Thomas C., Otte D. & Ono K. 1996. "A Review of driver airbag deployments in Europe and Japan to date". *Proceedings of 15th ESV*, Melbourne, Australia
- [7] Otte D. 1995. "Review of the air bag effectiveness in real life accidents demands for positioning and optimal deployment of air bag systems". 39th Stapp Car Crash Conference, 952701, San Diego.

UPDATE ON LATERAL IMPACT TEST PROCEDURE FOR CHILD RESTRAINT SYSTEMS

Heiko Johannsen

Technische Universität Berlin

Farid Bendjellal

Britax Childcare Group

Germany

François Renaudin

Dorel Europe

France

Peter Claeson

SIS Swedish Standards Institute

Sweden

Paper Number 11-0291

ABSTRACT

After years of research and discussion ISO published a side impact test procedure for CRS as Technical Specification ISO/TS 29062:2009. At the same time of the finalisation of the technical specification, the GRSP Informal Group on CRS decided to establish a more simple approach than specified in ISO/TS 29062:2009 and asked ISO for support. As a response to this request ISO prepared the Publicly Available Specification ISO/PAS 13396:2009 which summarises the most important input data for the development of a side impact test procedure. That represented a significant input to the Informal Working Group on CRS to develop their own test procedure. The new GRSP lateral impact test procedure is currently under validation. It is expected that the validation will be completed by spring 2011.

The new test procedure will become mandatory as part of the planned new regulation for the homologation of CRS.

INTRODUCTION

In lateral impact accidents two mechanisms are causing injuries; on the one hand the lateral acceleration and on the other hand intrusion of the side structure. This combination makes the development of a suitable test procedure more difficult compared to frontal impact test procedures. Proposals for lateral impact test procedures considered lateral intrusion only, lateral acceleration only and the combination of both. One of the problems for the combination was that the intrusion velocity in cars was higher than the Δv following the lateral acceleration. TRL developed the hinged door principle to address this issue which was the base for ISO and NPACS activities.

However, the hinged door principle is considered by a large number of organisations to be too complicated. In the following the latest developments with respect to lateral impact test procedures are summarised.

ACCIDENT ANALYSIS

The severity of injuries in side impacts depends on the seating position. It can be noticed that the severity of injuries is much higher for children sitting on the struck side than sitting on the non-struck side. The share of injuries on the non-struck side is comparable to frontal impacts, while the injury probability is much higher in struck side accidents, see Figure 1.

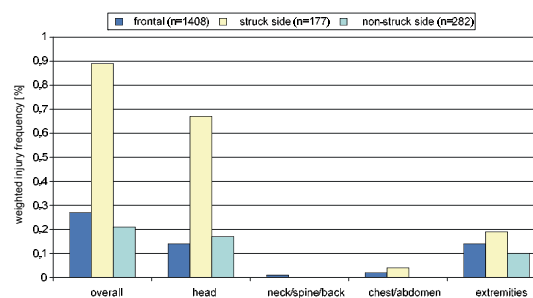


Figure 1. Injury frequency depending on the impact direction [Arbogast, 2004].

The relative number of children suffering MAIS 2+ injuries is much higher in lateral impact accidents than for the other impact directions, as shown in Figure 2.

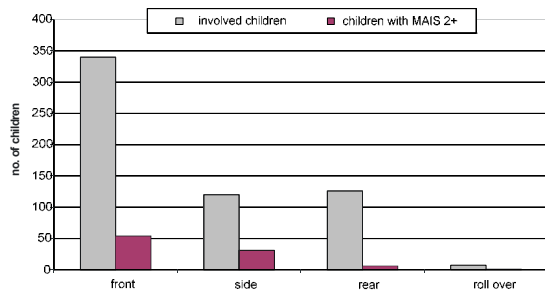


Figure 2. Share of different impact directions [Langwieder, 2002].

Regarding the different body regions the risk for severe injuries decreases from the head down to the legs. The frequently observed injuries of arms and legs are not of high severity, but may cause long term impairments. The focus for investigations concerning improvements of CRS should be primarily on the head but to certain extent also on neck and thorax/thorax, see Figure 3.

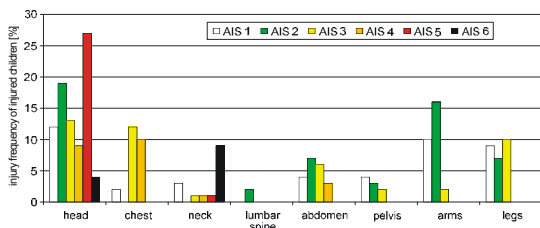


Figure 3. Injury risk of different body regions of 68 injured children in side impacts [Langwieder, 1996].

Looking at the distribution of injuries in lateral impacts from 1985 to 2001 it is obvious that the injury probability decreased since 1985 while the risk to suffer neck injuries increased and the chest remained unchanged, see Figures 4, 5, and 6.

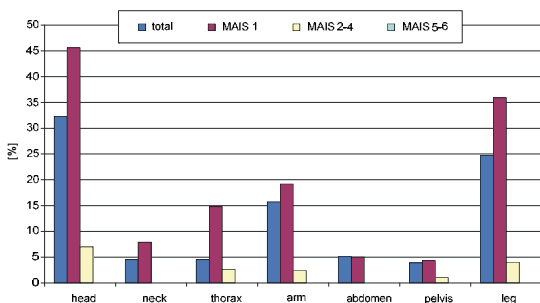


Figure 4. Injury probability of different body regions in side impact accidents between 1985 and 1990 [Otte, 2003].

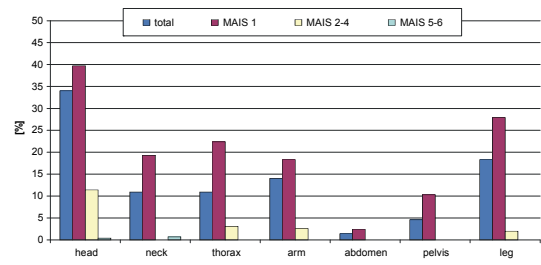


Figure 5. Injury probability of different body regions in side impact accidents between 1991 and 1996 [Otte, 2003].

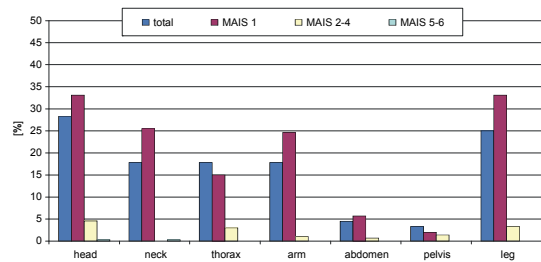


Figure 6. Injury probability of different body regions in side impact accidents between 1997 and 2001 [Otte, 2003].

These accident data show that side impact accidents are severe ones especially for those children (age up to 12 years) sitting at the struck side. Especially head, and to some degree neck and chest need to be protected.

In a study of the Swedish accident situation Jakobsson et al. [Jakobsson, 2005] did not find any moderate-severe (AIS2+) head injuries in children using rear-facing (RF) CRS involved in lateral impact accidents, while children using forward facing (FF) booster seats or the car belt only suffered from moderate-severe injuries (AIS2+) in side impacts.

Based on results of the EC funded CHILD project and the EEVC/WG18 Report (Feb 2006), non-head containment combined with intrusion loading is found to be the major reasons for head injuries in side impacts involving rearward facing and forward facing harness type CRS as well as high back booster and backless booster [Johannsen, 2006; EEVC, 2006].

Analysis of accident data involving children in side impacts from different sources and different regions of the world (Germany, Sweden and USA) indicates that the purely lateral impact (due to the accident data coding with $\pm 15^\circ$ deviation) is possibly more severe than angled ones while the share of perpendicular and angled impacts with forward component is nearly equal [Johannsen, 2007a]. Although all three sources show the same

tendency, final conclusions are not possible as the number of involved children is too small to allow statistical significant results. This data regards all types of impact objects and restraint use.

Henary et al [Henary, 2007] found when comparing the risk of injury between children (aged 0-23 months) in side impacts, using US crash data (NASS-CDS), a significant higher benefit for children in rearward facing compared to forward facing harness type CRS. The authors conclude that this is likely because a forward component in the vehicle travel direction in many of the cases will move the head forward during the crash.

The struck car is in many cases subject to an angled acceleration due to its initial speed. The main expected influence of a possible forward component would be an increase in head forward motion. Head forward trajectory can also be influenced by pre-braking conditions. Maltese et al [Maltese, 2007] mapped probable head contact points for 4 to 15 year old injured children (not using child seats) involved in a side impact seated on the struck side in the rear seat. The contacts were mainly found adjacent to the likely initial position of the head of the in-position rear seat child occupant, and adjusted forward. The authors state this forward adjustment is likely due to the forward component.

ACTIVITIES OF THE DIFFERENT WORKING GROUPS

ISO TC22 SC12 WG1

The ISO Working Group on Child Safety of Sub committee on Passive Safety and Crash Protection started in the nineties with the development of a side impact test procedure.

ISO 14646 was the first project concerning the standardisation of a lateral impact test procedure. After the disapproval of ISO DIS 14646 by a small margin ISO working group on child safety decided to summarise the knowledge gained for the development as a Technical Report. The ISO/TR 14646:2007 was published in 2007. A summary of the Technical Report is given in [Johannsen, 2007b].

ISO/TS 29062:2009 was the follow up project of ISO 14646 which concluded as a Technical Specification. In parallel to the ISO/TR 14646:2007 ISO restarted the project to publish a side impact test procedure. ISO/TS 29062:2009 was published in 2009. The test procedure is comparable to the NPACS test procedure. Similar to the original DIS 14646 procedure a hinged door test procedure was utilised.

Figure 7 shows the set-up according to ISO/TS 29062:2009 for FF CRS. In order to avoid a gap between backrest and panel the backrest is moveable in Y direction.

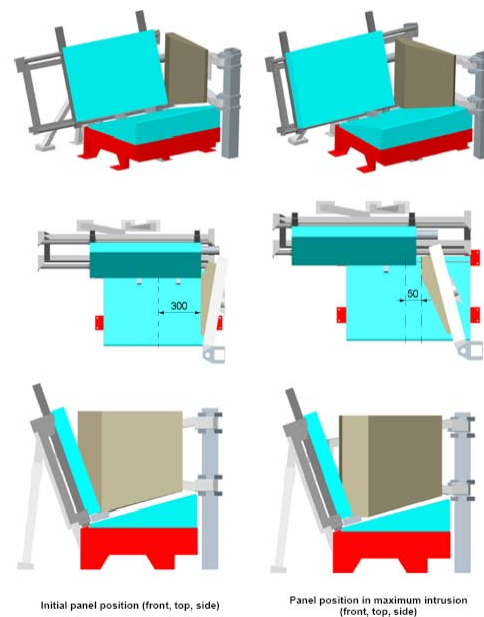


Figure 7. Side impact test bench according to ISO TS 29062 for FF CRS.

In order to test RF and FF CRS in comparable severity conditions the set-up is different for both CRS types. Using a hinged door test procedure it is important to have the maximum intrusion close to the dummy's head. The set-up for RF CRS is shown in Figure 8.

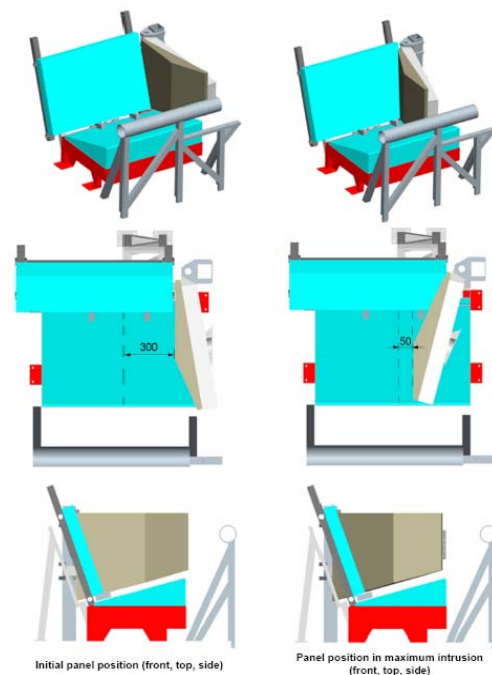


Figure 8. Side impact test bench according to ISO TS 29062 for RF CRS.

During the ISO voting process for the test procedure mentioned above the GRSP Informal Group on CRS reviewed several existing side impact test procedures for CRS and came to the conclusion that the ISO one would not be acceptable for ECE regulation. This finding resulted in two implications:

- GRSP decided to develop a suitable test procedure based on existing (and draft) procedures and asked ISO to provide essential input parameters for this development (see below).
- The ISO test procedure has scarcely been used since the publication of ISO/TS 29062:2009

ISO/PAS 13396:2009 is the ISO TC22 SC12 WG1 reaction to the official request for assistance expressed in April 2008 by GRSP IG CRS, ISO working group on child safety compiled a summary of ISO/TR 14646:2007 and added recent research results. A draft of the document was presented to GRSP IG CRS in April 2009. ISO/PAS 13396:2009 was published in November 2009.

In summary the ISO PAS stated the following:

Intrusion loading is the most frequent cause of injuries in side impacts. For the protection of children in car side impact, a combined assessment of body kinematics and energy management capabilities of the CRS is important.

Looking at the different body regions, the head needs to be protected with highest priority, followed by neck and chest.

The test input parameters are defined by the intrusion (specified by intrusion shape, intrusion depth and intrusion velocity), the bench acceleration and Δv , as well as by geometrical properties. The parameters are summarised below:

- intrusion velocity: maximum between 7 m/s and 10 m/s at approximately 30 ms close to the dummy's head;
- intrusion depth: dynamic intrusion depths should be between 200 mm and 300 mm;
- sled acceleration range: 10 g to 14 g (sled Δv should be approximately 25 km/h);
- intrusion surface height: approx. 500 mm with respect to CR point;
- initial distance between CRS centre line and intrusion surface: approximately 300 mm.

Based on the results of the analysis of impact angles, the test procedure should focus on perpendicular impact.

Table 1 lists the essential input parameters and their respective weight as a proposed tool to assess different test procedures.

Table 1.
Matrix of essential parameters to support the assessment of side impact test procedures [ISO/PAS 13396:2009, 2009]

Essential parameter	Reference value	Weighing factor
Loading conditions	intrusion loading	A
Loading conditions	assessment of occupant kinematics and energy management	A
Relevant body regions to be addressed	1. head 2. neck 3. chest	1: A 2: B 3: B
Maximum intrusion velocity	7 m/s to 10 m/s at approx. 30 ms close to the dummy's head	A
Maximum intrusion depths	200 mm to 300 mm	B
Sled acceleration range	10 g to 14 g	C
Sled Δv	approx. 25 km/h	B
Intrusion surface height	approx. 500 mm with regard to CR line	B
Initial distance between intrusion surface and CRS centre line	approx. 300 mm	B

GRSP IG CRS

In order to develop a new regulation for the homologation of CRS to replace current ECE R44, UNECE Working Party on Passive Safety (GRSP) formed an Informal Group on CRS to prepare the new standard. One of the aims of this group is the introduction of a lateral impact test procedure. Analysis of several lateral impact test procedures for CRS resulted in the judgement that these are either not reflecting enough real world needs (fixed door), are in development (NHTSA) or are too complicated so that repeatability and reproducibility issues can be expected (ISO and NPACS). Following that, the group decided to develop its own test procedure. As considerable experience was gained during the development of the ISO test procedures, GRSP sent a formal request to ISO to support this activity by summarising the most important parameters that need to be considered for the development (see above). The specifications described in ISO/PAS 13396:2009 were considered as important input data for the GRSP test procedure. The intrusion velocity profile was considered as the most important parameter, as shown in Figure 9.

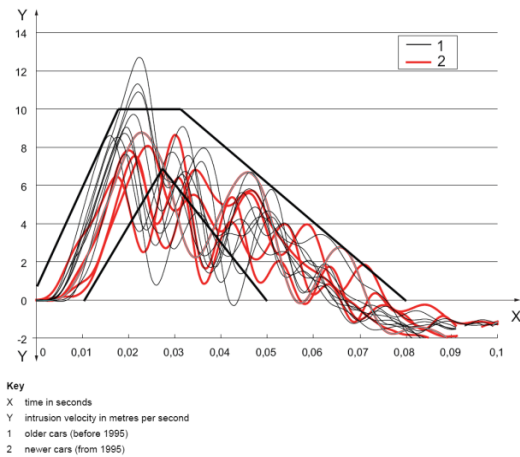


Figure 9. Intrusion velocity profile according to ISO/PAS 13396:2009.

Design requirements for the GRSP side impact test procedure were defined in order to fulfil the following characteristics:

- simple in order to ensure good:
 - repeatability
 - reproducibility
- reasonable cost
- potential to be used in different sled systems
 - deceleration sleds with different braking systems
 - acceleration sleds
- capable to replicate the basics of lateral impact

Following the advice of ISO/PAS 13396:2009 it is essential for a lateral impact test procedure for CRS to replicate intrusion loading and acceleration loading.

In addition the dimensions of the intrusion surface, the allowed degree of freedom of the ISOFIX anchorages amongst others were considered. As a first step the group decided to focus on the head: namely head containment with addition of parameters such as head acceleration and HIC. Given the lack of scientific validated criteria and limits for lateral impact it was decided to use the head criteria and limits as defined for frontal impact. This approach was deemed to be pragmatic. Table 2 shows the current proposal for the lateral impact criteria to be used for the new ECE regulation.

Table 2. Current proposal for lateral impact criteria

	Q0	Q1	Q1.5	Q3	Q6
HIC	600	600	600	800	800
a_{3ms} head	75g	75g	75g	80g	80g
head containment	Head shall not pass through head containment plane which is positioned in a distance of [55] mm from panel outside				

Following the experience of ISO TC22 SC12 WG1 the GRSP group considered the intrusion velocity as the main loading parameter which needs to be controlled precisely at the time of dummy loading. The intrusion velocity characteristics displayed in Figure 9 shows a fast increase of intrusion velocity in the beginning and a decreasing part of the velocity after the maximum. Figure 10 shows the general velocity change during lateral impact.

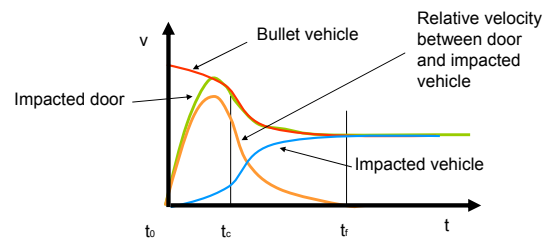


Figure 10. Velocity change during lateral impact (t_c : time of contact between CRS and side structure, t_f : time of end of crash phase).

As the velocity characteristic before the contact between CRS and side structure is felt to be irrelevant for the test procedure the idea of the GRSP method was to replicate only the period after the contact (t_c to t_f). Figure 11 shows the part of velocity characteristic that is considered for the GRSP test procedure.

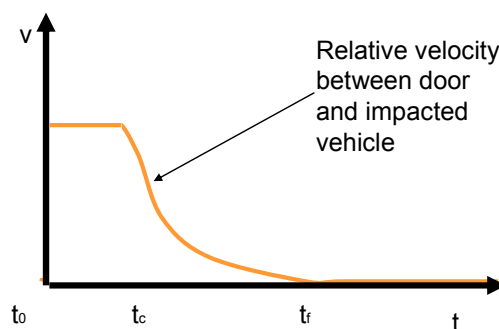


Figure 11. Velocity characteristics to be considered for the GRSP side impact test procedure for CRS.

In order to ensure the new test procedure can easily be installed in different labs the ECE R44 rear impact test procedure (initial velocity and stopping distance) was considered as a starting point. The

(new) frontal impact test bench is mounted in an angle of 90° relative to the sled. A velocity change corridor between test bench and intrusion plane defines the test severity. Figure 12 shows an example for the practical realisation of the test procedure.



Figure 12. Example for test set-up realisation.

Analysis of test severity became relevant because testing showed considerable high dummy readings especially looking at the smallest dummy for each CRS group. Initially the delta-v corridor was using the maximum intrusion velocity as observed in the ISO research as the start velocity. In addition to the high dummy loading observed in the testing programme the optimisation of a group 1 FF CRS with a support leg for Q1 dummy to reduce the head acceleration resulted in worse head acceleration in a car-to-car test, although the head acceleration was reduced by 20% in the test procedure. Following that the test results were compared with results from recent car tests.

In an ECE R95 like test with a small family car produced between 2002 and 2009 the same baby shell as in the test procedure was used. The comparison of test results show considerable higher dummy readings in the test procedure compared to the car test, see Figure 13.

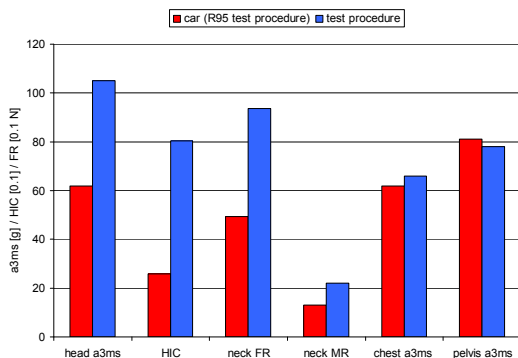


Figure 13. Comparison of dummy readings between test procedure and small family car test.

In a more severe lateral impact test involving the AEMDB, i.e. using a heavier trolley and a stiffer

barrier face compared to ECE R95, and a small van introduced in 2006, a comparable situation can be observed. For a infant carrier (baby shell) at the rear seat head loads and neck forces were considerably higher in the test procedure than in the car, while neck moments and chest and pelvis accelerations were at a comparable level, see Figure 14.

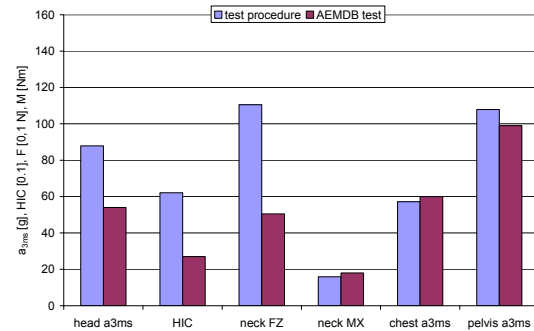


Figure 14. Comparison of dummy readings between test procedure and small van AEMDB car test RF CRS.

In a forward facing group I CRS with top tether and installed at the front passenger seat, the dummy readings were comparable, see Figure 15.

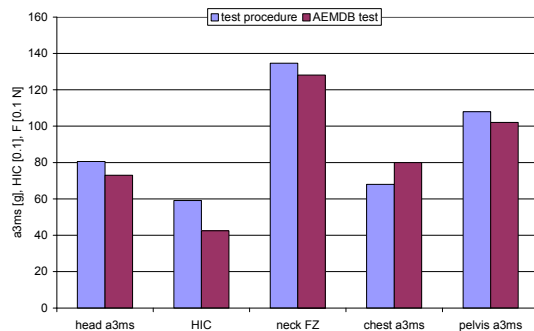


Figure 15. Comparison of dummy readings between test procedure and small van AEMDB car test FF CRS.

From past testing it is well known that the acceleration loading is smaller with heavier dummies, which is mainly caused by the higher mass in conjunction with a comparable force level defined by the padding stiffness of intrusion surface and CRS. In contrast it becomes more challenging to keep the head inside the CRS with larger dummies. That means that the validation results with smaller dummies are more important than those with larger ones with respect to dummy readings such as accelerations, forces and moments.

The analysis of the reasons for the higher severity indicated that the main idea of the test procedure (to consider the intrusion velocity profile for the loading relevant period only) was not considered

correctly. Indeed no analysis of the timing issue took place before.

Analysis of videos and time histories from different barrier-to-car and car-to-car lateral impact tests involving child dummies indicated that the time of maximum head loading would be the best reference.

Maximum head loading was identified in these tests between 35 and 70 ms with average at 50 ms, see Figure 16.

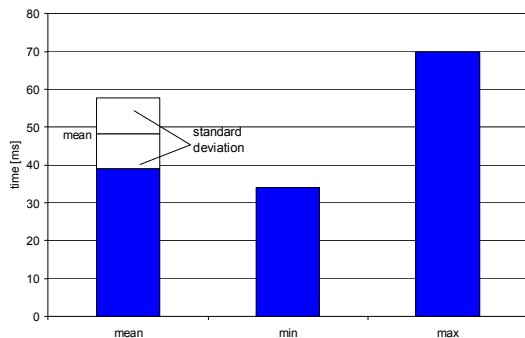


Figure 16. Time of maximum head acceleration in lateral impact tests with 6 different car models and 2 to 6 different CRS per car model.

As a result the average intrusion velocity at the time of maximum head acceleration (50 ms) would be approx. 3 m/s, see Figure 17.

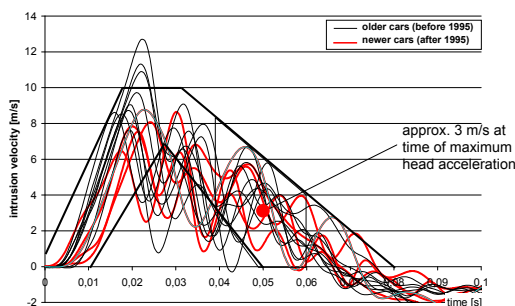


Figure 17. Relevant loading time in intrusion velocity characteristics proposed by ISO/PAS 13396:2009.

Description of the test procedure. Taking into account the new requirement for the relative velocity between the test bench and the intruding panel the following corridor was plotted, Figure 18. In order to adjust the severity in accordance with the findings mentioned above the timing of head acceleration was analysed in the test procedure. While in car tests the maximum head acceleration occurs at approx. 50 ms head loading takes place in the test procedure at approx. 40 ms. Following that the corridor was designed to reach an average delta-v of 3 m/s at 40 ms.

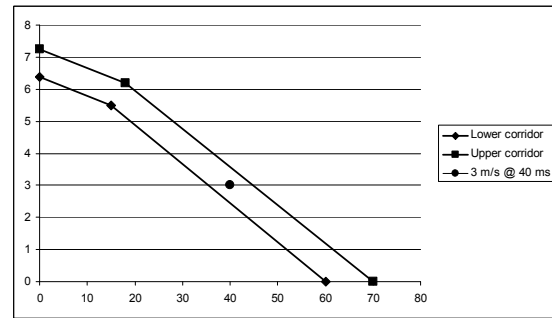


Figure 18. New lateral impact delta-v corridor.

Originally the corridor with reduced severity was more open in the beginning. However, based on numerical simulation results (see below) the corridor was made smaller. The stopping distance shall be 250 mm and the deceleration shall start when the distance between intruding surface and test bench centre line is 350 mm.

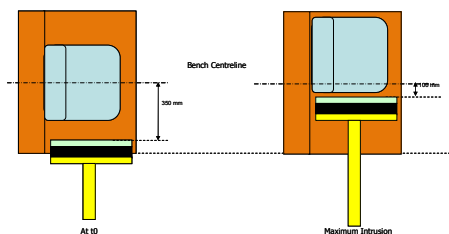


Figure 19. Definition of t_0 and intrusion.

The intrusion surface is defined to meet the requirements proposed by ISO/PAS 13396:2009 (height 500 mm above CR point) and covers the length of ISO R3 fixture in order not to miss any part of CRS, see Figure 20.

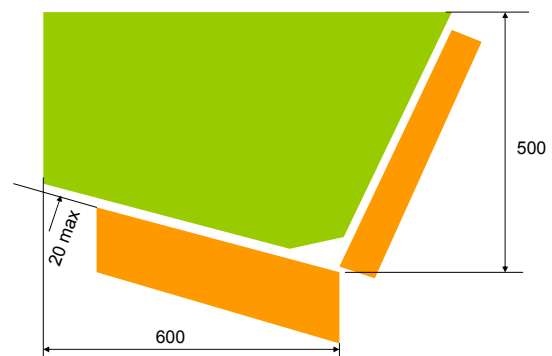


Figure 20. Dimensions of the intrusion surface.

The intrusion panel padding follows the ISO/PAS 13396:2009 proposal. In addition to the dummy readings the head containment will be determined. In order to have an objective criterion a head containment plane with a distance of 55 mm to the intrusion surface was defined. The dummy's head shall not pass beyond that plane, see Figure 21.

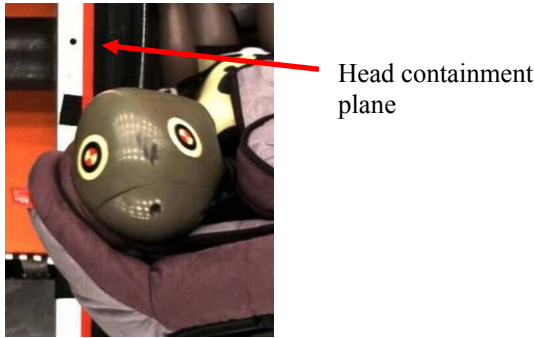


Figure 21. Head containment plane marked with red line, CRS failed criterion.

In addition to the technical parameters of the test procedure, CRS and dummy installation are of high importance in order to reach repeatable and reproducible test results. Therefore an installation procedure was defined. Key aspects of this installation procedure are summarised below:

- exact alignment of CRS with test bench centre line,
- exact alignment of dummy centre line with CRS centre line,
- arms shall be positioned symmetrical with elbows aligned with sternum,
- legs shall be positioned symmetrical,
- pre-impact dummy stability shall be controlled.

Validation of the test procedure took place considering the following areas to be important:

- feasibility,
- appropriate test severity,
- repeatability,
- reproducibility.

Concerning feasibility it was considered to be important that the test procedure is usable with different types of CRS (i.e., infant carriers, large RF CRS, CRS with top tether and CRS with support leg) and with different types of test facilities (i.e., acceleration vs. deceleration sled systems and different braking systems). These parameters were considered when preparing the test matrix for the check of repeatability and reproducibility.

Up to date the following labs have contributed to the validation programme:

- Britax (Deceleration - PU tubes),
- Dorel (Deceleration - hydraulic brake),
- IDIADA (Acceleration sled)
- TUB (Deceleration - bar brakes).

While the original delta-v corridor caused problems with PU tubes this issue was solved by the updated corridor. No other problems were observed with the other deceleration sled systems. The test procedure is less simple with acceleration sled systems. While

the intrusion surface can be fixed at the brake system of deceleration sleds, a double sled system is needed for an acceleration sled device. IDIADA decided to use a so called sled on sled system. The facility accelerates the main sled to which the intrusion surface is fixed. The test bench is fixed to another sled which is fixed to the main sled by a translational joint. In addition to the complexity of the sled system the interpretation of the input parameter is also less simple. While in deceleration sled devices the sled velocity is equal to the relative velocity between intruding surface and test bench, in the acceleration sled device both intrusion surface and test bench are moving. However, it was possible to install the lateral impact test procedure on an acceleration sled system and the test results are highly comparable with those of deceleration sled systems.

None of the tested CRS models (babysshell with base and support leg, group I RF with support leg, group I FF with support leg and group I FF with top tether) showed any issue to be reported.

That means that the feasibility of the test procedure is quite acceptable.

In order to check the severity level the AEMDB tests mentioned above are considered as reference.

The tests with an infant carrier even with the updated severity level indicate a considerably high dummy loading for the head in the test procedure. The other values are at a more comparable level, see Figure 22.

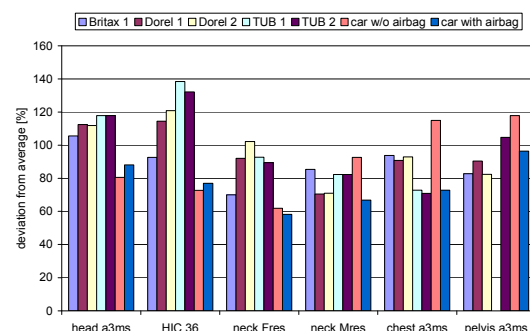


Figure 22. Comparison of results of test procedure and car tests for the baby shell.

In contrast to the infant carrier dummy readings in the group 1 FF CRS with top tether are at a comparable level, see Figure 23.

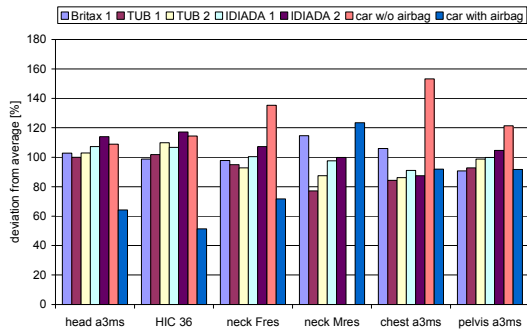


Figure 23. Comparison of results of test procedure and car tests for the group I CRS with TT.

A comparison of tests with old and new corridor with different CRS and different dummies shows that even the new corridor is challenging for industry especially when looking at the smallest dummy per CRS size group, Figure 24.

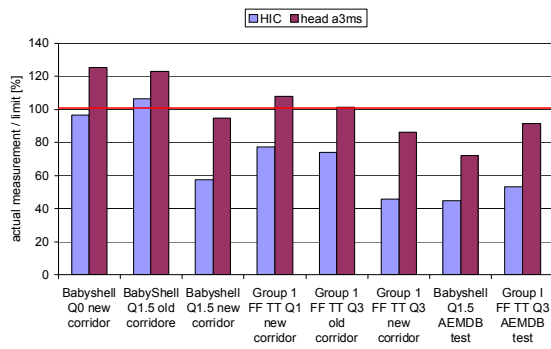


Figure 24. Comparison of head loading depending on severity level, dummy size and tested product.

During the tests for the validation of the protocol several products were found showing shortcomings with respect to the head containment criterion which is a must to protect children in lateral impact accidents.

Repeatability was analysed by running 5 tests with the same product in one lab. For different CRS products different labs were running the repeatability tests. The tests were performed using the original higher severity pulse. The coefficient of variation was used to assess repeatability. In well controlled dummy tests (e.g., pendulum tests) a coefficient of variation of 5% is considered to be good [Mertz, 2005]. For sled testing where variation is coming from the CRS, the dummy and CRS installation as well as variation in the sled behaviour higher variations can be expected. For head and pelvis acceleration the 5% limit is passed for all labs and CRS types. HIC and chest acceleration variation are close to 5% but exceed the threshold for one CRS type or in one lab, see Figure 25.

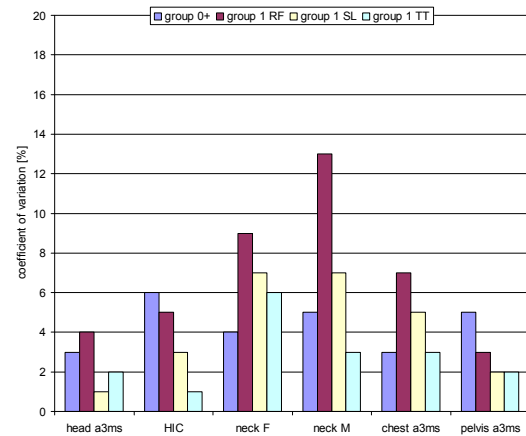


Figure 25. Analysis of repeatability.

The analysis of reproducibility took place using the new test severity. The plan was to test different types of CRS in at least 3 different labs. Unfortunately the programme has not been finalised. In these three labs at least 2 tests for each product were conducted. Again the coefficient of variation was used to assess reproducibility. For most of the body regions, except the head, the coefficient of variation in the reproducibility tests exceeded 10%, see Figure 26.

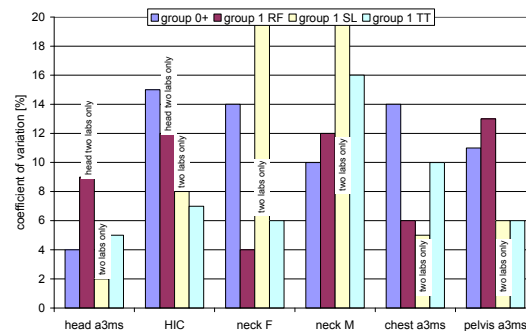


Figure 26. Analysis of reproducibility.

The analysis of repeatability and reproducibility indicates that the test procedure is sufficiently repeatable and reproducible for the main target body region, the head. Following the observation that reproducibility of head a_{3ms} is much better than HIC it is recommended to take only head a_{3ms} as head criterion into account.

In parallel to the testing validation programme parameter studies using numerical simulation and sled testing took place. The main aim of the parameter studies by simulation was to assess the influence of CRS position and delta-v characteristics on the test results. A group 0+ model in combination with Q1.5 dummy model was used for this study. Generally the dummy readings of physical tests and simulation runs were in a comparable level although the CRS model was

not explicitly validated for lateral impact conditions.

The variation of the sled pulse showed considerable differences in the dummy readings. The sled pulse was varied in a way that borders of the corridor were used. The delta-v curves used for this study are shown in Figure 27. The time of “engagement” of the head is visualised for information.

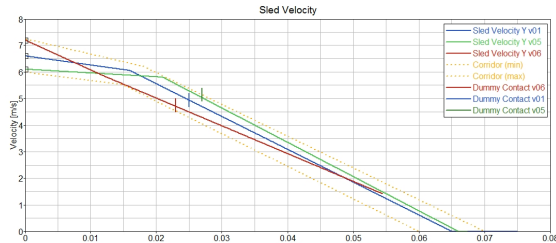


Figure 27. Sled velocity variation for numerical parameter analysis.

In the study the head a3ms varied between -20 and +40% compared to the baseline test, see Figure 28.

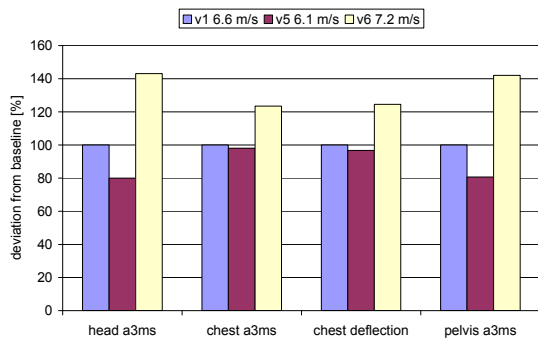


Figure 28. Influence of pulse variation on dummy readings.

The main reason for the variation seems to be the CRS velocity at the time of impact as shown in Figure 29.

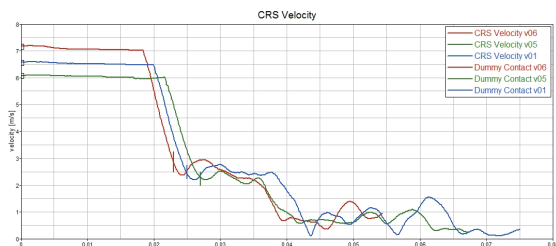


Figure 29. CRS velocity profiles for the sled delta-v variation.

Small Deviations in the positioning of the CRS with respect to the bench centre line seems to cause a smaller variation, see Figure 30 and Figure 31.

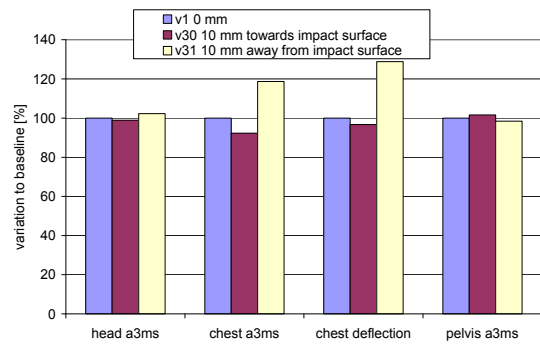


Figure 30. Dummy readings depending on CRS positioning.

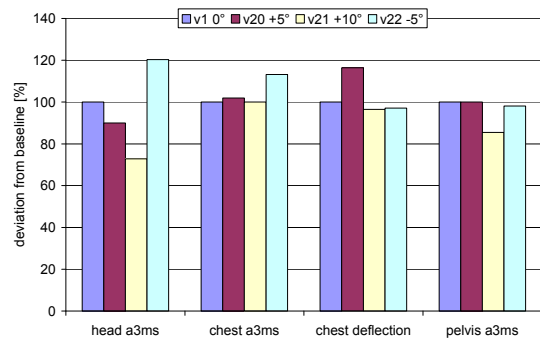


Figure 31. Dummy readings depending on CRS angle from upright to reclined.

In further sled tests the influence of the variable ISOFIX anchorages was checked and angled tests with 10° impact angle were analysed.

Restricting the ISOFIX anchorage points seems not to have major influence on the dummy readings for the tested products, see Figure 32. Earlier analysis of the timing of the movement of the anchorages is supporting this result. The movement of the ISOFIX anchorages seems to start after maximum dummy readings.

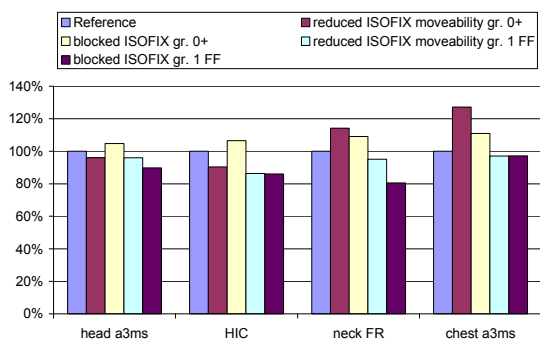


Figure 32. Dummy readings depending on the allowed travel amount of ISOFIX anchorages.

The influence of introducing an impact angle depends mainly on the individual product. However, for most of the tested CRS the influence was small, see Figure 33.

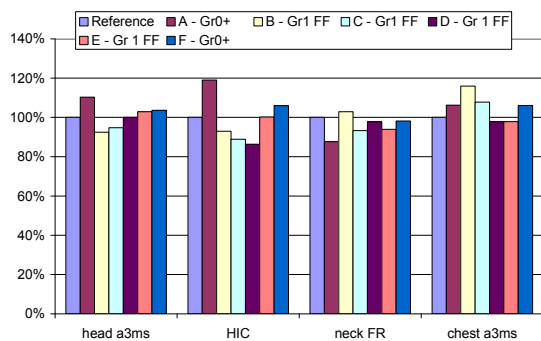


Figure 33. Dummy readings depending on impact angle.

CONCLUSIONS

Existing test procedures for the assessment of the lateral impact performance of child restraint systems were felt to be either too complicated to be used for the homologation of CRS or do not represent real world side accidents in a sufficient way. Following that the GRSP Informal Group on CRS developed a new test procedure utilising the knowledge gained in ISO TC22 SC12 WG1. This test procedure has been analysed in order to check the feasibility with different sled systems and different CRS types, test severity as well as repeatability and reproducibility. The results to date indicate that the procedure is feasible at different sled systems (deceleration sleds: PU tubes, bar brake and hydraulic brake; acceleration sled: sled on sled were tested so far) with different ISOFIX integral harness CRS types. The severity level tends to be higher than in reference tests for infant carriers and at an equal level for larger CRS. However, for larger CRS the fulfilment of the head containment criterion is more challenging. Good repeatability and reproducibility were obtained at least for the head acceleration, which is rated as the target body region. Although validation of the test procedure is still ongoing, it is expected that the procedure will be ready on time for introduction into ECE regulation.

ACKNOWLEDGEMENTS

Part of the work presented in this paper was co-funded by the European Commission within the 7th Frame Work Programme (CASPER project, Grant Agreement no. 218564).

Further information concerning the CASPER project is available at the CASPER web site www.casper-project.eu.

REFERENCES

Arbogast, K.B.; Chen, I.; Durbin, D.R.; Winston, F.K.
Injury Risks for Children in Child Restraint

Systems in Side Impact Crashes
IRCOBI Conference, Graz 2004

Crandall, J.; Sherwood, C.
Factors Influencing the Performance of Rear Facing Restraints in Frontal Vehicle Crashes
3rd International Conference – Protection of Children in Cars, Munich, 2005

EEVC Working Group 18
Report Child Safety
February 2006

Henry B, Sherwood CP, Crandall JR, Kent RW, Vaca FE, Arbogast KB, Bull MJ;
Car safety seats for children: rear facing for best protection. *Injury Prevention* 2007; 13:398-402

Johannsen, H.; Weber, S.; Schindler, V.:
CHILD Technical Report Selection of Side Impact Test Procedure
2006

Johannsen, H.; Menon, R.A.
Short Report Forward Component in ISO Side Impact Test Procedure for CRS
ISO TC22 / SC12 / WG1 / TF1, 2007a (ref. ISO/TC22/SC12/WG 1 N 797)

Johannsen, H.; Barley, G.; Carine, S.; Claeson, P.; Lundell, B.; Nojiri, K.; Renaudin, F.; van Rooij, L.; Siewertsen, A.
Review of the Development of the ISO Side Impact Test Procedure for Child Restraint Systems
ESV Conference, Lyon, 2007b

Jakobsson, L.; Isaksson-Hellmann, I.; Lundell, B.
Safety for the Growing Child – Experience from Swedish Accident Data
19th ESV Conference, Washington DC, June 2005

Langwieder, K.; Hell, W.; Willson, H.
Performance of Child Restraint systems in Real-Life Lateral Collisions
40th STAPP-Conference, Albuquerque, 1996.

Langwieder K.
Verletzungsfolgen für Kinder als Insasse bei Pkw-Unfällen
Innovative Kindersicherungen im Pkw, 2002 (in German).

Maltese MR, Locey CM, Jermakian JS, Nance ML, Arbogast KB
Injury causation scenarios in belt-restrained nearside child occupants
Stapp Car Crash Journal. Vol 51, 2007

Mertz, H.
Calculation Methods & Acceptance Levels for Assessing Repeatability and Reproducibility (R &

R)
ISO/TC22/SC12/WG5 Document N751, 2004

Otte, D.
Injury Risk of Children in Cars
1st Conference Protection of Children in Cars,
Cologne, 2003